[American Journal of Science, Vol. 320, October, 2020, P. 677–729, DOI 10.2475/10.2020.02]

ZIRCON U-Pb GEOCHRONOLOGY AND Nd-Pb ISOTOPE GEOCHEMISTRY OF BLUE RIDGE BASEMENT IN THE EASTERN GREAT SMOKY MOUNTAINS, U.S.A.: IMPLICATIONS FOR THE PROTEROZOIC TECTONIC EVOLUTION OF THE SOUTHEASTERN LAURENTIAN MARGIN

D.P. MOECHER*, F.C. HARRIS*, E.A. LARKIN*, R.J. QUINN*, K.B. WALSH*, D.F. LOUGHRY, JR.*, E.D. ANDERSON*, S.D. SAMSON**, A.M. SATKOSKI**, and E. TOHVER***

ABSTRACT. **The Mesoproterozoic to Paleozoic history of the southeastern Laurentian margin involved repeated collisional and accretionary tectonomagmatic events that reworked and recycled older continental crust of preceding events. The Great Smoky Mountains Basement Complex (GSMBC) within the southern Appalachian Blue Ridge exposes complexly deformed orthogneiss and paragneiss that preserve a record of Laurentian margin evolution from *ca.* 1.9 Ga to 450 Ma. The GSMBC consists primarily of: (1) 1.34 to 1.31 Ga (pre-Elzevirian) granodioritic orthogneiss and entrained mafic xenoliths that represent some of the oldest crust in Appalachian Grenville massifs (correlated with pre-Elzevirian crustal components in the Adirondack, Green Mountains, New Jersey Highlands, and French Broad massifs), (2) *ca.* 1.15 to 1.05 Ga augen and granitic orthogneiss produced during Shawinigan and Ottawan phases of Grenville-age magmatism and metamorphism, respectively, and (3) paragneiss derived from protoliths with either Grenville-age (1.1–1.0 Ga) or post-Grenville (Neoproterozoic) depositional ages based on presence/absence of *ca.* 1.0 Ga metamorphic zircon and 1.9 to 1.1 Ga detrital zircon. All lithologies experienced Taconian metamorphism and variable migmatization. Pre-Ottawan paragneiss exhibits major detrital zircon ages modes at 2.0 to 1.6 and 1.4 to 1.3 Ga that require a component of older Proterozoic crust in the sediment source region. Detrital zircon grains in post-Ottawan paragneiss exhibits the full spectrum of Grenville-age modes that correlate with the five phases of Grenville magmatic/metamorphic events in eastern Laurentia. These paragneiss samples also contain scattered 750 to 600 Ma detrital zircon grains that constrain their maximum depositional age to late Neoproterozoic. The sedimentary protoliths of the latter paragneiss consist largely of detritus from exhumation of all Grenville crustal age components during post-orogenic exhumation and crustal extension leading up to Late Neoproterozoic breakup of Rodinia.**

Most zircon U-Pb age systematics exhibit variable discordance that can be attributed to disturbance of the U-Pb system and/or new zircon growth during either high-grade Ottawan (*ca.* 1.04 Ga) or Taconian (*ca.* 0.46 Ga) regional metamorphism and migmatization. Neodymium T_{DM} model ages for granodioritic orthogneiss and paragneiss range from 1.8 to 1.6 Ga, indicating that the rocks were derived from recycling of Proterozoic crust (that is, they are not juvenile), consistent with the 1.9 to 1.6 Ga detrital zircon grains in pre-Ottawan paragneiss and with 1.8 to 1.7 Ga inherited zircon in some 1.33 Ga orthogneisses and a 1.35 Ga xenolith. Whole rock Pb isotope compositions of GSMBC rocks overlap the field of compositions characteristic of Amazonian crust and of other basement rocks from the south-central Appalachians. The Pb isotopes and geochronology in orthogneiss, mafic xenoliths, and pre-Ottawan paragneiss are consistent with a correlation of the GSMBC with the Mars Hill terrane within the French Broad massif and with the greater Grenvillian south-central Appalachian basement (SCAB) that is considered exotic to Laurentia, and transferred during Rodinian collision prior to *ca.* 1.2 Ga. Similarities in protolith ages and Pb isotopes

*University of Kentucky, Department of Earth and Environmental Sciences, Lexington, Kentucky 40506, U.S.A.
**Syracuse University, Department of Earth Sciences, Syracuse, New York 13244, U.S.A.
***Instituto de Geosciências, Universidade de São Paolo, 05508-080, São Paolo, Brazil

point to the Paraguá terrane of Amazonia (southwestern Brazil and eastern Bolivia) as a likely match for SCAB. Initial Amazonia-Laurentia collision occurred at *ca.* 1.35 to 1.32 Ga with final transfer of SCAB to Laurentia occurring after 1.20 Ga within the sinistral oblique collision zone between Laurentia and Amazonia defined by previous workers.

Key words: Appalachian tectonics, Grenville orogeny, zircon, U-Pb geochronology, Amazonia-Laurentia collision

INTRODUCTION

A fundamental question in continental evolution is the extent to which crust develops by addition of juvenile material versus reworking of older crust. In the case of Laurentia, growth and cratonization occurred by both mechanisms (for example, Hoffman, 1988; Condie, 1990; Whitmeyer and Karlstrom, 2007; Condie and Aster, 2010; Rivers and others, 2012). Juvenile terranes comprised much of the Paleoproterozoic crustal growth (Yavapai, Mazatzal, Granite-Rhyolite belts) whereas more evolved crustal material was added since then (Grenville, Appalachian belts).

The Grenville province in Ontario, Quebec, and New York includes rocks ranging in age from *ca.* 1800 Ma to 950 Ma (Rivers, 1997, 2008; Hynes and Rivers, 2010; Rivers and others, 2012; McLelland and others, 2013), some of which are pre-orogenic (older than *ca.* 1400 Ma) with others formed during Grenville orogenesis.[1] Evolution of the Grenville orogen probably involved syn-collisional extensional events (Rivers and others, 2012; McLelland and others, 2013), and then was fully rifted in the Neoproterozoic and subsequently reworked (metamorphosed, deformed) to varying degrees by several Paleozoic collisional events (Taconian, Neo-Acadian, Alleghanian) that further obscured Precambrian characteristics (Rankin, 1975; Hatcher, 1987; Robinson and others, 1998). Adding to the complexity of eastern Laurentian crustal evolution, whole-rock Pb isotope compositions of Grenvillian rocks exposed in central and southern Appalachian basement massifs require the presence of an exotic Amazonian crustal component (Sinha and others, 1996; Loewy and others, 2003; Tohver and others, 2004; Fisher and others, 2010), implying growth by continental collision and terrane transfer.

This study focuses on the evolution of southeastern Laurentian crust exposed in the Great Smoky Mountains basement complex where a range of Precambrian lithologies is well-mapped and documented (Hadley and Goldsmith, 1963; Quinn, ms, 1991; Montes, ms, 1997; Massey and Moecher, 2005; Merschat and Cattanach, 2008; Merschat, ms, 2009; Southworth and others, 2012; Larkin, ms, 2016) (fig. 1). The study area includes the southwesternmost extent of the Grenvillian French Broad basement massif where Paleozoic tectonometamorphism resulted in crustal imbrication, high grade metamorphism and polyphase folding of Mesoproterozoic basement and Neoproterozoic cover. This basement consists of the oldest rocks in the southern Blue Ridge basement (*ca.* 1.37–1.30 Ma: Moecher and others, 2018; also see Tollo and others, 2010, 2017) and records a protracted history of eastern Laurentian continental evolution from at least the Mesoproterozoic through the Ordovician. We use zircon U-Pb geochronology of basement ortho- and paragneisses, major and trace element chemistry, detrital zircon age systematics, and Nd and Pb isotope compositions to unravel the nature of bedrock types, processes, and sequence of events that produced the present configuration of continental basement. The protracted history of high-

[1] The Grenville orogeny *sensu strictu* consists of Ottawan (*ca.* 1.09-1.02 Ga) and Rigolet (*ca.* 1.02-0.98 Ga) phases (Rivers and others, 2012). The Shawinigan (1190-1120 Ma) and Elzeverian (1250-1210 Ma) are recognized as distinct orogenies. Laurentian continental margin arc rocks that formed in the interval *ca.* 1380-1300 do not have a formal uniform designation and are referred to here as "pre-Elzevirian" for brevity.

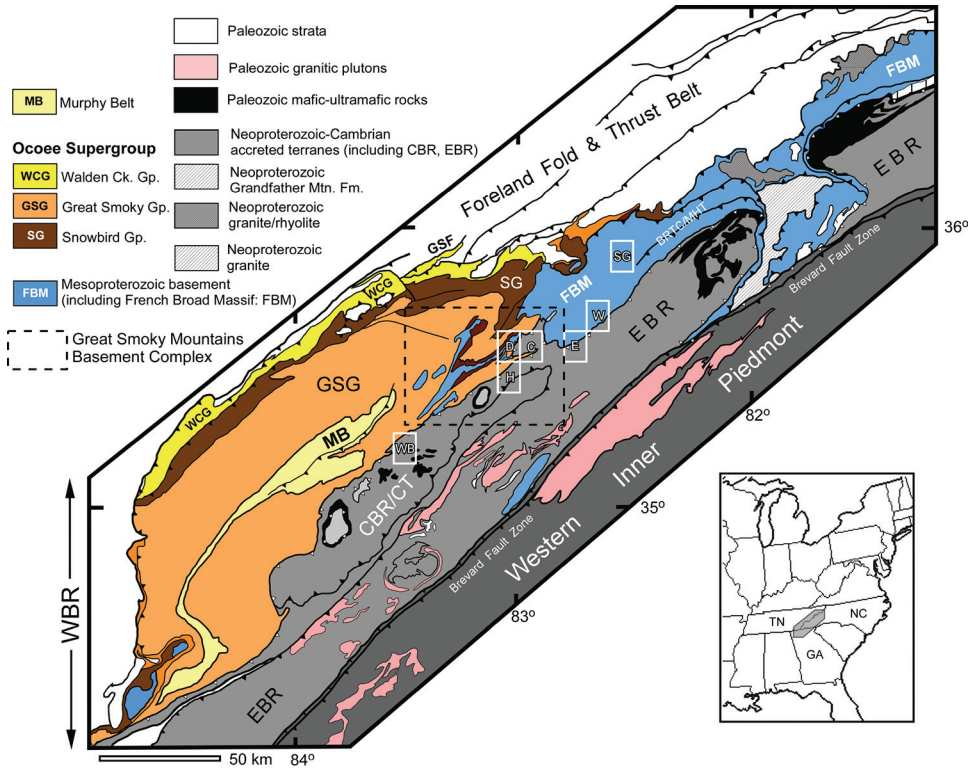

Fig. 1. Geologic map showing the distribution of terranes in the southern Appalachian Blue Ridge province with locations and units discussed in text (geology after Rankin and others, 1990). Sampled 7.5 minute quadrangles (white boxes) abbreviations: C: Clyde; D: Dellwood; E Enka; H: Hazelwood; SG: Sams Gap; WB: Wayah Bald; W: Weaverville. Other abbreviations: CBR/CT: Cartoogechaye terrane of the Central Blue Ridge province; EBR: Eastern Blue Ridge; FBM: French Broad Massif of the Western Blue Ridge; GSF: Great Smoky Fault; GSG: Great Smoky Group; MB: Murphy Belt; SG: Snowbird Group; WCG: Walden Creek Group. Dashed black box is region of the informally designated Great Smoky Mountains basement complex of this study. BRTC/MHT: Blue Ridge Thrust Complex within the greater French Broad Massif (Troupe and others, 2004) that cuts the informally designated Mars Hill terrane (Carrigan and others, 2003) of the French Broad Massif.

grade regional metamorphism impacts U-Pb systematics, as shown by zircon inheritance, discordance due to Pb loss, and complex zircon growth and dissolution patterns that factor into the interpretation of age results. Nd and Pb isotopes, along with zircon textures, aid in seeing through the complex geologic history to arrive at constraints on the ultimate sources of crustal components of southeasternmost Laurentia and its collision with Amazonia to assemble Rodinia.

GEOLOGIC BACKGROUND

Interpretation of the new geochronology must consider the sequence of Precambrian and Paleozoic tectonometamorphic events that created and modified lithologies constituting southern Appalachian crystalline basement. Mesoproterozoic rocks are exposed in basement massifs along the length of the Appalachian orogen (Hatcher, 1987; Rankin and others, 1989; Ratcliffe and others, 1991; Hatcher and others, 2004; Southworth and others, 2010; Tollo and others, 2010) and have temporal affinities with Mesoproterozoic rocks of the Grenville province in Canada and the Adirondacks. The present study relies on the syntheses of McLelland and others (2010, 2013),

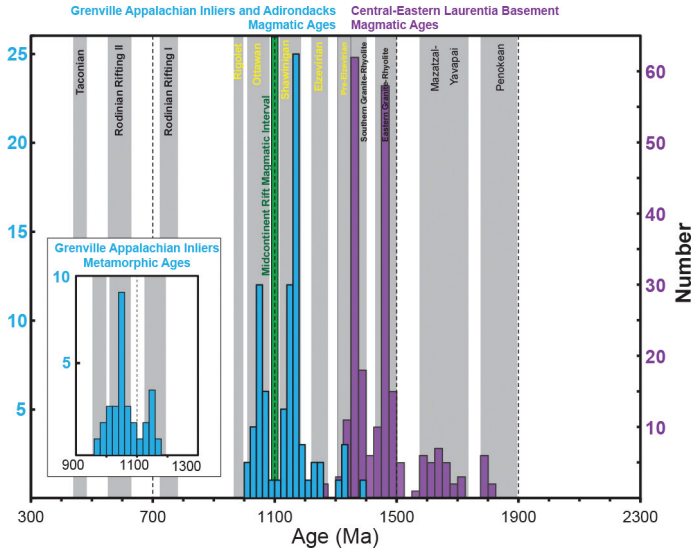

Fig. 2. Compilation of SHRIMP U-Pb zircon ages for eastern Laurentia Precambrian basement illustrating ages of major magmatic and metamorphic zircon-forming events in eastern Laurentia used for interpretation of the results of this study. Data from Southworth and others (2010), McLelland and others (2013), Bickford and others (2015), and this study.

Southworth and others (2010), and Rivers and others (2012) for orogen-scale comparisons and interpretations of results. Most Mesoproterozoic rocks in western North Carolina and southwestern Virginia constitute the French Broad massif of the Western Blue Ridge province (fig. 1) and are granitic orthogneisses with protolith crystallization ages of either *ca.* 1050 or *ca.* 1150 Ma (Southworth and others, 2010; Tollo and others, 2010, 2017), which correspond to the Ottawan phase of the Grenville orogeny and the Shawinigan orogeny, respectively (Rivers, 1997, 2008, 2012; McLelland and others, 2010, 2013) (fig. 2). Two older Mesoproterozoic magmatic events have been identified in the Adirondacks and Appalachian basement massifs: the *ca.* 1260 to 1220 Ma Elzevirian and *ca.* 1370 to 1300 Ma pre-Elzevirian phases of development of the eastern Laurentian margin. Magmatism of Shawinigan age is aerially the most extensive and voluminous magmatic event within the Grenville orogen (Labrador to west Texas) (Rivers and others, 2012). High-grade metamorphism accompanied the Elzevirian, Shawinigan, Ottawan, and Rigolet phases, with the Ottawan being the regionally most extensive metamorphic event (Rivers and others, 2012). The dominance of Shawinigan magmatism and Ottawan metamorphism is reflected in the relative proportion of igneous versus metamorphic zircon ages for each event (fig. 2). Neodymium isotope analysis of the *ca.* 1350 Adirondack orthogneisses supports their origin as juvenile magmatic additions to Laurentia (Daly and McLelland, 1991; McLelland and others, 1993), whereas most of the 1050 and 1150 Ma granitic gneisses from the southern Appalachian inliers that have been analyzed have protoliths with a major component of evolved Laurentian crust (Carrigan, and others, 2003; Bream and others, 2004; Fisher and others, 2010). In spite of the temporal similarities of Blue Ridge basement rocks with Grenville-age rocks elsewhere, Pb isotope compositions are compelling evidence that much of the southern Blue Ridge represents crust exotic to Laurentia (Loewy and others, 2003; Tohver and others, 2004a; Fisher and others, 2010; McLelland and others, 2010, 2013; Rivers and others, 2012). The timing and process of this transfer remain matters of debate.

Although it has a complex Precambrian evolution, the present architecture of crystalline rocks in the southern Appalachians (GA-NC-SC-TN) (fig. 1) has long been interpreted in terms of Paleozoic tectonics including Middle Ordovician (Taconian) accretion of continental margin terranes that formed within or along the post-Rodinian, rifted passive margin of Mesoproterozoic Laurentia bordering Iapetus (Hatcher, 1987; Rankin and others, 1989; Hatcher and others, 2004). The Western Blue Ridge terrane includes Grenville basement and its late Neoproterozoic to Cambrian cover sequences (Ocoee Supergroup, Chilhowee Group) that represent the rifted Laurentian continental margin. The Eastern Blue Ridge (EBR) consists primarily of the widespread Ashe-Tallulah Falls and other metasedimentary sequences (Otto, Cowrock, *et cetera*), interpreted to be marginal marine transitioning to oceanic slope and rise sequences. The EBR province includes mafic lithologies tectonically mixed with metasediments ("block-in-matrix" structures: Raymond and others, 1989), now primarily amphibolites, mafic granulites, eclogites, and metaperidotites, interpreted to represent remnants of oceanic lithosphere. All of these sequences are interpreted to be thrust sheets, some with terrane designation, accreted before, and metamorphosed during, Taconian collision/subduction with their boundaries being cryptic thrust faults. The largest sequence is the Cartoogechaye terrane within the Central Blue Ridge (fig. 1), which is everywhere migmatitic at upper amphibolite to granulite facies and distinguished by mafic enclaves ranging in size from outcrop to map scale (Hatcher and others, 2004). The challenge remains to resolve the pre-Taconian history of the basement and cover sequences, including the ages and affinities of the former and the provenances of the latter.

The type area for the Great Smoky Mountains Basement Complex is the Dellwood quadrangle in western North Carolina, originally mapped by Hadley and Goldsmith (1963; also see Southworth and others, 2012) (fig. 3). Mesoproterozoic gneisses are interpreted, based on evidence in lower grade equivalents, to be nonconformably overlain by Neoproterozoic syn-rift clastic sediments of the Ocoee Supergroup (Southworth and others, 2012). Detrital zircon and detrital monazite ages of low-grade Ocoee metaclastic rocks support a predominantly local Grenville basement source and late Neoproterozoic depositional age (Bream and others, 2004; Aleinikoff and others, 2010; Moecher and others, 2011, 2019; Chakraborty and others, 2012; Kelly and Moecher, 2014). Middle Ordovician (Taconian) regional metamorphism resulted in development of chlorite to sillimanite-grade conditions from north to south across the Great Smoky Mountains region (Hadley and Goldsmith, 1963; Moecher and others, 2004; Massey and Moecher, 2005; Corrie and Kohn, 2007; Clemons and Moecher, 2009; Moecher and others 2011; Spaulding, ms, 2014), culminating in upper amphibolite to locally granulite facies conditions, with widespread migmatization and ductile deformation in nearly all basement units.

The study area in the eastern Great Smoky Mountains region is primarily within the Dellwood, northern Hazelwood, and western Clyde 7.5 minute quadrangles (figs. 1 and 3), which expose rocks that were formed during, or were affected by, the entire Mesoproterozoic to lower Paleozoic geologic history discussed above. Evidence for the protoliths and the nature of original contacts are generally absent so that whole-rock geochemistry, isotopic systematics, and geochronology are required to assign a crustal affinity. Bedrock mapping (1:24,000) of the north half of the Hazelwood 7.5 minute quadrangle (Larkin, ms, 2016; also see Southworth and others, 2012, and Merschat, ms, 2009) was conducted to assess potential southward extensions of basement lithologies of the Great Smoky Mountains basement complex from the type locality. The Clyde quadrangle had been mapped in detail (Merschat and Cattanach, 2008) so that correlatives of the Dellwood basement lithologies can be compared. Representative samples for whole-rock major and trace element geochemistry, whole-rock Sm-Nd

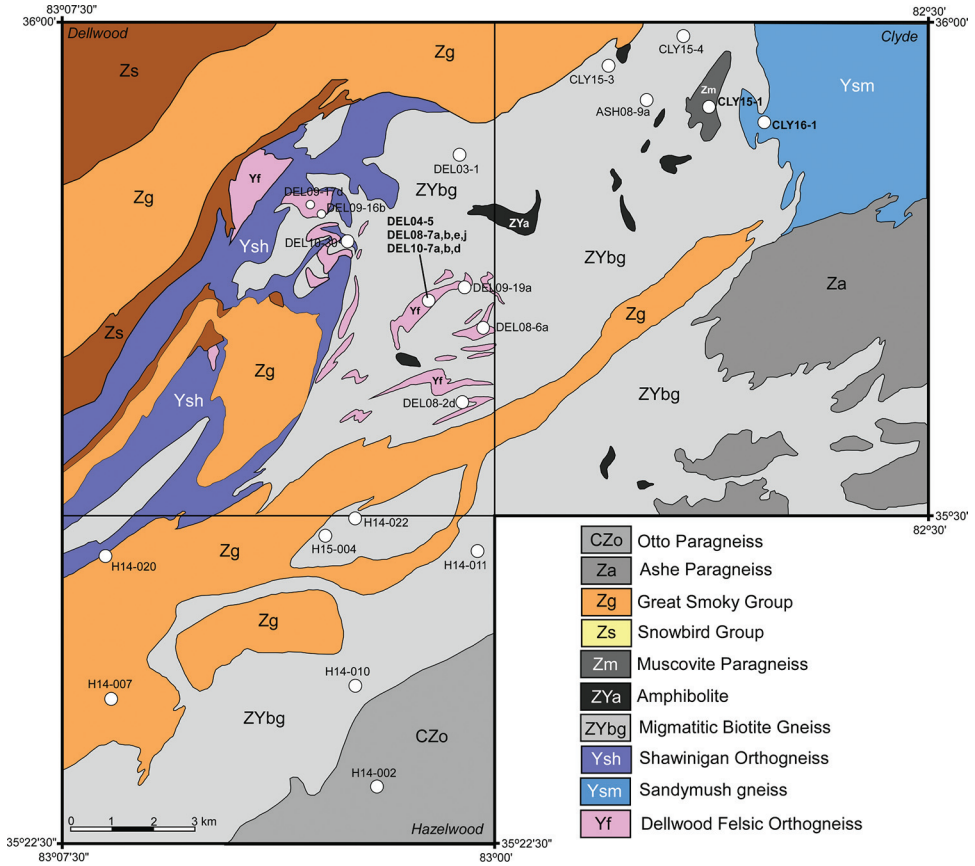

Fig. 3. Geologic map of study area showing distribution of map units (modified from Hadley and Goldsmith, 1963; Merchat and Cattanach, 2008; Southworth and others, 2012; and Larkin, ms, 2016) and sample localities. Designation of map units partly reflects the results of geochronology presented in this study.

and feldspar Pb isotope geochemistry, and U-Pb zircon geochronology were collected from basement lithologies in all three quadrangles (Loughry, ms, 2010; Anderson, ms, 2011; Quinn, ms, 2012; Larkin, ms, 2016; Walsh, ms, 2018). In addition, samples were collected from basement northeast (Enka, Sams Gap, Weaverville 7.5 min. qudrangles) and southwest of the main study area (Wayah Bald 7.5 min. quadrangle), respectively. Zircon U-Pb geochronology focussed on crystallization ages of orthogneiss protoliths and ages of detrital and/or metamorphic zircon in presumed sedimentary protoliths of paragneisses, all in the context of zircon growth textures imaged by SEM.

SAMPLE DESCRIPTIONS

General descriptions of sampled lithologies are summarized below and in table 1. Detailed lithologic descriptions of map units may be found in Hadley and Goldsmith (1963), Southworth and others (2012), Larkin (ms, 2016), and Moecher and others (2018), with descriptions of specific samples in Loughry (ms, 2010), Quinn (ms, 2012), Larkin (ms, 2016) and Walsh (ms, 2018). Field photographs of representative lithologies are shown in figure 4.

Following Hadley and Goldsmith (1963; also see Southworth and others, 2012) the dominant basement lithologies in the Dellwood quadrangle are:

TABLE 1

Description of Samples used for Geochronology

Sample	Lithology[1]	Mineral Assemblage[2]	Textural Details
Meta-igneous rocks			
DEL04-5	Granodioritic orthogneiss	Pl-Qtz-Bt-Mc-Ep-Sc-Ap-Ttn-Hbl	Foliation = discontinuous mm-scale folia of dynamically recrystallized Bt+Ep+Qtz
DEL08-6c	Monzogranitic orthogneiss	Pl-Qtz-Mc-Hbl-Bt-Ep-Ttn-Ap	Foliation = discontinuous mm-scale folia of dynamically recrystallized Bt+Ep+Qtz wrapping feldspar porphyroclasts with grain boundary recrystallization
DEL08-7a	Granodioritic orthogneiss	Pl-Qtz-Bt-Hbl-Grt-Sc-Ep-Opq	Equigranular, unfoliated, Grt poikiloblasts and coronas
DEL08-7d	Amphibolite	Hbl-Pl-Bt-Grt-Sc-Qtz	Equigranular, granoblastic
DEL08-7e	Granodioritic orthogneiss	Pl-Mc-perthite-Qtz-Bt-Hbl-Grt-Cpx-Opq	Equigranular, unfoliated, Grt coronas on Cpx and Opq, Hbl-I (primary) and Hbl-II (retrograde symplectite after Cpx)
DEL08-7j	Deformed tonalitic orthogneiss	Pl-Hbl-Qtz-Bt-Sc-Ep	Foliation = compositional banding (mafic/felsic layers) and parallel alignment of Hbl+Bt folia; dynamic recrystallization of Qtz+Bt seams
DEL08-10a	Qtz monzodioritic gneiss	Pl-Hbl-Bt-Qtz-Ep-Ttn-Ap	Foliation = compositional banding: alternating mafic/felsic layers and parallel alignment of Bt flakes; dynamic recrystallization of Qtz+Bt seams and Pl grain boundaries
DEL09-16b	Qtz monzodioritic orthogneiss	Pl-Qtz-Orthoclase perthite-Hbl-Bt-Ttn-Sc-Ep-Ap	Unfoliated, equigranular
DEL09-17d	Monzogranitic orthogneiss	Pl-Qtz-Mc perthite-Bt-Ttn-Ep	Equigranular, unfoliated leucosome in migmatitic gneiss
DEL09-19a	Monzogranitic orthogneiss	Pl-Mc-Qtz-Bt-Ttn	Equigranular, unfoliated leucosome in migmatitic gneiss
DEL10-7A	Amphibolite xenolith	Pl-Bt-Hbl-Grt-Sc-Grt-Qtz	Equigranular, granoblastic, unfoliated; Grt symplectites
DEL10-7B	Granodioritic orthogneiss	Pl-Qtz-Mc-Bt-Hbl-Grt	Equigranular, unfoliated
DEL10-7D	Amphibolite xenolith	Hbl-Pl-Bt-Ep-Ttn	Equigranular, granoblastic, unfoliated
DEL10-11	Syenogranitic orthogneiss	Mc perthite-Pl-Qtz-Bt-Ep-Hbl	Weakly foliated – dynamic recrystallization of Qtz and grain boundary recrystallization of Pl and Mc
DEL10-30	Porphyroclastic granodioritic orthogneiss	Mc perthite-Pl-Qtz-Bt-Ep	Foliation = penetrative dynamic recrystallization of Qtz+Bt around relict Kfs phenocrysts;
H14-020	Alkali feldspar granitic augen orthogneiss	Mc-Pl-Qtz-Bt-Ttn-Ep	Inequigranular, weakly foliated: Abundant dynamic recrystallization of Qtz+Bt wrapping relict, recrystallized Mc phenocrysts;
H15-003	Dark grey porphyroclastic Bt-orthogneiss	No thin section	Weakly foliated, foliation defined by weak parallelism of isolated, recrystallized Kfs porphyroclasts and leucosomes
SG18-1	Granitic orthogneiss	Mc-Pl-Qtz-Bt-Ms-Ep	Originally porphyritic, protomylonitic retrograde greenschist facies ductile overprint

TABLE 1
(continued)

Sample	Lithology[1]	Mineral Assemblage[2]	Textural Details
Metasedimentary rocks			
DEL08-2e	Migmatitic paragneiss, ~15% leucosome	Pl-Bt-Ms-Qtz-Ttn-Ep	Foliation defined by parallelism of leucosome bands and Mu+Bt folia
DEL14-001	Protomylonitic paragneiss	Qtz-Pl-Ms-Bt-Grt	Penetrative recrystallization of Qtz, mica fish and crenulated micas
H14-002	Metapsammitic paragneiss (Otto Fm.)	Qtz-Pl-Mc-Bt-Ms	Weak banding with sparse leucosomes
H14-007	Metapsammite (Copper Hill Fm.)	Qtz-Pl-Mc-Bt-Ms	Massive metasandstone interlayered with Ky-Str-Grt-Bt-Ms-Pl-Qtz metapelitic gneiss with sparse leucosomes
H14-011	Amphibolite enclave in migmatitic paragneiss	Hbl-Pl-Grt-Bt-Qtz-Opq; Pl-Qtz-Bt-Grt	Amphibolite enclave: unfoliated, equigranular, granoblastic; host leucosome: equigranular, granoblastic
H15-004	Bt-Mu paragneiss	Pl-Qtz-Bt-Ms	
DEL03-1	Migmatitic Bt paragneiss, ~50% leucosome	Pl-Mc-Qtz-Bt-Ms	Foliation defined by isoclinally folded leucosomes bordered by melanosome, and folia of dynamically recrystallized Qtz+Bt+Pl
ASH08-9	Migmatitic Bt paragneiss, ~50% leucosome	Pl-Qtz-Bt-Ms-Ep	Foliation defined by isoclinally folded leucosomes bordered by melanosome, and folia of dynamically recrystallized Qtz+Bt+Pl
CLY15-1	Ms-Bt paragneiss	Pl-Qtz-Mu-Bt-Grt-Ap	No definitive leucosomes; foliation defined by parallelism of Ms+Bt wrapping around Grt poikiloblasts; penetrative dynamic recrystallization of all Qtz
CLY15-3	Ms-Bt paragneiss	Pl-Qtz-Ms-Bt	No definitive leucosomes; foliation defined by parallelism of Ms+Bt; penetrative dynamic recrystallization of all Qtz
CLY15-4	Ms-Bt paragneiss	Pl-Qtz-Ms-Bt	No definitive leucosomes; foliation defined by parallelism of Ms+Bt; penetrative dynamic recrystallization of all Qtz
CLY16-1	Bt paragneiss	Pl-Qtz-Bt-Ep-Ttn leucosome; Bt-Pl-Qtz-Ttn-Ep melanosome	Isoclinally folded 1 cm thick tonalitic leucosomes bounded by Bt melanosomes interlayered with protomylonitic melanosomes
WB15-1	Bt-Grt paragneiss	Qtz-Pl-Bt-Grt	Equigranular, granoblastic, weak foliation defined by parallelism of scattered Bt flakes
E19-1	Metagraywacke	Qtz-Pl-Kfs-Bt-Mu	Equigranular, granoblastic, weak foliation defined by parallelism of scattered Bt and Mu flakes
W19-2	Metagraywacke	Qtz-Pl-Kfs-Bt-Ms-Grt	Equigranular, granoblastic, weak foliation defined by parallelism of scattered Bt and Mu flakes

[1]: Plutonic rock lithologic designations based on whole rock composition (table 2) and classification of Streckeisen and Le Maitre (1979).
[2]: Assemblage listed in order of abundance; abbreviations after Whitney and Evans (2010).

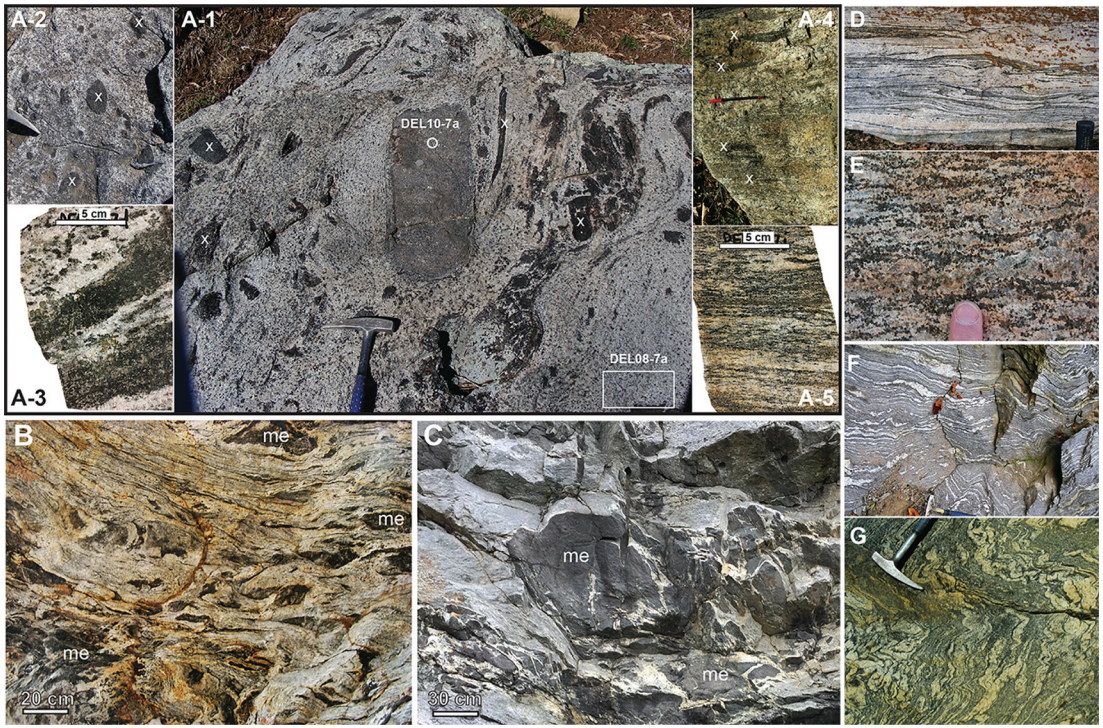

Fig. 4. Photographs of representative lithologies from the Dellwood (NC) 7.5 minute quadrangle region analyzed for this study. (A-1) Outcrop of xenolith-bearing granodioritic orthogneiss at the type locality (shown as locations DEL08-7 and DEL10-7 on fig. 3). A weak compositional banding is developed around mafic masses. White circle is location of core taken from dated xenolith sample DEL10-7a. White box outlines region of outcrop DEL08-7a that typifies least deformed orthogneiss and similar to features of dated orthogneiss samples DEL08-7e and DEL10-7b). (A-2) Pavement outcrop of undeformed orthogneiss containing numerous small xenoliths (denoted by white x). (A-3) Sawn surface of unfoliated clinopyroxene-bearing orthogneiss sample DEL08-7e with mafic xenoliths (now garnet amphibolite); (A-4) pavement outcrop 10 meters south of A-1 showing flattened mafic xenoliths (denoted by black x) in weakly foliated orthogneiss; (A-5) sawn surface of dated sample DEL08-7j showing foliation defined by parallelism of layers containing variable mafic mineral content. (B) Outcrop at location DEL08-6 (fig. 3) showing mafic enclaves interpreted to be deformed xenoliths in strongly foliated granodioritic orthogneiss (sample DEL08-6c was collected from the outcrop). (C) Roadcut in Sams Gap quadrangle (fig. 3) of foliated light gray granitic orthogneiss containing mafic enclaves sampled for geochronology (SG18-1 and -2, respectively). (D) Migmatitic, isoclinally-folded orthogneiss mapped as hornblende gneiss by Hadley and Goldsmith (1963), dated here via SIMS as Shawinigan in age (*ca.* 1150 Ma). (E) Migmatitic, isoclinally folded gneiss mapped as hornblende-biotite gneiss (sample DEL08-19, preliminarily SIMS age is Shawinigan). (F) Weakly foliated augen orthogneiss (sample DEL08-16b, preliminarily SIMS age is Shawinigan). (G) Post-Ottawan migmatitic biotite paragneiss (sample DEL08-2e) with relatively low proportion of leucosome. (H) Pre-Ottawan migmatitic biotite gneiss (sample ASH08-9) with relatively high proportion of leucosome.

(1) Light-gray, non-migmatitic plagioclase + K-feldspar + quartz + biotite + hornblende + clinopyroxene + garnet granodioritic orthogneiss (samples DEL08-7a, -7e; DEL10-7b) containing mafic xenoliths or enclaves in various stages of disaggregation and magmatic or tectonic mixing with the host orthogneiss (figs. 4A-1 to 4A-3). A weak flow banding in the host orthogneiss envelops the rounded xenoliths that range in size from a few centimeters to 1 meter in maximum dimension. Although not all occurrences are foliated, the presence of metamorphic hornblende, biotite, garnet, scapolite, and epidote (Loughry, ms, 2010; Quinn, ms, 2012; table 1) supports the interpretation that this unit was metamorphosed, that is, it experienceed the thermal and baric conditions, but not necessarily the same degree of strain, as the surrounding terrane (thus the designation "orthogneiss"). The orthogneiss grades laterally into foliated, variably folded orthogneiss overprinted by late ductile deformation (probably late Paleozoic, discussed below) and with mafic bands, schlieren and rafts interpreted to be deformed xenoliths (samples DEL04-5, DEL08-6c and -7j) (figs. 4A-4 and 4A-5, 4B). The deformed orthogneiss may be monzonitic to tonalitic and have slightly higher mafic mineral content (mainly hornblende) due to tectonic mixing of granodiorite and mafic xenoliths during deformation and metamorphism (table 2). Two mafic xenoliths in granodioritic orthogneiss were sampled for geochronology (DEL10-7a, -7d: for example, fig. 4A-1) in order to test that they are older than host orthogneiss.

Berquist (ms, 2005) conducted U-Pb zircon and Nd isotope analysis of granitic orthogneiss containing abundant mafic enclaves (fig. 4C) exposed in the Blue Ridge Thrust Complex of the Western Blue Ridge northeast and along strike of the basement exposures of the Great Smoky Mountains basement complex (fig. 1) (Trupe and others, 2004). A SIMS zircon U-Pb upper intercept age of *ca.* 1370 Ma was obtained for porphyroclastic granitic orthogneiss. This age is significant as it is among the oldest reliable magmatic ages reported in the French Broad massif. Because of the age and lithologic similarity we resampled the roadcut that exposes orthogneiss dated by Berquist (ms, 2005; data published in Fisher and others, 2010) (sample SG18-1) and abundant 0.1 to 1 meter-scale mafic enclaves (now amphibolite: hornblende + plagioclase + biotite + titanite + epidote) (SG18-2) (fig. 4C) for zircon U-Pb geochronology to compare with granodioritic orthogneiss from the Great Smoky Mountains basement complex.

(2) Variably migmatitic hornblende-biotite orthogneiss (fig. 4D), compositionally banded (alternating hornblende + biotite-richer or poorer layers), most of which was originally mapped as the same unit as the felsic orthogneiss (above) (Hadley and Goldsmith, 1963), but turns out to be of diverse age and affinity based on zircon U-Pb geochronology (discussed below) (samples DEL08-10a, -16a, -17d, -19a; DEL10-11, collected for igneous and/or metamorphic zircon).

(3) Granitic to granodioritic, variably foliated, non-migmatitic augen and protomylonitic orthogneiss with a demonstrable plutonic protolith (samples DEL10-30; H14-020) (fig. 4E).

(4) Medium gray, migmatitic plagioclase + biotite + muscovite + K-feldspar + quartz + garnet paragneiss (DEL08-2e; DEL03-1; ASH08-9) that varies in volume of leucosome and thickness of leucosome bands (figs. 4G and 4H). Although originally mapped (Hadley and Goldsmith, 1963) and sampled as a single unit (Loughry, ms, 2010), the detrital zircon geochronology demonstrates that this map unit consists of two paragneisses of distinctly different age and origin (as discussed further below).

(5) Map-scale garnet + clinopyroxene amphibolite bodies, probably large boudins (Anderson and Moecher, 2009). Hornblende from the largest body in Dellwood quadrangle yields ^{40}Ar-^{39}Ar plateau ages of 440 to 450 Ma, interpreted to record cooling from peak Taconian metamorphism (Aleinikoff and others, 2007) and supporting previous work that high-grade metamorphism in the region occurred at *ca.* 460 Ma

TABLE 2

Whole Rock Major Element Analyses

Sample	CLY15-1	CLY15-2	CLY15-3	CLY15-4	WB15-1	CLY16-1	DEL14-001	H14-007	H14-011	H14-020	DEL08-2d	DEL04-5	DEL08-6C
Quad.	Clyde	Clyde	Clyde	Clyde	Wayah Bald	Clyde	Hazel.	Hazel.	Hazel.	Hazel.	Dell.	Dell.	Dell.
Lith.	pgn	pgn	pgn	pgn	pgn	pgn	pgn	pgn	pgn	agn	pgn	ogn	ogn
SiO_2	67.55	64.94	70.02	70.39	69.16	73.72	72.81	71.17	74.98	74.24	66.78	68.77	66.46
TiO_2	0.89	1.06	0.76	0.79	1.00	0.33	0.67	0.75	0.65	0.18	0.78	0.27	0.33
Al_2O_3	14.30	14.91	13.30	12.97	12.06	12.16	12.02	10.12	12.37	13.46	13.56	15.60	14.90
Fe_2O_3	6.45	6.31	5.06	4.64	6.33	3.00	4.93	4.03	3.75	1.44	4.71	0.22	0.27
FeO	nd	nd	nd	nd	nd	nd	nd	nd	nd	nd	nd	2.18	2.62
MnO	0.12	0.07	0.08	0.08	0.12	0.04	1.60	1.16	1.32	0.48	1.57	0.04	0.04
MgO	1.82	1.67	1.59	1.41	2.47	0.96	1.68	1.29	1.72	1.23	1.79	0.88	1.00
CaO	1.77	3.00	1.52	1.52	1.32	2.62	1.35	1.25	2.17	2.6	2.08	2.77	3.06
Na_2O	1.78	3.24	1.60	1.58	2.21	2.82	2.55	2.3	3.22	5.88	4.19	3.57	3.48
K_2O	2.70	3.20	3.75	3.66	2.49	1.11	0.16	0.16	0.11	0.07	0.17	3.65	3.85
P_2O_5	0.19	0.46	0.16	0.16	0.13	0.04	0.06	0.06	0.04	0.02	0.08	0.14	0.18
LOI	2.44	1.13	2.15	2.80	2.70	3.19	0.89	1.18	0.69	0.67	3.77	0.35	3.74
Total	100.01	99.99	99.99	100.00	99.99	99.99	98.72	93.46	101.02	100.27	99.48	98.44	99.93
A/CNK	1.3	0.9	1.2	1.2	1.2	0.9	1.3	1.3	1.0	0.9	1.4	0.9	0.8
Rock Type										alk. feld. granite		grano-diorite	monzo-granite

TABLE 2
(continued)

Sample	DEL08-7a	DEL08-7d	DEL08-7e	DEL08-7j	DEL10-7a	DEL10-7b	DEL10-7d	DEL10-11	DEL10-30	DEL08-10A	DEL09-16B	DEL09-17D	DEL09-19A
Quad.	Dell.	Dell.	Dell.	Dell.	Dell.	Dell.	Dell.	Dell.	Dell.	Dell.	Dell.	Dell.	Dell.
Lith.	ogn	mx	ogn	ogn	mx	ogn	mx	ogn	agn	og	agn	agn	ogn
SiO_2	64.51	58.81	51.31	66.32	48.52	71.27	49.16	65.82	63.76	59.09	56.2	72.83	71.99
TiO_2	0.38	0.94	1.3	0.5	1.24	0.23	1.42	0.34	0.67	0.72	1.11	0.23	0.32
Al_2O_3	15.74	14.44	16.43	15.83	20.41	15.49	16.31	14.95	16.58	15.94	15.7	12.83	12.82
Fe_2O_3	0.33	0.70	0.88	0.31	0.90	0.18	0.92	0.17	0.37	0.56	0.76	0.15	0.20
FeO	2.93	6.28	7.88	2.79	8.99	1.78	9.19	1.69	3.69	5.07	6.85	1.32	1.77
MnO	0.04	0.11	0.18	0.04	0.13	0.02	0.20	0.02	0.10	0.1	0.1	0.02	0.03
MgO	1.20	3.60	4.67	1.54	4.71	0.64	5.73	0.56	1.51	2.80	3.74	0.40	0.58
CaO	3.67	5.29	7.17	3.68	8.68	2.67	9.08	1.77	3.64	5.52	5.19	1.61	1.61
Na_2O	3.70	2.97	3.94	4.43	3.80	3.27	3.58	2.62	3.39	3.67	2.36	2.54	2.47
K_2O	2.91	2.10	1.28	1.63	2.45	3.55	1.51	6.79	3.58	2.20	3.63	4.81	5.10
P_2O_5	0.25	0.32	0.49	0.26	0.98	0.08	0.28	0.11	0.21	0.31	0.47	0.03	0.12
LOI	4.00	3.67	3.49	2.31	0.63	0.33	0.80	0.32	0.82	3.40	3.07	3.06	2.78
Total	99.66	99.23	99.02	99.64	101.44	99.50	98.18	95.16	98.32	99.38	99.18	99.83	99.79
A/CNK	1.1	0.7	0.6	1.1	0.6	0.9	0.5	0.9	0.9	0.8	0.7	0.9	0.9
Rock Type	grano-diorite		grano-diorite	tonalite		grano-diorite		syeno-granite	grano-diorite	qtz. monzo-diorite	qtz. monzo-diorite	monzo-granite	monzo-granite

Abbreviations: agn: augen gneiss; amx: amphibolite xenolith; hgn: hornblende gneiss; mx: mafic xenolith; ogn: orthogneiss; pgn: paragneiss. Rock type based on IUGS chemical classification (Streckeisen and Le Maitre, 1979). A/CNK = molar $Al_2O3/(CaO+Na_2O+K_2O)$.

(Moecher and others, 2004; Corrie and Kohn, 2007; Anderson and Moecher, 2009; Moecher and others, 2011).

Lithologies in the northern half of the Hazelwood quadrangle sampled for igneous and detrital zircon include the following:

(6) Metapsammite within the Copper Hill Fm. of the Great Smoky Group (H14-007), a quartzose and feldspathic muscovite-biotite paragneiss, massive to layered and weakly foliated with rare thin (~0.1 – 1.0 cm) leucosomes. The Copper Hill Formation correlates with lower-grade feldspathic arenites elsewhere in the Western Blue Ridge of the Great Smoky Mountains region.

(7) Variably migmatitic biotite + garnet paragneisses similar to (4) above (samples DEL14-001, H15-004).

(8) Migmatitic plagioclase + hornblende + biotite + garnet gneiss with mafic enclaves (H14-011).

The following map units were sampled in the Clyde quadrangle (Merschat and Cattanach, 2008):

(9) Variably migmatitic biotite-muscovite-feldspar-quartz paragneisses mapped as part of the Cartoogechaye terrane, inferred to be late Neoproterozoic to early Cambrian in age (CLY15-1 and -3, fig. 3).

(10) Layered gneiss mapped as part of the Grenville crystalline basement complex Sandymush Formation (Ysm, fig. 3) of the Mars Hill basement terrane and inferred to underlie the paragneisses in (8) (sample CLY16-1).

Two samples of non-migmatitic metagraywacke paragneiss of the Ashe Metamorphic Suite (AMS; Merschat and Cattanach, 2008) were also analyzed for detrital zircon (fig. 3) (E19-1, W19-1). The AMS is the most aerially extensive accreted Laurentian margin terrane. It is included here because of its volume and potential temporal relationship with the Ocoee supergroup as a Laurentian margin sediment package and with the other paragneisses of the study. A single sample of non-migmatitic felsic plagioclase + biotite + quartz + garnet + K-feldspar paragneiss from the Wayah Bald granulite complex was analyzed in order to assess along-strike provenance variability of potential accreted terranes (WB15-1).

METHODS

Whole-rock analysis of major, minor, and trace elements was conducted on a 4-kW Bruker S4 Pioneer wavelength dispersive X-ray fluorescence spectrometer at the Kentucky Geologic Survey. The majority of zircon U-Pb geochronology was conducted by laser ablation-inductively coupled plasma-mass spectrometry (LA-ICP-MS) at the University of Arizona. Additional zircon U-Pb ages were conducted at Curtin University using the sensitive high-resolution ion microprobe (SHRIMP IIB) and at the University of California-Los Angeles using the CAMECA ims1270 secondary ion mass spectrometer (SIMS). Whole rock Sm-Nd and Pb isotope analysis of feldspar was conducted at Syracuse University. Whole rock Pb isotope analysis was conducted at the University of Texas at Austin. Details of all analytical methods and data reduction are presented in the Appendix – METHODS. Results of XRF, Sm-Nd, and Pb isotope analysis are presented in tables 2, 3, and 4 respectively. Results of LA-ICP-MS U-Pb geochronology are presented in Supplemental Materials-Appendices 1 (orthogneisses and xenoliths) and 2 (paragneisses), SHRIMP IIB analyses are presented in Appendix 3, and SIMS analyses in Appendix 4, http://earth.geology.yale.edu/%7eajs/SupplementaryData/2020/Moecher.

Approaches for Addressing Zircon U-Pb discordance

Discordance in zircon U-Pb systematics is present in nearly all samples of this study. This is not surprising as all rocks experienced upper amphibolite facies, Taconian regional metamorphism and the generation of a melt phase (leucosomes) in

TABLE 3

Sm and Nd isotope data

Sample	Age (Ma)	2σ (Ma)	Nd (ppm)	Sm (ppm)	$^{147}Sm/^{144}Nd$	$^{143}Nd/^{144}Nd$	2σ	εNd(0)	$^{143}Nd/^{144}Nd(T)$	εNd(T)	T_{DM} (Ga)
DEL04-5	1145	70	20.9	3.64	0.1053	0.511859	6	-15.2	0.510939	0.4	1.66
DEL08-10a	1125	83	39.1	7.13	0.1103	0.511891	2	-14.6	0.511186	-2.1	1.69
DEL08-2d	na		42.5	8.40	0.1194	0.512106	3	-10.4	na	na	1.52
DEL08-6c	1227	45	32.1	5.43	0.1023	0.511846	3	-15.4	0.511054	-0.6	1.64
DEL08-7a	1292	65	26.0	3.26	0.0757	0.511606	3	-20.1	0.510970	-0.1	1.59
DEL10-7a	1381	6	53.7	9.68	0.1090	0.511809	6	-16.2	0.510821	-0.7	1.79
DEL10-11	1175	30	28.2	4.03	0.0864	0.511649	3	-19.3	0.511184	-3.4	1.67
DEL10-29	1175	11	8.3	1.14	0.1023	0.511872	13	-14.9	0.511121	-0.8	1.60
DEL10-7b	1331	8	9.2	0.98	0.0645	0.511552	3	-21.2	0.510919	1.3	1.52
DEL10-7c	1342	53	24.6	5.45	0.1337	0.512114	3	-10.2	0.510905	0.6	1.76
DEL10-7d	1342	53	30.3	6.30	0.1256	0.512118	2	-10.1	0.510905	2.1	1.60
DEL10-7e	1331	8	23.0	2.61	0.0686	0.511546	4	-21.3	0.510919	0.5	1.57
MP04-2	~1050		82.7	14.7	0.1072	0.512008	6	-12.3	0.511269	-0.3	1.48
FC08-2	1040	8	30.9	6.21	0.1214	0.512022	2	-12.0	0.511296	-2.0	1.68

Depleted mantle model ages (T_{DM}) and $\epsilon_{Nd}(T)$ values calculated using present day $^{143}Nd/^{144}Nd = 0.512638$ and $^{147}Sm/^{144}Nd = 0.1967$ for CHUR and depleted mantle evolution model of (DePaolo, 1981); na: not applicable to metasediment.

TABLE 4

Pb Isotope Compositions

Whole Rock	Rock Type	Age (Ma)	$^{206}Pb/^{204}Pb$	$^{207}Pb/^{204}Pb$	$^{208}Pb/^{204}Pb$
DEL08-7a	Felsic orthogneiss	1325	17.04	15.54	37.00
DEL10-7b	Felsic orthogneiss	1325	17.22	15.56	37.01
DEL08-7e	Felsic orthogneiss	1325	17.23	15.56	37.35
DEL08-6c	Felsic orthogneiss	1335	17.37	15.58	37.50
DEL08-7d	Mafic xenolith	1360	17.38	15.57	37.22
DEL08-7j	Felsic orthogneiss	1330	17.40	15.58	37.41
DEL10-7c	Felsic orthogneiss	1330	17.60	15.58	37.61
ASH 08-9	Paragneiss	1050	18.14	15.68	39.53
CLY 19-1	Paragneiss	1050	18.19	15.63	39.87
DEL-03-1	Paragneiss	1050	18.43	15.71	40.78
Feldspar	**Rock Type**	**Age (Ma)**	$^{206}Pb/^{204}Pb$	$^{207}Pb/^{204}Pb$	$^{208}Pb/^{204}Pb$
DEL10-7e	Felsic orthogneiss	1330	16.94	15.46	36.71
DEL04-5	Felsic orthogneiss	1315	16.98	15.48	36.86
FC08-02	Augen orthogneiss	1150	17.05	15.51	36.71
DEL10-7d	Mafic xenolith	1350	17.11	15.47	37.07
MP04-2	Granite	1040	17.26	15.50	36.96
DEL10-11	Felsic Orthogneiss	1160	17.34	15.56	37.85
DEL10-7a-1	Mafic xenolith	1360	17.34	15.43	36.89
DEL10-7a-2			17.40	15.41	36.88
DEL10-30-1	Augen orthogneiss	1160	17.64	15.54	38.16
DEL10-30-2			17.64	15.54	38.18
DEL10-2a-1	Paragneiss	600*	17.68	15.54	37.08
DEL10-2a-2			17.70	15.52	37.08
DEL10-30	Augen orthogneiss	1150	17.73	15.50	38.04
DEL10-29	Augen orthogneiss	1150	17.74	15.57	37.21

*: depositional age.

paragneisses. The oldest plutonic rocks (*ca.* 1.35 Ga) and detrital zircon in paragneisses must have also experienced high-grade Grenville (Elzevirian, Shawinigan and/or Ottawan-Rigolet) metamorphism. Discordance in Mesoproterozoic metaplutonic rocks in this study is typically manifested as arrays of analyses that may be approximately linear and projecting to an upper intercept, or concordant within error and spread 100 to 300 m.y. down concordia with the oldest ages forming a cluster of nearly concordant analyses. These patterns of discordance are similar to that observed elsewhere for zircon U-Pb analyses in metaigneous rocks with protracted high-grade post-magmatic histories (Mezger and Krogstad, 1997; Halpin and others, 2012; Spencer and others, 2016). For the present study we calculate weighted mean $^{207}Pb/^{206}Pb$ and Concordia Ages for the oldest cluster of concordant analyses (usually 98–102% concordant).

Discordance of U-Pb data in detrital zircon from paragneiss of this study is common, ranging up to 60 percent. The number of ages that are more than 5 percent discordant (our preferred cutoff for inclusion in age histograms) ranges up to 50 percent of analyzed grains. In most samples of paragneiss with a high proportion of discordant analyses, the discordant array defines a linear trend on a concordia diagram with a lower intercept and distinct population of ages at *ca.* 460 Ma (figs. 5A-5C and supplemental Tera-Wasserberg plots). Interpretation of discordance in detrital zircon data sets is complex and compounds the many uncertainties known to plague the

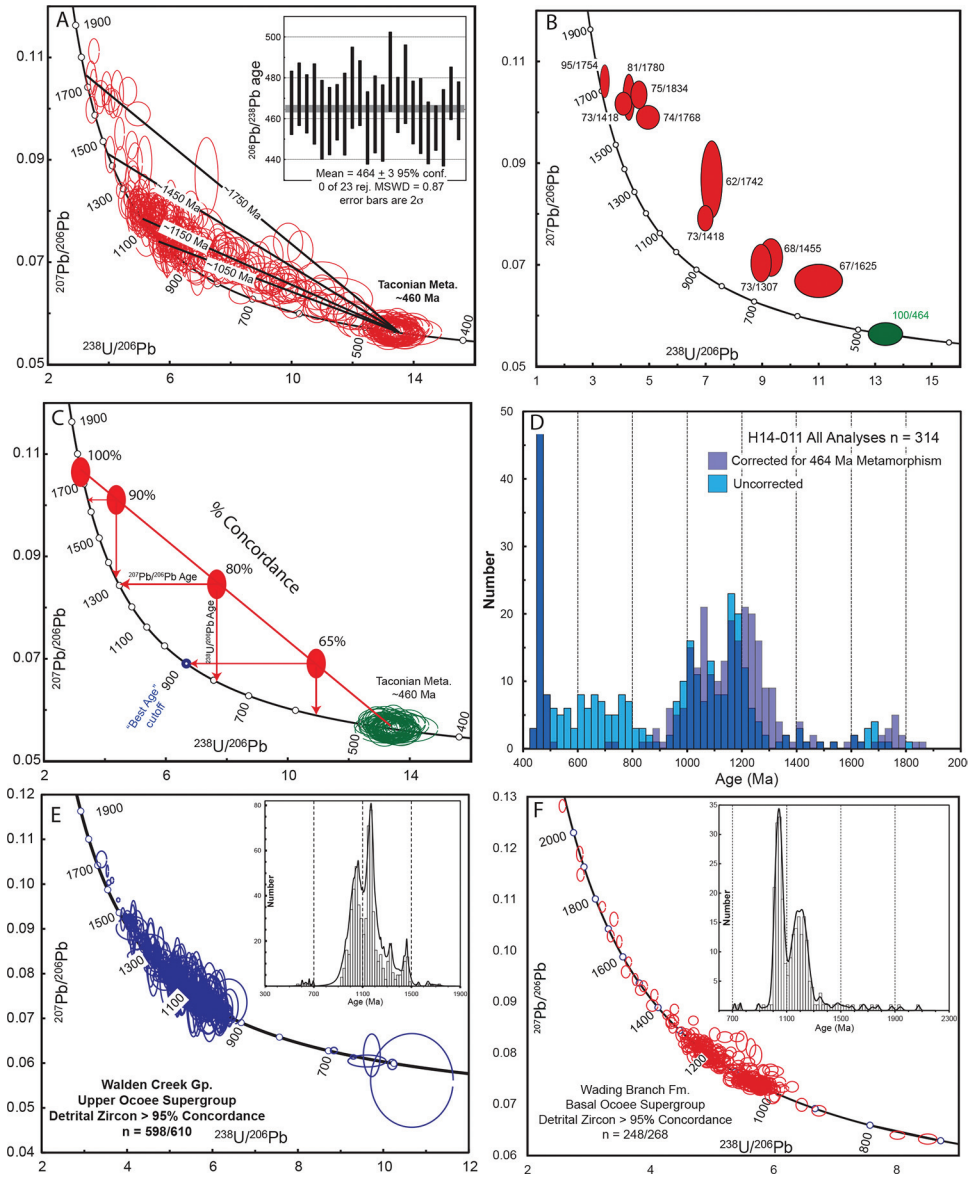

Fig. 5. Tera-Wasserburg concordia plots illustrating effects of disturbance of detrital zircon U-Pb systematics in high-grade, migmatitic paragneisses exemplified by sample H14-011. (A) Lines schematically illustrating trends of discordant arrays for various initial ages of zircon grains with U-Pb systematics disturbed by high grade Taconian metamorphism (*ca.* 460 Ma). Inset shows weighted mean age of metamorphic zircons. (B) Representative zircon U-Pb analyses with percent discordance and age when extrapolated back to concordia. (C) Schematic diagram illustrating the effect of selection of detrital zircon "best age" for use in plotting on an age histogram. (D) Histogram showing detrital zircon ages using analyses that are uncorrected versus corrected for disturbance of the U-Pb system during Taconian high-grade metamorphism (only Precambrian ages were corrected). The primary outcome of correction is to eliminate abundant apparent (erroneous) Neoproterozoic "best" ages. (E and F) Detrital zircon analyses from the basal (Wading Branch Fm.) and upper (Walden Creek Group) Ocoee Supergroup that experienced only greenschist-facies Taconian metamorphism and no disturbance of the U-Pb system reflected in the high proportion of analyses that are < 5% discordant (data from Chakraborty and others, 2012, and Moecher and others, 2019).

interpretation of zircon U-Pb ages (Mezger and Krogstad, 1997). One approach for addressing discordance in detrital samples is to apply a subjective discordance filter whereby analyses that are more than 30 percent (for example, Fosdick and others, 2014), 20 percent (for example, Peck and others, 2019), 15 percent (Carter and others, 2006) or 5 percent (Spencer and others, 2015, and used here) are excluded from the age histogram (Nemchin and Cawood, 2005; Spencer and others, 2016). However, discordant analyses may contain important age and provenance information. For example, if the age of a major lead loss event is known from independent evidence, discordant ages can be corrected back to concordia (Mezger and Krogstad, 1997), increasing the number of geologically meaningful ages. Also, analyses of older zircons (for example, 1 Ga) that are as little as 5 percent discordant may still be tens of millions of years younger than their true age, and if of sufficient number, be misinterpreted as a detrital age population, shift populations to erroneously lower apparent ages, and affect maximum depositional ages (fig. 5D). Discordance filters may not be a problem for large datasets ($n = 300$), in which a statistically meaningful number of ages remain after rejection, or for young detrital zircons (Phanerozoic) where the $^{206}Pb/^{238}U$ age is accepted as relatively accurate. However, for samples with $n < 150$ (typical of our earliest analyses and older detrital zircon populations observed here), discordance will result in age spectra that lack a sufficient number of ages to define a geologically meaningful age population.

Even with a discordance filter, discordant ages require criteria for plotting one of the three U-Pb ages – the so called "best" or "preferred" age (Gehrels and others, 2008; Spencer and others, 2016). Commonly the $^{206}Pb/^{238}U$ age is the "best age" for analyses less than 900 Ma, and the $^{207}Pb/^{206}Pb$ age for analyses older than 900 Ma (fig. 5C). Because the former age can be significantly younger than the $^{207}Pb/^{206}Pb$ age, the "best" or "preferred" age may also be geologically misleading or even erroneous. Figure 5 illustrates the nature of the problem in using, filtering, and correcting discordant detrital zircon U-Pb analyses for one of the paragneisses of this study. Evidence will be presented that high-grade Taconian regional metamorphism occurred throughout the study area at 460 ± 10 Ma, consistent with previous geochronology in the region (Miller and others, 1998; Moecher and others, 2004, 2011; Corrie and Kohn, 2007). By calculating a two-point chord, discordant ages were projected through the discordant analysis back to concordia using 460 ± 10 Ma as a lower intercept (figs. 5A-5B). The calculated upper intercept usually has a large error but the age spectrum of corrected ages eliminates erroneous ages (those in the *ca.* 900–600 Ma age range) and confirms the presence of older ages (*ca.* 1700–1900 Ma) that support a relatively old crustal component documented further below (figs. 5A and 5D). For comparison, figures 5E and 5F show Tera-Wasserburg plots for detrital zircons from two metaclastic units of the Ocoee Supergroup in the Great Smoky Mountains region that did not experience high-grade metamorphism and disturbance of the U-Pb system during Taconian regional orogenesis (92 and 93% of analyses $< 5\%$ discordant).

Finally, even grains yielding dates less than ± 5 percent discordant may not be geologically meaningful. Post-analysis CL imaging revealed that in some cases the laser spot overlapped two zircon growth zones. These 'mixed' ages tend to be slightly more discordant (3–5%) and yield slightly younger dates for a magmatic age mode defined by grains with the spot entirely in the magmatic zone of a grain. Thus even grains with a discordance filter of 5 percent may not be appropriate to include in the detrital zircon histogram. Post-analysis CL imaging of dozens of grains in the highest-grade, most migmatitic paragneisses reveals the nature and scale of the problem and is discussed further in the RESULTS section.

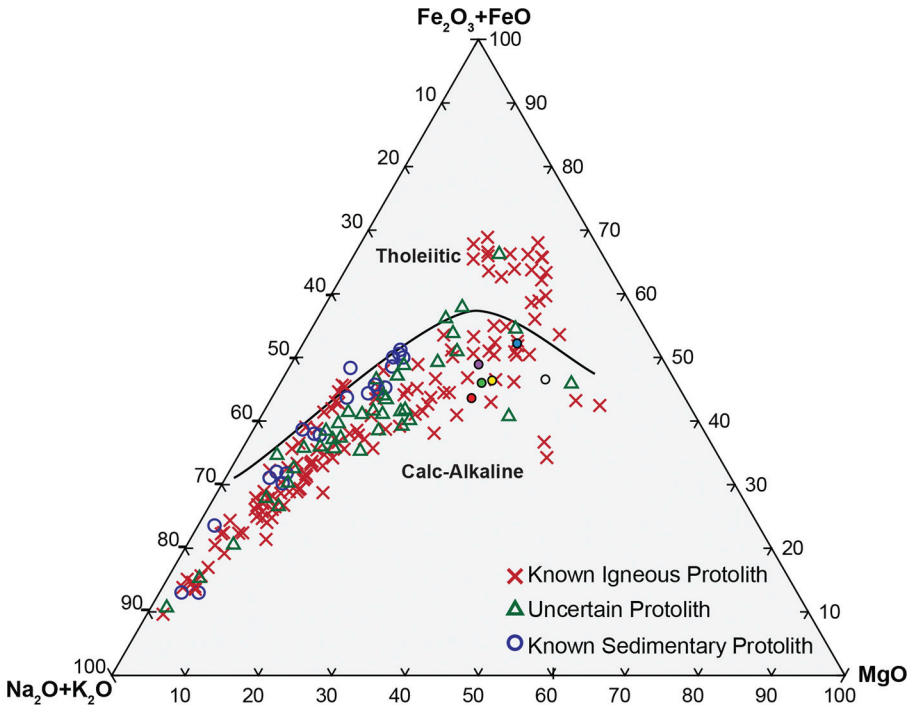

Fig. 6. AFM diagram illustrating range of whole rock geochemistry of crystalline bedrock units of the Dellwood, Hazelwood and Clyde quadrangles. Samples that plot in tholeiitic field are metamafic rocks (primarily amphibolites). Lithologies with likely sedimentary protoliths (for example, units from the Ocoee Supergroup: Chakraborty, ms, 2010; Chakraborty and others, 2012) have bulk compositions consistent with little chemical weathering and derivation from local basement sources, which is also consistent with detrital zircon U-Pb provenance analysis (Chakbraborty and others, 2012; Moecher and others, 2019).

RESULTS

Whole-Rock Geochemistry

Protoliths of many of the gneisses in the study area are often challenging to infer from gross lithologic characteristics due to the high metamorphic grade, extent of migmatitzation, and complex deformation. Early mapping (Hadley and Goldsmith, 1963) interpreted the oldest basement complex map units to be metastratified volcanic and sedimentary rocks (paragneisses) based primarily on their layered appearance. The same interpretation was made by the USGS in a more recent map compilation (Southworth and others, 2012). Although those and the present studies recognized the porphyritic granitic orthogneiss units (fig. 4H), neither previous study described the xenolith-bearing tonalitic to granodioritic orthogneiss documented here (figs. 4A-4E) nor presented whole rock geochemistry for purported paragneisses. An initial distinction was made for samples that are demonstrably meta-igneous (augen orthogneisses and amphibolites) or metasedimentary (metapsammites and metapelites) (table 2). On an AFM ternary diagram, mafic rocks (amphibolites, including mafic xenoliths and enclaves) cluster in the tholeitic field, whereas granitic igneous lithologies including the felsic orthogneiss are arrayed along a calc-alkaline trend (fig. 6). Their bulk major element compositions are mostly granodiorite, tonalite, and granite (table 2). Metasedimentary lithologies also plot along the calc-alkaline trend (fig. 6). We do not assign petrogenetic significance to this array as the rocks defining it range in age from *ca.* 1.35

TABLE 5

Summary of zircon U-Pb ages for meta-igneous rocks

Sample	Lithology	Concordia Age[1]	Weighted Mean Age	Interpretation
DEL04-5	Foliated granodioritic orthogneiss	1311 ± 6 1041 ± 4	1315 ± 8 1044 ± 8	Protolith crystallization age Metamorphic age
DEL08-6c	Foliated, folded granodioritic orthogneiss	1334 ± 8	1343 ± 11	Protolith crystallization age
DEL08-7a	Granodioritic orthogneiss	1324 ± 6	1324 ± 7	Protolith crystallization age
DEL08-7e	Granodioritic orthogneiss	1324 ± 7	1327 ± 10	Protolith crystallization age
DEL08-7j	Foliated tonalitic orthogneiss	1326 ± 11	1335 ± 15	Protolith crystallization age; *ca.* 1870 Ma inheritance
DEL10-7a	Mafic xenolith	1365 ± 10	1362 ± 11	Crystallization age
DEL10-7b	Granodioritic orthogneiss	1336 ± 9	1337 ± 13	Crystallization age
DEL10-7d	Mafic xenolith	1337 ± 16	1339 ± 27	Protolith crystallization age; *ca.* 1775 Ma inheritance
DEL10-11	Granitic orthogneiss	--	1160 ± 15 1038 ± 20	Crystallization age Metamorphic age
DEL10-30	Porphyritic granitic orthogneiss	1164 ± 8	1160 ± 10	Crystallization age
DEL14-020	Porphyritic granitic orthogneiss	1147 ± 17	1146 ± 15	Crystallization age
SG18-1	Granodioritic orthogneiss	1357 ± 6	1352 ± 8	Crystallization age
SG18-2	Mafic enclave in orthogneiss	--	1043 ± 8	Metamorphic age; *ca.* 1150 xenocrystic magmatic cores ~= intrusion age

[1]: All ages are $^{207/206}$Pb ages, errors are 2σ; Concordia and mean ages calculated from selected analyses (see text).

to 0.6 Ga. Many of the migmatitic biotite-plagioclase paragneisses lacking a definitive protolith overlap the trend, consistent with either igneous and/or immature clastic sediment protolith derived from weathering of the rocks defining the calc-alkaline trend, tend to have higher A/CNK values (1.2–1.4) compared to meta-igneous rocks (0.8–1.1) (table 2). Further inferences regarding igneous versus sedimentary protolith for the migmatitic biotite gneisses are based on zircon morphology, zircon zoning characteristics, U-Pb age distributions, and comparison with lower grade temporal equivalents of the paragneisses (Ocoee Supergroup) that have an obvious sedimentary origin, as discussed below.

Geochronology: Meta-Igneous Rocks

Results of zircon U-Pb geochronology for various map units of the Great Smoky Mountains basement complex will be summarized below from oldest to youngest (demonstrably) meta-igneous rocks (also compiled in table 5). All ages use ^{207}Pb/^{206}Pb ages cited at the 2σ level. We analyzed grains from the 50 to 125 micron and 125 to 250 micron size fractions.

Felsic orthogneiss – unfoliated.—The following samples are the same map unit, sampled from scattered exposures of the least deformed felsic orthogneiss at the type locality in the Dellwood quadrangle (figs. 4A-4E) or at the Sams Gap quadrangle. In all samples, three zircon growth zones/generations are apparent in CL images. The bulk of each grain is concentrically oscillatory-zoned (generation 1), overgrown first by a

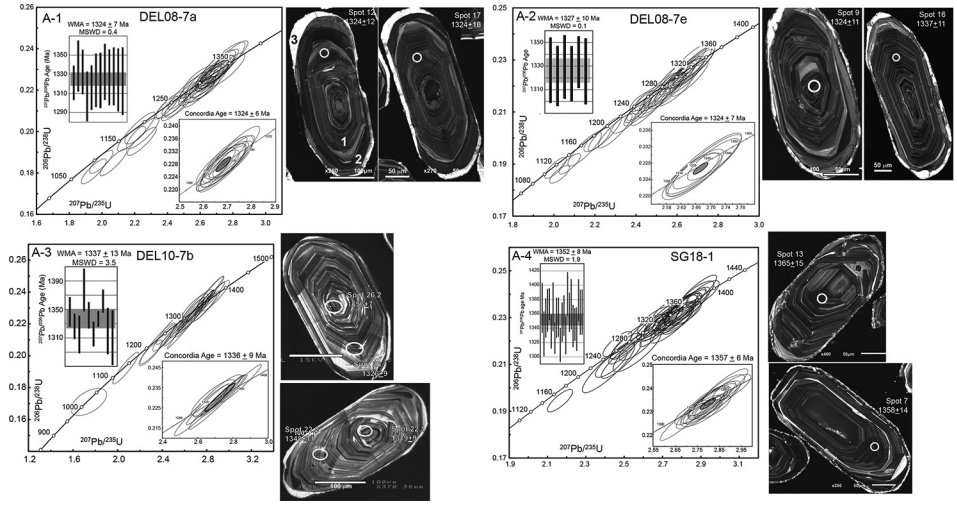

Fig. 7. (A): Wetherill U-Pb zircon concordia, weighted mean age plots, and representative zircon CL images (to right of each plot) for samples of least deformed felsic orthogneiss from Dellwood and Sams Gap quadrangles. (B) Same as in A for deformed (foliated, folded) orthogneiss samples. Error bars, error ellipses, and cited ages are all at 2σ level of precision. White circle is location of laser spot (20 microns in diameter) for each analysis and number is the date and 2σ error in Ma.

darker relatively thick intermediate zone (generation 2), which is, in turn, overgrown by thin bright rims (generation 3) (fig. 7A). Oscillatory-zoned sectors represent the bulk of the zircon growth in these samples and were targeted for U-Pb analysis via LA-ICP-MS or the SHRIMP II (DEL10-7b only). The other zones were too thin for targeting with confidence without overlapping growth generations.

DEL08-7a: A cluster of the oldest least discordant analyses yields a Concordia Age of 1324 ± 6 Ma (n = 12) and a weighted mean age of 1324 ± 7 Ma (fig. 7A-1).

DEL08-7e: A cluster of the oldest least discordant analyses yields a Concordia Age of 1324 ± 7 Ma (n = 6) and a weighted mean age of 1327 ± 10 Ma (fig. 7A-2).

DEL10-7b: A cluster of the oldest, least discordant ages defines a Concordia Age of 1336 ± 9 Ma (n = 10) and a weighted mean age of 1337 ± 13 Ma (fig. 7A-3).

SG18-1: A cluster of the oldest, least disconcordant ages defines a Concordia Age of 1357 ± 6 Ma (n = 23) and a weighted mean age of 1352 ± 8 Ma (fig. 7A-4). The pattern of discordance is consistent with SHRIMP analyses for samples from the same locality by Berquist (ms, 2005) (upper intercept = 1375 ± 63 Ma, weighted mean of oldest least discordant analyses = 1343 ± 13 Ma).

Felsic orthogneiss – foliated/folded.— Zircon grains in the deformed felsic orthogneiss exhibit euhedral, oscillatory-zoned cores, overgrowths of varying thickness, and bright rims, similar to generations 1–3 in undeformed felsic orthogneiss. All samples exhibit a generation of zircon filling trans-granular fractures (for example, fig. 7D). The overgrowths were of sufficient thickness for analysis in only one sample. In all cases analyses spread along Concordia similar to felsic orthogneisses interpreted to be the protolith of the deformed samples.

DEL08-6c: The oldest least discordant dates yield a Concordia age of 1334 ± 8 Ma (n = 8) and a weighted mean age of 1344 ± 8 (fig. 7B-1).

DEL04-5: Zircon grains exhibit thick (60–100 μm) light gray sector-zoned overgrowths on generation 1 zircon cores (fig. 7B-2). Two populations of ages are distinguished. A cluster of the oldest least discordant analyses yields a Concordia Age of 1311 ± 6 Ma (n = 18) and weighted mean age of 1315 ± 8 Ma. The second

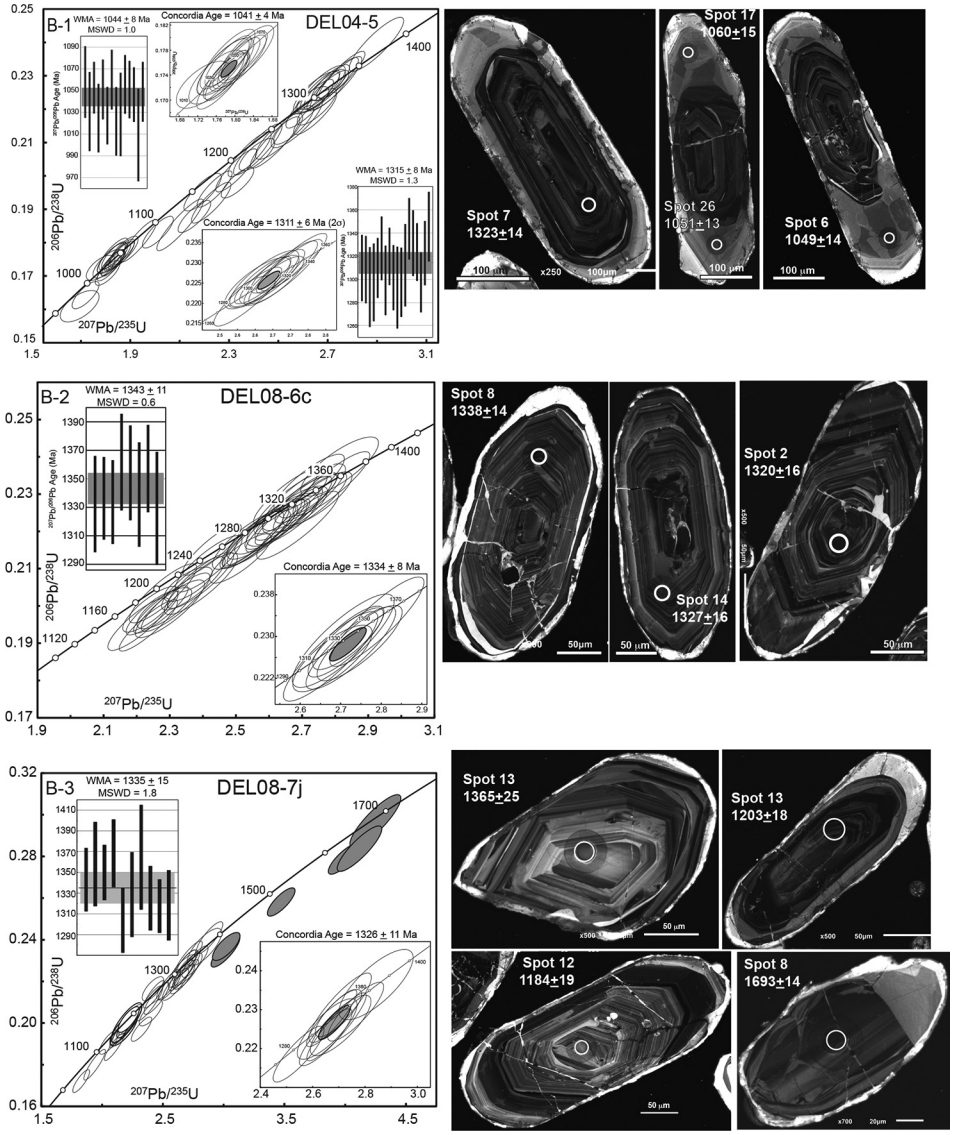

Fig. 7. Continued

population of ages obtained from the thick overgrowths yields a Concordia Age of 1041 ± 4 Ma (n = 14) and weighted mean age 1044 ± 8 Ma.

DEL08-7j: Two discordant arrays are apparent (fig. 7B-3). One array is similar to the relatively undeformed felsic orthogneisses above in spreading along concordia. The oldest cluster of least discordant ages yields a Concordia Age of 1326 ± 11 Ma (n = 10) and a weighted mean age of 1335 ± 15 Ma. A second array of discordant analyses (gray error ellipses) ranges from *ca.* 1400 to 1700 Ma and is interpreted to be related to inheritance of an older zircon component.

Mafic xenoliths and enclaves.—The DEL10-7 samples below are from mafic xenoliths entrained within the lithology respresented by samples DEL08-7a and DEL10-7b

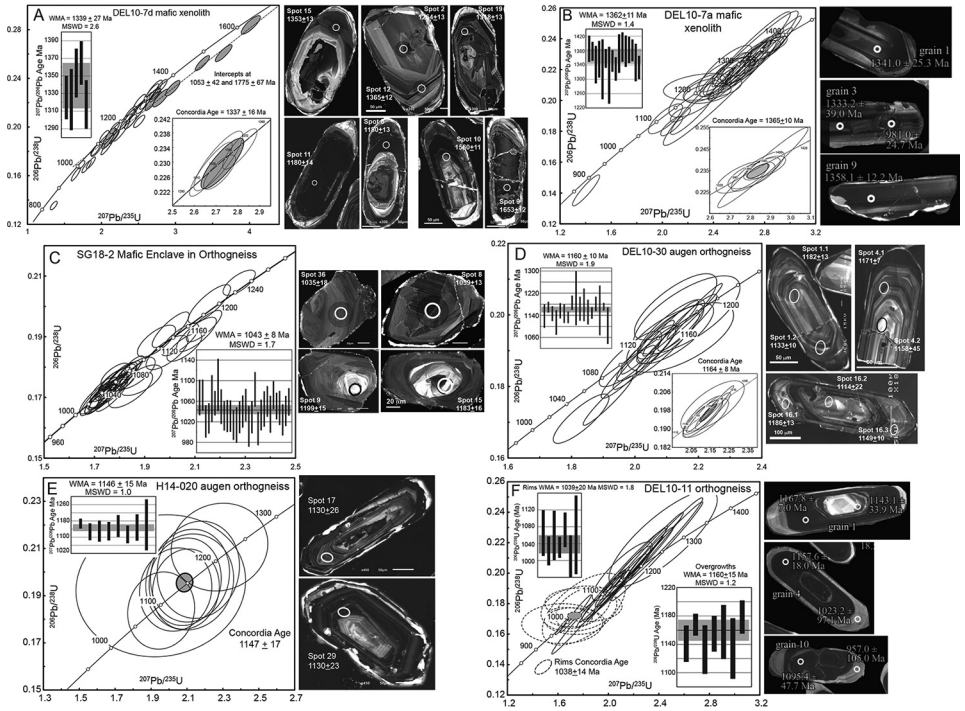

Fig. 8. Wetherill U-Pb zircon concordia, weighted mean ages, and representative zircon CL images for mafic xenoliths in felsic orthogneiss from the type locality (A, B); mafic enclave in orthogneiss from Sams Gap quadrangle (C); granitic orthogneisses mapped as Grenville in age (Southworth and others, 2012) or exhibiting textural evidence of having a granitic protolith (D, E); and orthogneiss mapped as hornblende-biotite gneiss but found to have a Grenville age (F). A, B, C and F are LA-ICP-MS analyses, D is a SHRIMP II analysis, and E is a SIMS analysis. CL images of dated zircons from xenolith sample DEL10-7a and DEL10-11 are from Quinn (ms, 2012).

above. The SG18-2 sample is from a mafic enclave in felsic orthogneiss sample SG18-1 above (fig. 4C).

DEL10-7d: Zircon grains are highly variable in terms of zoning pattern, brightness, and shape with trans-granular fractures filled with a bright generation of zircon (fig. 8A). Analyses define two apparent discordant arrays similar to sample DEL08-7j above. The oldest cluster of analyses yields a Concordia Age of 1337 ± 16 Ma (n = 5) and a weighted mean of 1339 ± 27. Older analyses (shown as gray error ellipses) are for oscillatory-zoned zircon cores (ages of ~1400–1700 Ma) and likely are due to inheritance of xenocrystic zircon. Younger analyses are for thick, dark, sector-zoned overgrowths and are consistent with metamorphic age of approximately 1.0 Ga.

DEL10-7a: Zircon grains for this sample were analyzed on the Nu multicollector by LA-ICPMS in 2012. Zircons are blocky (2:1 to 3:1) with the bulk of the zircon being dark oscillatory zoned centers and thin bright rims (fig. 8B). A cluster of the oldest least discordant dates from the oscillatory zoned centers yields a Concordia Age of 1365 ± 10 Ma (n = 16) and weighted mean age of 1362 ± 11 Ma a (fig. 8B).

SG18-2: Zircon consists of two generations: bright oscillatory zoned cores and dark sector-zoned to banded/layered overgrowths (fig. 8C). Analyses from the dark sector-zoned generation define a concordant cluster with a weighted mean age of 1043 ± 8 Ma (n = 30). This age is interpreted as a metamorphic age based on the style of CL zoning. The bright cores yield variably discordant older ages of 1100 to 1250 Ma

that do not define a coherent population and are interpreted to be relict magmatic grains with variably disturbed U-Pb systematics (fig. 8C).

Augen and protomylonitic orthogneisses.—**DEL10-30:** Large prismatic zircon grains are oscillatory-zoned with thin bright rims (Fig. 5.3 in Quinn, ms, 2012). SHRIMP II analyses for a cluster of the least discordant oldest analyses yield a Concordia Age of 1164 ± 8 Ma (n = 7) and weighted mean age of 1160 ± 10 Ma (n = 17) (fig. 8D).

H14-020: Zircon grains are equant to prismatic with rare xenocrystic cores and thick oscillatory-zoned rinds interpreted to represent the bulk of magmatic zircon growth (fig. 8E). All SIMS analyses (n = 9) yield a Concoria Age of 1147 ± 17 Ma and a weighted mean age of 1146 ± 14 Ma (fig. 8E).

DEL10-11: Zircons exhibit two CL zones: dark oscillatory zoned elongate overgrowths on xenocrysts or antecrysts of varying complexity, overgrown in turn by thin, light CL rims of variable thickness (fig. 8F). Both zones were analyzed via the Nu multicollector LA-ICP-MS. The dark inner zone yield a weighted mean age of 1160 ± 15 Ma for a cluster of least discordant analyses (n = 7), interpreted as a magmatic age. A Concoridia Age could not be calculated due to the spread of ages. The bright outer zone yielded Concordia and weighted mean ages of 1038 ± 14 Ma and 1039 ± 20, respectively (fig. 8F), interpreted as a metamorphic age.

Miscellaneous orthogneisses.—These samples typify the migmatitic hornblende-biotite orthogneisses originally mapped as the same unit as the felsic orthogneiss (Hadley and Goldsmith, 1963) (fig. 4D) and dated via SIMS as part of an early reconnaissance study (Loughry, ms, 2010). There is an insufficient number of analyses to calculate precise dates. Analyses tend to spread along concordia similar to the orthogneiss samples described above (Appendix fig. A8). Based on the oldest cluster of ages, three samples are consistent with a Shawinigan magmatic crystallization age (*ca.* 1150 Ma: DEL09-16b, -17d, -19a), similar to the augen and protomylonitic orthogneisses above (fig. 8). One sample is consistent with a *ca.* 1300–1350 Ma magmatic crystallization age, similar to the *ca.* 1.32 to 1.35 felsic orthogneisses (fig. 7).

Meta-igneous rocks – summary.—Analyses of oscillatory-zoned, euhedral zircon crystals in multiple samples of granodioritic to tonalitic orthogneiss in the Dellwood quadrangle of the Great Smoky Mountains basement complex yield arrays of analyses consistent with magmatic crystallization ages for the orthogneiss protolith of 1.34 to 1.31 Ga (table 5). Zircon from amphibolite enclaves in orthogneiss interpreted to have been mafic xenoliths yields ages consistent with crystallization of the amphibolite protolith being slightly older than its magmatic host (1.36–1.34 Ga: table 5). Another orthogneiss sample along strike to the northeast of the Great Smoky Mountains basement complex but within the Western Blue Ridge extends the time span of the magmatic event that generated the granodioritic orthogneiss protolith to *ca.* 1.35 Ga. Ages for a mafic enclave in the latter orthogneiss are consistent with its origin as a dismembered mafic dike that intruded at *ca.* 1.15 Ga and metamorphosed at 1.04 Ga (table 5).

One tonalitic orthogneiss (DEL08-7j) and one mafic xenolith (DEL10-7d) exhibit evidence of an inherited crustal component in the form of zircons with ages of 1.4 to 1.7 Ga (figs. 7B-3 and 8A, respectively). The deformed orthogneiss is interpreted, based on field evidence (fig. 4A-4 and -5), to be a lithologic-tectonic mixture of granodioritic orthogneiss host and mafic xenolith. The older inherited zircons in the tonalitic orthogneiss are therefore interpreted to be introduced via the mafic xenolith component of this mixed lithology.

The tectonomagmatic event that generated the granodioritic to tonalitic protoliths of 1.36 to 1.31 Ga orthogneiss in the study area is tentatively correlated with earliest magmatism of the Grenville orogenic cycle (the *ca.* 1400–1300 Ma "Dysart-Mount Holly" event of McLelland and others, 2013), referred to here simply as

"pre-Elzevirian", the significance of which is discussed below. A second major magmatic event is indicated by augen and migmatitic orthogneisses with ages of 1.15 to 1.13 Ga. This magmatic event is correlated with the widespread Shawinigan orogeny recognized throughout the Grenville orogen in Canada, the Adirondacks, and Appalachian basement inliers. Evidence of metamorphism, including *ca.* 1040 Ma overgrowths on magmatic zircon, correlates with the Ottawan phase of the Grenville Orogeny. Previous geochronology on crystalline rocks of the Great Smoky Mountains basement complex supports the Shawinigan and Ottawan igneous and metamorphic ages determined here (Southworth and others, 2012). Notabley absent from the new geochronology are meta-igneous rocks with ages of 1.3 to 1.2 Ga (Elzevirian phase of the Grenville orogenic cycle: McLelland and others, 2013), although there is evidence for its presence within the detrital zircon record, discussed below.

Geochronology: Metasedimentary Rocks

Paragneiss samples were treated as metasedimentary with application of the "large n" approach to detrital zircon provenance analysis (dating of ~300 zircon grains: Pullen and others, 2014). Approximate centers of grains were targeted for laser ablation analysis without consideration for texture or paragenesis (magmatic vs. metamorphic) because of the large number of grains. However, all samples were re-imaged via CL after dating for location of the laser spot relative to zircon growth zones. Those images were critical to accurate interpretation of zircon age distributions in paragneisses.

Two groups of variably migmatitic paragneiss are distinguished based on depositional age inferred from the youngest detrital zircon population and oldest metamorphic zircon grains, the relative fraction of zircon comprising each age mode, and the patterns of zircon growth textures observed in CL. Paragneisses with a pre-Ottawan depositional age exhibit (1) a high proportion of metamorphic zircon that is 980 to 1080 Ma; (2) youngest magmatic detrital zircon ages of early Shawinigan age; (3) zircon age spectra with multiple age modes in the range 1300 to 1900 Ma with zircon grains comprising these modes consisting of detrital magmatic cores with metamorphic overgrowths. In contrast, paragneisses with post-Ottawan depositional ages are characterized by (1) the youngest detrital magmatic grains being 800 to 550 Ma; (2) their age spectra exhibit the complete record of Grenville orogenic phases, being dominated by the Ottawan-Shawinigan doublet; and (3) Paleoproterozoic grains are rare.

In the discussion to follow, dominant zircon age modes in the range 900 to 1400 Ma are discussed in the context of tectonic phases of the "Grenville Cycle" (McLelland and others, 1996) as illustrated in figure 2. For zircon age modes in the range 1500 to 1900 we use the "Geon" terminology of Rivers (1997) in order to not imply a provenance from a specific Laurentian crustal age province.

Pre-Ottawan migmatitic paragneisses.—**DEL03-1**: This lithology consists of leucosome in greater proportion than host gneiss. Only 63 percent of the measured dates are less than 5 percent discordant with no clear pattern of discordance (Appendix fig. A9). Dominant age modes occur at *ca.* 996, 1045, and 1341 Ma, corresponding to Rigolet, Ottawan, and pre-Elzevirian phases (fig. 9A). Other older ages suggest 1.7 to 1.9 Ga provenance. Zircon grains defining the *ca.* 996 and 1045 Ma age modes are uniformly subequant, dark to medium gray in CL, and exhibit "fir tree" sector zoning or tapered layer zoning (fig. 9). These grains and the dark generation of zircon are interpreted as having a metamorphic paragenesis based on similar zircon textures documented in high-grade paragneisses elsewhere (Vavra and others, 1996, 1999; Kunz and others, 2018). Zircon grains older than 1.1 Ga are generally equant, subrounded, and consist of bright, anhedral, oscillatory-zoned (magmatic) cores with dark overgrowths of variable thickness similar in zoning characteristics to the *ca.* 1.0 Ga generation of

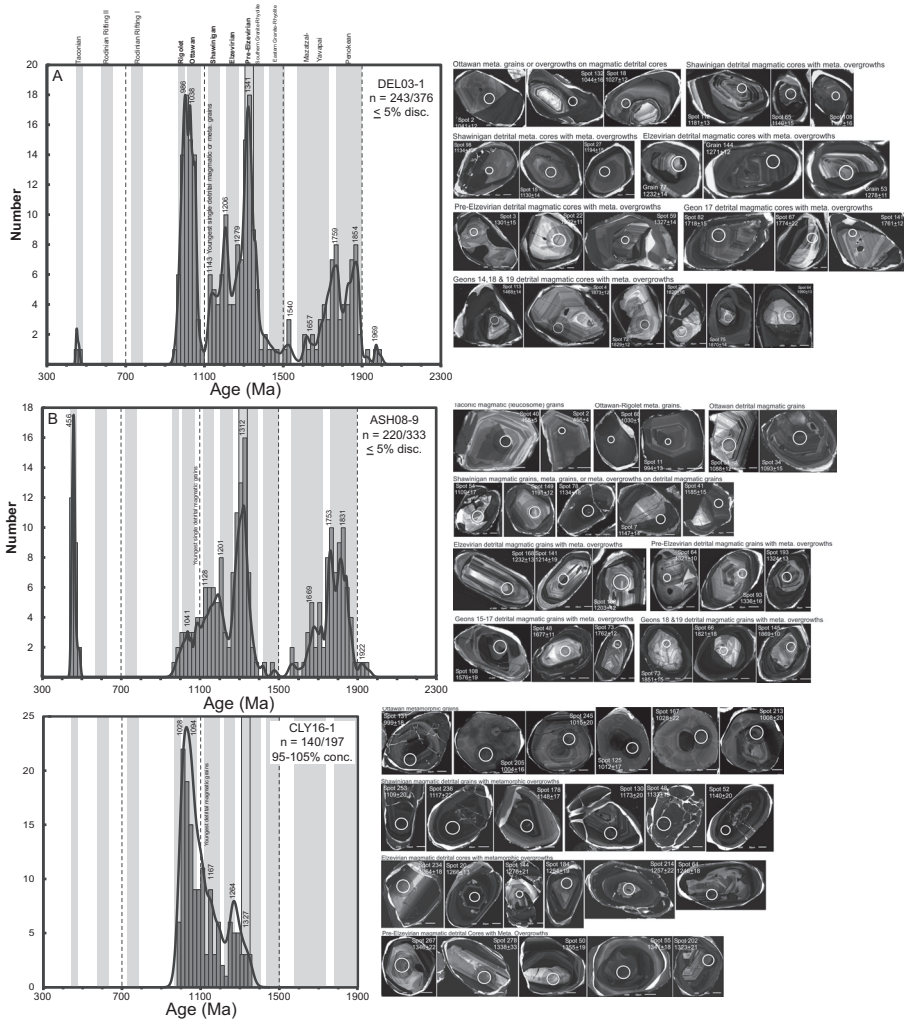

Fig. 9. Zircon U-Pb age histograms for pre-Ottawan migmatitic paragneisses from Dellwood (A) and Clyde quadrangles (B, C). Also shown are representative CL images of zircon textures for grains comprising the dominant age modes. White circle on each zircon grain is 20 microns in diameter.

metamorphic grains (fig. 9). These grains are interpreted as detrital magmatic grains that experienced metamorphism at *ca.* 1.0 Ga. This sample thus has a sedimentary protolith containing detrital zircon of primarily Paleoproterozoic and Mesoproterozoic age that experienced Ottawan high grade metamorphism. The *ca.* 1.0 Ga metamorphic ages and the youngest detrital magmatic zircon ages of *ca.* 1.14 Ga bracket the depositional age of the protolith. The high proportion of grains that are > 5 percent discordant may be explained by Ottawan high-grade metamorphism that affected U-Pb systematics. The lesser effects of regional Taconian metamorphism on zircon U-Pb systematics are reflected in the minor zircon growth at *ca.* 450 Ma (fig. 9).

ASH08-9: This sample also contains leucosome in greater volume than host gneiss. 66 percent of analyses are less than 5 percent discordant. The dominant age modes are 1830–1750, 1310, 1200–1040, and 450 Ma (fig. 9B). Grains with dates in the range

1200 to 2000 Ma consist of anhedral, embayed, oscillatory zoned fragments with sector-zoned to banded overgrowths (fig. 9). These grains are interpreted to consist of detrital magmatic grains that experienced high grade metamorphism, which produced the overgrowths . Although fewer in number than in DEL03-1, the *ca.* 990 to 1030 Ma ages are from grains that are equant, rounded, dark in CL, sector-zoned or layered; also, this age group includees some dark overgrowths on magmatic cores. The dark generation of zircon is interpreted to have formed during high-grade late-Ottawan to Rigolet metamorphism. The oldest metamorphic grains (*ca.* 1200 Ma) and the youngest detrital magmatic grains (1080 Ma) bracket the depositional age of the protolith. The *ca.* 450 Ma age grains are oscillatory-zoned, consistent with magmatic growth in leucosome melt during Taconian metamorphism. The pattern of discordance (Appendix fig. A9) suggests disturbance of the U-Pb system by *ca.* 460 Ma metamorphism as illustrated in figure 2.

CLY16-1: This is a two-mica paragneiss with a relatively low volume of leucosome compared to the two samples above. 89 percent of the zircons are less than 5 percent discordant (Appendix fig. A9). A dominant age mode skewed to younger ages is resolvable into 1028 and 1094 Ma components, with minor resolvable modes at 1167, 1264, and 1327 Ma (fig. 9C). The majority of zircon grains in this sample are equant to elliptical, rounded, relatively dark in CL, and have a core-overgrowth morphology with the overgrowth commonly exhibiting sector-zoning or tapered banding (fig. 9C). These grains are interpreted to represent zircon growth during high-grade Ottawan or Rigolet phase metamorphism. Many grains appear fractured and healed with a distinct generation of zircon filling fractures (fig. 9C). Grains associated with the three oldest age modes consist of oscillatory- zoned cores with dark, sector-zoned to banded overgrowths (fig. 9C), consistent with detrital magmatic grains that experienced Rigolet-Ottawan metamorphism. Ages greater than 1400 Ma are absent from this sample, in contrast to the previous two samples. The youngest detrital magmatic grains are *ca.* 1120 Ma and the oldest metamorphic grains are *ca.* 1060 Ma.

Post-Ottawan Paragneiss: Dellwood quadrangle.—**DEL08-2e:** This migmatitic paragneiss is shown in fig. 4I. The sample processed for zircon concentration was selected for having a low proportion of leucosome. 86 percent of the analyses are less than 5 percent discordant (Appendix fig. A10-A) without the distinct pattern of discordance illustrated by sample H14-011 (fig. 5). The age distribution consists of two dominant modes centered at 1033 and 1147 Ma, with the latter having a resolvable shoulder at 1215 Ma, and a fourth minor age mode at 1323 Ma (fig. 10A). There are scattered dates between 1400 and 2000 Ma and between 700 and 900 Ma, with three grains at ~450 Ma.

Zircon grains from this sample (fig. 10) typify the textural characteristics of zircon in other post-Ottawan paragneisses, but share characteristics with the pre-Ottawan paragneisses. Detrital zircon grains comprising the Rigolet-Ottawan age mode exhibit CL zoning consistent with either a metamorphic or magmatic origin. Their presence constrains the maximum depositional age of the paragneiss protolith to be post-Rigolet (~1000 Ma). Grains comprising the Shawinigan, Elzevirian, and pre-Elzevirian modes consist of detrital magmatic cores with metamorphic overgrowths. Many grains of all ages and types have thin (~10 mm) bright rims. Although not correlated via mapping with late Neoproterozoic to early Cambrian clastic rocks of the Great Smoky Mountains region, the age spectrum of paragneiss sample DEL08-2e is similar in most respects to the lower (Wading Branch Fm.) and upper (Walden Creek Group) Ocoee Supergroup (fig. 10A), the former occurring noncomformably on Grenville basement and the latter stratigraphically underlying the basal Cambrian Chilhowee Group. The youngest magmatic detrital zircons in all these samples (550–750 Ma), U-Pb SHRIMP dating of diagenetic xenotime overgrowths on detrital zircon in Ocoee metasediments

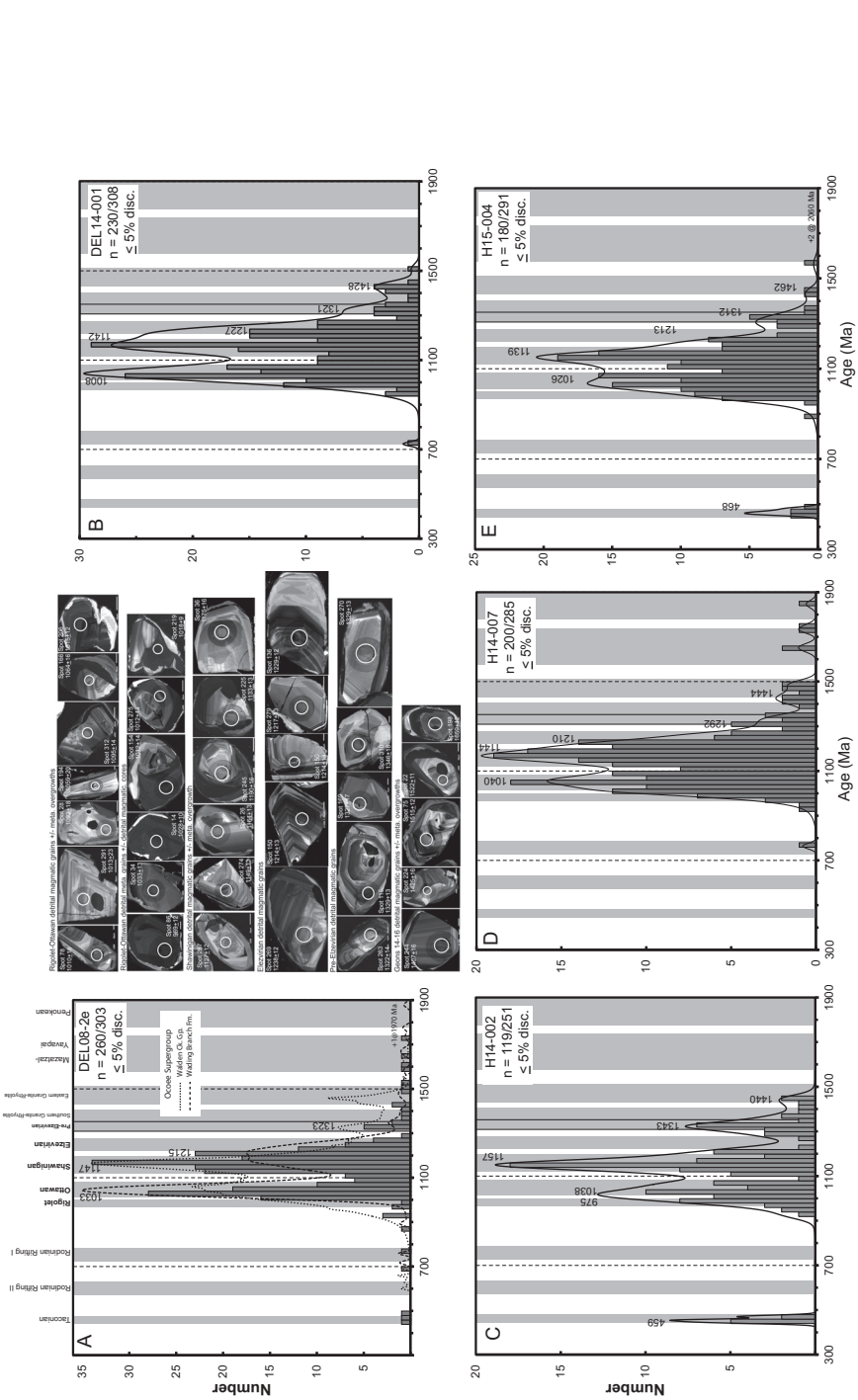

Fig. 10. Detrital zircon U-Pb age histograms for post-Ottawan paragneisses and metapsammites from Dellwood and Hazelwood quadrangles. Included in A for comparison are probability density distributions for detrital zircon from clastic units of the Ocoee Supergroup from the Great Smoky Mountains region (basal Ocoee: Wading Branch Fm.; uppermost Ocoee: Walden Creek Gp.) (Chakraborty and others, 2012; Moecher and others, 2019). Also shown are representative CL images of zircons comprising the major age modes for sample DEL08-2e, which are typical of zircon textures for post-Ottawan paragneiss samples. White circles are 20 μm laser spot with spot number and date. Figure 5 discusses post-Ottawan paragneiss sample H14-011 also from Hazelwood quadrangle.

(Aleinikoff and others, 2010), and the overlying Lower Cambrian strata constrain the depositional age of the Ocoee units to latest Neoproterozoic. The similarity of the paragneiss age spectrum and Ocoee units permits a tentative temporal correlation that is explored further below with evidence from additional paragneiss samples.

Post-Ottawan Paragneisses: Hazelwood quadrangle.—These samples occur farther south and at slightly higher grade than the Dellwod quadrangle sample above. All samples contain a high proportion of grains that are greater than 5 percent discordant with the array of discordant analyses defining a trend toward *ca.* 450 Ma (Appendix fig. A10).

DEL14-001: leucosome-poor Bt-Ms paragneiss similar to DEL08-2e above and is correlated based on mapping (Larkin, ms 2016) to be the same map unit. 75 percent of the ages are less than 5 percent discordant (Appendix fig. A10). Five resolvable age modes occur at 1008, 1142, 1227, 1321, and 1428 Ma (fig. 10B).

H14-011: migmatitic gneiss containing enclaves of mafic garnet amphibolite and a high proportion of leucosome (~30%), discussed above in the context of age discordance. The discordance-corrected spectrum (fig. 5D) exhibits a major peak at *ca.* 460, a range of ages from 1000 to 1250 Ma, and a small cluster of ages in the range 1700 to 1900 Ma. A weighted mean age for grains defining the youngest age mode is 465 ± 3 Ma (n = 56, MSWD = 1.5) (fig. 5D). This age agrees with previous studies that determined the peak of Taconian regional metamorphism in the study area (Central Blue Ridge/Cartoogechaye terrane) was at 460 ± 5 Ma (Moecher and others, 2004; Corrie and Kohn, 2007; Anderson and Moecher, 2009; Moecher and others, 2011).

H14-002: quartz- and feldspar-rich, mica-poor, leucosome-poor metapsammite of the Otto Formation. Only 47 percent of the analyses are less than ±5 percent discordant. Resolvable age modes occur at 1350, 1160, 1000, and 460 Ma (fig. 10C).

H14-007: quartz- and feldspar-rich, mica-poor metapsammite within the mostly metapelitic Copperhill Formation. 70 percent of the analyses are less than ±5 percent discordant. Most ages are in the range of 1300 to 1000 Ma, plus a few older ages between 1600 and 1800 Ma (fig. 10D).

H15-004: migmatitic, thinly banded, biotite gneiss with *ca.* 1 cm., regularly spaced leucosomes. 62 percent of the analyses are discordant and define arrays between *ca.* 450 and 1000 to 1400 Ma (Appendix fig. A10). Most ages are between 1300 and 1000 Ma. (fig. 10E).

Post-Ottawan Paragneisses - Clyde Quadrangle.—Representative detrital zircon textures are shown in figure 11. Most zircons are oscillatory-zoned in CL, consistent with an ultimate magmatic paragenesis, but with dark or light metamorphic overgrowths of variable thickness (fig. 11). All samples contain a scattering of ages younger than 900 Ma.

CLY15-1: This quartz- plagioclase-muscovite-biotite-garnet paragneiss contains the lowest volume of leucosome and the highest proportion of nearly concordant zircons (90%) among the Clyde quadrangle paragneiss samples (Appendix fig. A11). Two dominant age modes occur at *ca.* 1150 and 1050 Ma , with scattered dates in the ranges 600 to 700 and 1400 to 1900 (fig. 11A). The age distribution is identical to the biotite paragneiss sample DEL08-2e from Dellwood quadrangle (above).

CLY15-3: leucosome-poor biotite-muscovite gneiss. 74 percent of dated grains are less than 5 percent discordant with resolvable age modes at 1011, 1060, 1162, 1227, and 1317 Ma, and scattered ages younger than 950 Ma or in the range 1400 to 1900 Ma (fig. 11B).

CLY15-4: 83 percent of dated grains are less than 5 percent discordant, and yield modes at *ca.* 1000 and 1150 Ma. No Paleoproterozoic or Archean grains were found (fig. 11C).

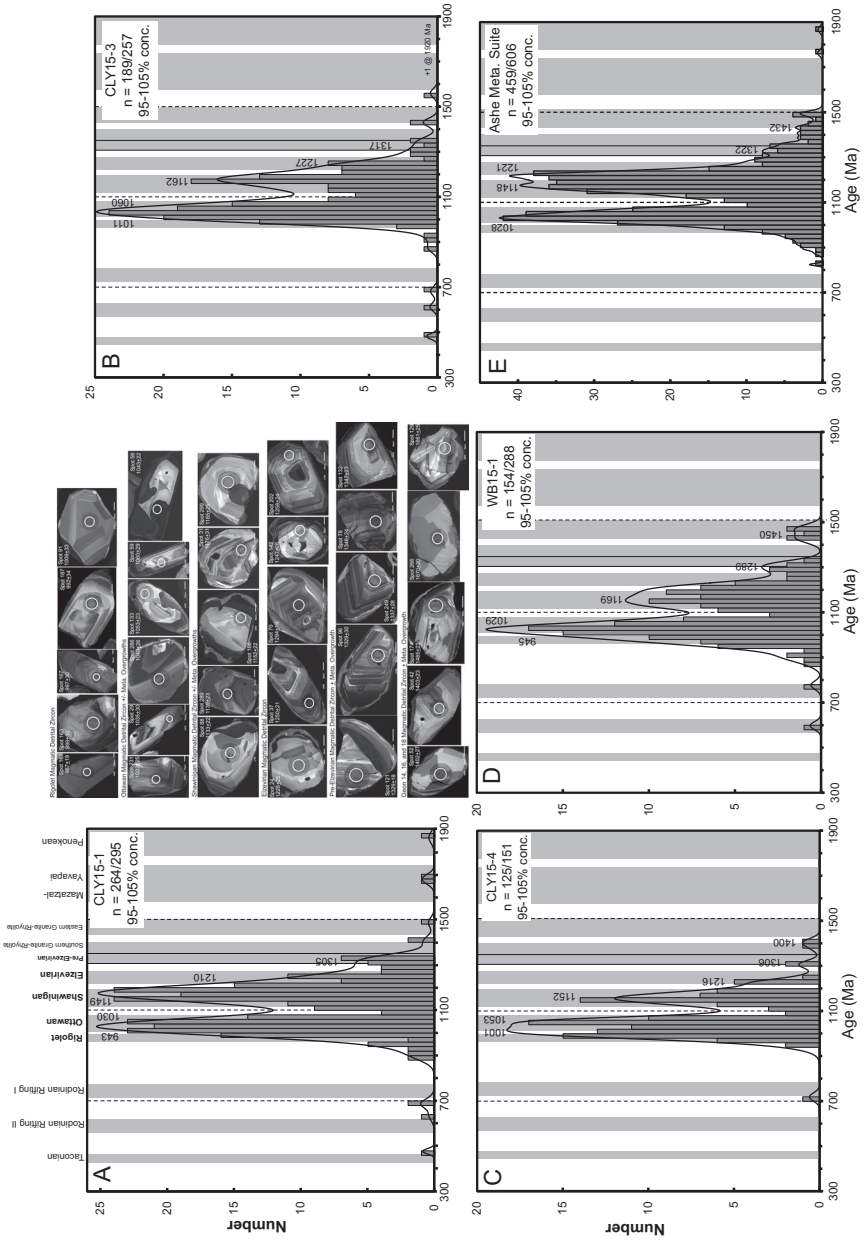

Fig. 11. Detrital zircon U-Pb geochronology for paragneisses from the Clyde quadrangle (A-C), the Trimont Ridge complex of the Cartoogechaye terrane (Hatcher and others, 2004) in the Wayah Bald quadrangle (D), and a composite of two samples of the Ashe Metamorphic suite (E). CL images next to A are representative grains for the dominant age modes with spot number, date, and location of 20 μm laser spot (white circle).

Post-Ottawan Paragneisses: Wayah Bald quadrangle (Trimont Ridge Complex).—**WB15-1:** This is a mica-poor garnet-bearing quartzo-feldspathic gneiss located within the area of the Taconian granulite facies zone (Eckert and others, 1989). 54 percent of dated grains are less than 5 percent discordant, and yield major age modes at approximately 1030 and 1200 Ma with minor modes at 1290 and 1450 and no Paleoproterozoic or Archean grains (fig. 11D).

Ashe Suite metagraywacke: Enka and Weaverville quadrangles.—**E19-1, W19-1**: These mica-poor quartzofeldspathic gneisses interpreted as metagraywacke (Merschat and Cattanach, 2008) lack leucosomes entirely. A composite age spectrum for both samples is shown in figure 11E. 76 percent of the grains are less than 5 percent discordant with the majority of the discordant analyses being consistent with disturbance of Shawinigan and Ottawan-age grains during Taconian metamorphism (Appendix fig. A11). The age spectrum exhibits three resolvable age modes at 1030, 1150, and 1220 Ma, minor modes at 1320 and 1450 Ma, plus two grains at *ca.* 1800 Ma (fig. 11E). Neoproterozoic, Paleoproterozoic and Archean grains are absent.

Metasedimentary rocks: interpretation.—The paragneisses were provisionally interpreted as having a sedimentary protolith based on mineralogy (quartz-rich; muscovite-, sillimanite-, or garnet-bearing), high A/CNK values (table 2), and lack of relict primary magmatic textures that would be consistent with a plutonic origin. The strongest supporting evidence for this interpretation is the presence in most samples of multiple zircon age modes spanning *ca.* 550 to 2300 Ma (table 6), the close match of detrital zircon age spectra with lower grade metaclastic units in the study area (fig. 10A), and the diversity of CL zoning patterns and rounded morphologies among zircons. It is unlikely that a single plutonic or volcanic protolith would exhibit multiple zircon age modes defined by oscillatory-zoned (magmatic) zircon grains exhibiting a variety of growth zoning characteristics.

The *ca.* 450 Ma age mode (Taconian metamorphism) is also present to varying degrees in the majority of samples (table 6) but varies in amplitude. Its presence is consistent with previous work (Moecher and others, 2004; Corrie and Kohn, 2007; Anderson and Moecher, 2009; Moecher and others, 2011) that documents the peak of Paleozoic regional metamorphism in this area of the southern Blue Ridge was Middle Ordovician (Taconian) in age. The tectonic implication of these ages is that all map units were assembled before the Taconian. Although the Taconian metamorphic overprint had profound influence on the appearance of the rocks, obscuring primary lithologic features and their zircon systematics, these ages have no implications for provenance other than bracketing the younger end of the depositional age range and will not be discussed further.

Two groups of paragneiss were distinguished based on zircon ages and textures. Post- Ottawan clastic sequences exhibit the complete range of Grenville age modes in approximate relative proportion to crystallization ages of Grenville magmatic and metamorphic rocks in the Adirondacks and Appalachian basement massifs defined by SHRIMP U-Pb ages (fig. 2; table 5). Neoproterozoic ages between *ca.* 800 and 550 Ma are present and although not defining a specific age mode they broadly correlate with the two periods of post-Rodinian rift magmatism recognized from the magmatic and detrital record along the southeastern Laurentian margin (Aleinikoff and others, 1995; Cawood and others, 2001; Thomas and others, 2004). These ages also constrain the maximum depositional age of post-Ottawan sediments to be late Neoproterozoic. Samples within this group also have in common a resolvable Granite-Rhyolite province age mode (1400–1500 Ma) and scattered ages of 1600 to 2300 Ma. Post-Ottawan paragneisses have detrital zircon age distributions similar to greenschist-facies Ocoee Supergroup metaclastic rocks with late Neoproterozoic depositional ages (figs. 5 and 10), further supporting the sedimentary origin for the paragneisses deduced from

TABLE 6

Summary of Zircon U-Pb Age Modes[1] in Paragneisses

Sample	Taconian[2]	Neo-Proterozoic	Rigolet	Ottawan	Shawinigan	Elzevirian	Pre-Elzevirian	Granite Rhyolite	Geons 15-20
Post-Ottawan									
DEL08-2e	461	rare[3]	-	1033	1147	1215	1323	rare	rare
DEL14-001	-	-	-	1008	1142	1227	1321	1428	-
H14-002	459		975	1038	1157	rare	1343	1440	-
H14-007	-	rare	-	1040	1144	1210	1292	1444	rare
H14-011	464	rare	-	1020	1160	1229	1291	rare	10 grains 1600-1900
H15-004	468	-	-	1026	1139	1213	1312	1462	rare
CLY15-1	rare	rare	943	1030	1149	1210	1305	rare	rare
CLY15-3	rare	rare	1011	1060	1162	1227	1317	rare	-
CLY15-4	-	-	1001	1053	1152	1216	rare	rare	-
Ashe Composite	-	rare	-	1028	1148	1221	1322	1432	rare
WB15-1	rare	-	945	1029	1169	-	1289	1450	-
Pre-Ottawan									
DEL03-1	rare	-	996	1045	1143	1206, 1279	1341	1458	1540, 1657, 1759, 1854 1969
ASH08-9	456	-		1041	1128	1201	1312	rare	1669, 1753, 1831, 1922
CLY16-1	-	-	-	1028, 1094	1167	1264	1327	-	-

[1]: ages cited are most probable age of mode using "Unmix" routine of Isoplot v.4 (Ludwig, 2009).
[2]: mean age calculated if n ≥ 3 grains.
[3]: 1-5 grains with no resolvable age mode.

detrital zircon age modes and textures. The overall age patterns are generally consistent with an eastern Laurentian margin provenance, which supports the inferences of previous work on assembly of the crystalline southern Appalachians (for example, Hatcher, 1987).

The second group of paragneisses consists of two samples (DEL03-1, ASH08-9) that are distinguished from the post-Ottawan paragneisses in that: (1) they are dominated by detrital zircons of pre-Elzevirian and Paleoproterozoic age; (2) contain broadly Grenville zircons (1200–900 Ma) but not with the characteristic Ottawan-Shawinigan/Elzevrian 'doublet' of the post-Ottawan sediments; (3) exhibit a generation of metamorphic zircon of Ottawan-Rigolet age; (4) lack grains from the time interval 1400 to 1600 Ma; (5) lack Archean grains; and (6) lack Neoproterozoic-aged grains. A third sample that is distinctly different than the post-Ottawan sediments (CLY16-1) lacks the Paleoproterozoic ages but also contains a high proportion of Rigolet-Ottawan metamorphic zircon. The presence of the Rigolet-Ottawan generation of metamorphic zircon in these three samples requires their depositional age to be between *ca.* 1040 and 1106 Ma, the latter being the youngest definable magmatic age mode for ASH08-9. These units are thus pre-Ottawan in age but represent broadly syn-orogenic Grenville sediments with a provenance that would be interpreted from a Laurentian perspective as being dominated by eastern Laurentia (pre-Elzevirian) and central to northeastern Laurentia terranes (broadly Penokean-Yavapai-Mazatzal) and their extensions into the Grenville province in Canada (Penokean-Labradorian-Makkovikian). Early Paleoproterozoic and Archean-age grains are noticeably absent from all detrital samples of this study. The ultimate origin and tectonic implications of two distinctly different groups of metasedimentary rocks is discussed below.

Isotope Geochemistry

Nd isotopes.—All samples have negative values of $\epsilon_{Nd}(t)$ with Nd isotope evolution trends that intersect the depleted mantle curve (T_{DM}) at 1.6 to 1.8 Ma (fig. 12). The latter ages are 200 to 500 m.y. older than the crystallization age and argue for presence of an older (evolved) crustal age component in the source region, that is, the Dellwood rocks are not juvenile. The correspondence of T_{DM} ages with the oldest detrital zircon ages in paragneisses (1.5–1.9 Ga) supports the interpretation that the older age component is primarily metasedimentary (discussed below).

Pb isotopes.—Figure 13 compares whole rock and feldspar Pb isotope compositions for samples of this study with whole-rock Pb isotope compositions for basement gneisses from Laurentian (Granite-Rhyolite, Adirondacks, Ontario Grenville), Amazonia and various localities from the southern and central Appalachians. In general, Amazonian samples have higher values of $^{207}Pb/^{204}Pb$ for a given $^{206}Pb/^{204}Pb$ value than Laurentian samples (fig. 13A). The Laurentian and Amazonian whole rock values define distinct fields and trends, although there is considerable overlap at lower (less radiogenic) values of the isotope distributions. South-central Appalachian Grenville-age basement samples have $^{207}Pb/^{204}Pb$ and $^{206}Pb/^{204}Pb$ values that overlap the Amazonian trend (fig. 13A), supporting the hypothesis of an exotic (not native Laurentian) origin and terrane transfer following Amazonian collision with Laurentia during assembly of Rodinia (Carrigan and others, 2003; Loewy and others, 2003; Tohver and others, 2004; Fisher and others, 2010).

Whole rock Pb isotope compositions for three Dellwood pre-Ottawan paragneisses and seven 1.34 to 1.31 Ga felsic orthogneisses all fall above the Stacey and Kramers (1975) Pb evolution line, overlapping Amazonian and south central Appalachian basement values (fig. 13B). The most radiogenic samples are paragneisses. In contrast, feldspar Pb isotope compositions for a greater variety of Dellwood rocks straddle the terrestrial Pb isotope evolution trend (Stacey and Kramers, 1975) with most samples falling in the lower range of $^{207}Pb/^{204}Pb$ values of the Amazonian field. However, one

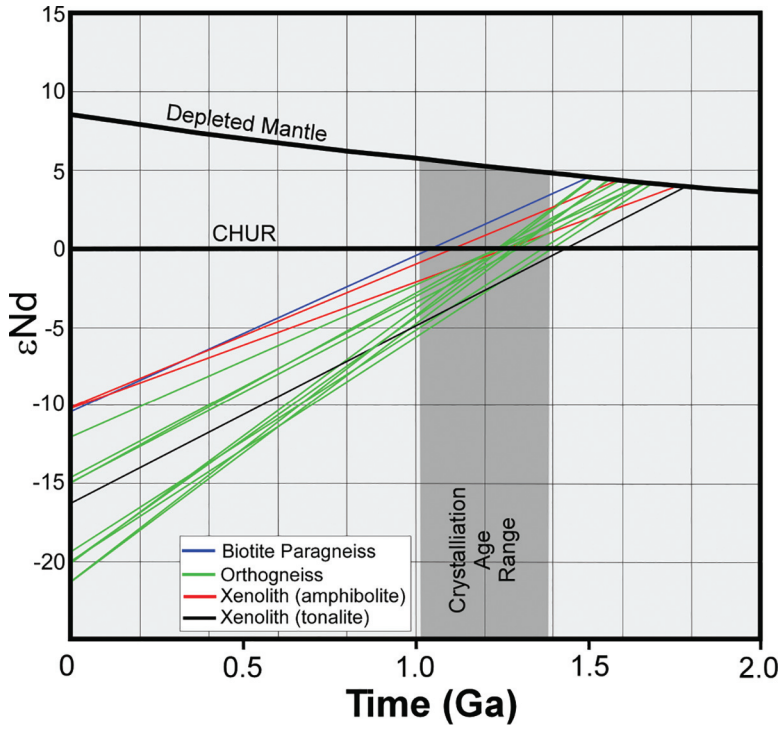

Fig. 12. Nd isotope evolution diagram for selected samples from the study area. T_{DM} ages are consistent with recycling of Paleoproterozoic crust as a source for crustal components in the eastern Great Smoky Mountains basement complex. Also see Fisher and others (2010) for a more regionally extensive dataset.

of the mafic enclaves falls well within the Laurentian field (fig. 13; DEL10-7a, dated at 1362 ± 11 Ma). The three other samples with lowest $^{207}Pb/^{204}Pb$ values for given $^{206}Pb/^{204}Pb$ values (more "Laurentian-like") are two *ca.* 1330 Ma felsic orthogneisses and the other mafic xenolith (DEL10-7d: 1339 ± 27 Ma). Shawinigan and Ottawan granitic/augen orthogneisses (DEL10-11, -29, -30, MP04-2, FC08-02) all have higher $^{207}Pb/^{204}Pb$ and fall within the Amazonia field, consistent with the range of values for other Western Blue Ridge Grenville granitoids, including a sample analyzed by Fisher and others (2010) from the same locality as the orthogneiss (sample SG18-1: 1352 ± 8 Ma) dated here. Replicates of paragneiss sample DEL08-2 are consistent with a provenance that is dominantly Laurentian even though it occurs intimately deformed within the Great Smoky Mountains basement complex (fig. 13).

TECTONIC IMPLICATIONS

Basement Age Components

Grenvillian-age basement inliers within the greater Appalachian orogen are recognized as sharing most of their tectonic history with rocks of the Grenville province in the Adirondacks and Canada, in which the Shawinigan (~1.15 Ga) and Ottawan (~1.05 Ga) orogenic phases generated the majority of magmatic and high-grade metamorphic rocks, respectively (Southworth and others, 2010; Rivers and others, 2012; McLelland and others, 2013: fig. 2). Elzevirian-age rocks (*ca.* 1.25–1.21 Ga) are present but volumetrically much less abundant in the Appalachians and Adirondacks than in the Canadian Grenville. The pre-Elzevirian event is also volumetri-

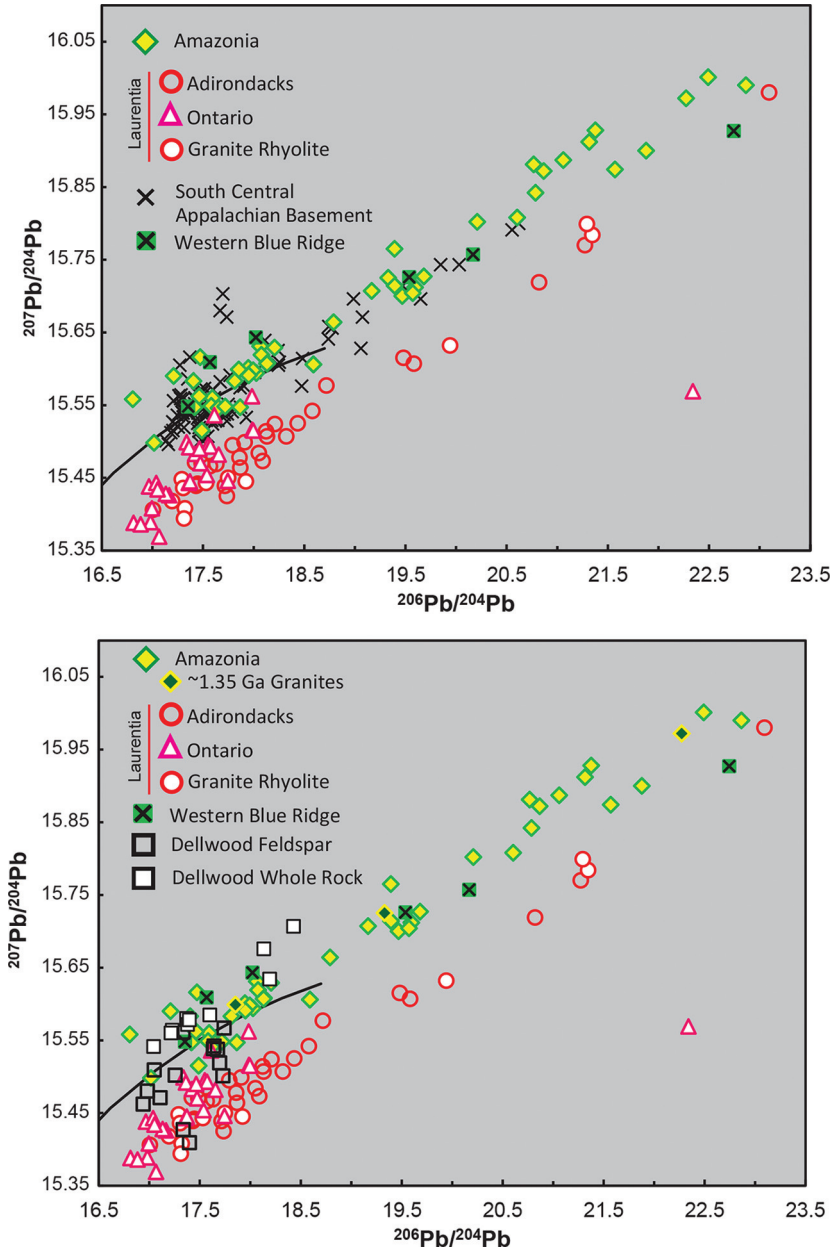

Fig. 13. (A) Pb isotope compositions from previous studies illustrating the distinction between Amazonian and Laurentian crust, along with values for south-central Appalachian basement samples that were used to infer an "exotic" Amazonian origin for Grenville-age crust. (B) Whole rock and feldspar Pb isotope compositions of Dellwood samples compared to Amazonian and Laurentian arrays. Samples labeled "~1.35 Ga granitoids" are from the Pensamiento Granite Complex of the Paraguá Terrane, southwestern Brazil (Tohver and others, 2004a, 2006), and are emphasized here due to their similarity in age and Pb isotope systematics to the granodioritic orthogneisses of this study. Western Blue Ridge granitoids with Amazonian Pb isotope compositions are highlighted in green for the same emphasis. See text for discussion. Data sources: Amazonia: Tohver and others (2004); Ontario: DeWolf and Mezger (1994); Adirondacks: Sinha and McLelland (1999); Eastern Granite Rhyolite and Mars Hill terrane: Fisher and others (2010); south-central Appalachian basement: Sinha and others (1996), Loewy and others (2003), Fisher and others (2010).

cally minor but is important to recognize as it is proposed to record the final phase of 1.5 to 1.3 Ga Laurentian margin continental magmatism before commencement of the Grenvillian orogenic cycle (Hanmer and others, 2000; McLelland and others, 2013). Fragments of 1.4 to 1.3 Ga pre-Elzevirian arc crust are interpreted to have rifted from the Laurentian margin at *ca.* 1.3 Ga forming back-arc basins that record Elzevirian sedimentation (deposition of the "Grenville Supergroup": McLelland and others, 2013) and subduction-related magmatism and metamorphism accompanying closure of the basins during Shawinigan convergence. The occurrence of pre-Elzevirian rocks in the most outboard extent of the Grenville province in eastern Laurentia (northern Appalachian basement massifs) is also interpreted in terms of the fragmented arc model (McLelland and others, 2013). Thus, the Grenville orogen mostly developed cratonward of pre-Elzevirian rocks currently exposed in the Green Mountains (Ratcliffe and others, 1991; Aleinikoff and others, 2011), Hudson Highlands (Ratcliffe and Aleinikoff, 2008), New Jersey Highlands (Volkert and others, 2010), northern French Broad massif (Tollo and others, 2010, 2017), and southern French Broad massif (this study).

The Great Smoky Mountains basement complex records Shawinigan magmatism and metamorphism, in support of the shared history summarized above (Southworth and others, 2010, 2012; Aleinikoff and others, 2012). Although none were dated for this study, Ottawan-age granites are present in the Western Blue Ridge of the Great Smoky Mountains region (Miller and others, 2000; Ownby and others, 2004) where the Max Patch granite is basement for the Ocoee Supergroup cover and is dated at 1040 Ma (K. Makovsky, pers. comm.). The only evidence for Elzevirian magmatism detected in this study is via detrital zircon analysis (discussed further below).

Most importantly the present study provides ample outcrop and geochronologic documentation that pre-Elzevirian crust is a significant component of the southeastern Laurentian margin. The pristine nature of some of the samples (fig. 4), wider occurrence of highly deformed temporal equivalents, and ubiquity of detrital zircons of corresponding age in metasedimentary sequences demonstrate that the pre-Elzevirian event is just as common in the southern Appalachians as it is in the northern Appalachians and Adirondacks. In support of the occurrence of pre-Elzevirian crust Tollo and others (2010, 2017) report the occurrence of a 1327 ± 7 Ma meta-igneous granofels and widespread 1.33 to 1.27 Ma inherited zircons in Shawinigan orthogneisses in the Mount Rogers area of the northeasternmost French Broad massif. Also, a significant number of detrital zircon grains of pre-Elzevirian age occur in paragneisses of the Mars Hill terrane (Aleinikoff and others, 2013), supporting the results presented here.

Although determination of precise magmatic crystallization ages for the felsic orthogneiss protolith and xenoliths is complicated by zircon U-Pb discordance, the concordia and weighted mean ages are consistent with a crystallization age of 1.34 to 1.31 Ga for the orthogneiss and 1.36 to 1.34 Ga for the xenoliths in the Great Smoky Mountains basement complex (table 5). The sample from the Western Blue Ridge basement exposed in the Blue Ridge Thrust Complex (SG18-1) exhibits concordia and weighted mean ages that are slightly older (1.35 Ma) than the Great Smoky Mountains basement complex samples, but consistent with being a component of the same pre-Elzivirian crustal age province. Magmatic crystallization ages for both occurrences of pre-Elzevirian orthogneiss protoliths fall within the range of ages obtained for other pre-Elzevirian rocks in Appalachian basement massifs discussed above, demonstrating a close temporal correlation.

Insights from Detrital Zircon Geochronology

Detrital zircon U-Pb geochronology provides a rich record of crustal evolution by defining magmatic events associated with formation of continental crust (for example,

Condie and Aster, 2010; Cawood and others, 2013; Roberts and Spencer, 2015; Spencer, 2020). A sufficiently large detrital zircon sample set (n = ~300 per sample, as in this study: Pullen and others, 2014) from thirteen locations permits (1) resolution of age distributions for volumetrically minor crustal components; (2) resolution of crustal components that are close in age or may be the only evidence for ultimate sediment source terranes that are long eroded or covered (as in the case of much of Laurentia after the Cambrian); and (3) identification of terranes involved in the magma-generating collisional orogenesis. The *ca.* 2000 detrital zircon U-Pb ages and their textures presented here provide the evidence for greater resolution of provenance and tectonics in eastern Laurentia while also revealing cryptic crustal age components.

Detrital zircon ages from post-Ottawan paragneisses emphasize the dominant role of the Ottawan and Shawinigan phases of the Grenville orogeny in the evolution of the southeastern Laurentian margin deduced from prior detrital zircon studies of Neoproterozoic to Phanerozoic clastic rocks in eastern Laurentia (Eriksson and others, 2003; Thomas and others, 2004; Becker and others, 2005; Chakraborty and others, 2012; Moecher and others, 2019). However, additional insights emerge from our dataset:

1. Although constituting a relatively small fraction of dated detrital zircon grains, the oldest Grenville age component in post-Ottawan paragneisses and Ocoee Supergroup sediments is the pre-Elzevirian mode (*ca.* 1300–1375 Ma). It is also present in metaclastic rocks of the Roan Mountain region (Aleinikoff and others, 2013). The ubiquity of this age mode demonstrates that pre-Elzevirian basement rocks were present in the source terrane of the paragneiss protoliths. The most probable ages calculated for each detrital sample (table 6) indicate the age of this event is 1340 to 1320 Ma, consistent with the interpretation of the crystallization ages for felsic orthogneiss based on the oldest least discordant cluster of U-Pb ages. The ubiquity of the age mode further implies that the orthogneiss protoliths were spatially more extensive than the relatively limited (quadrangle scale) region of this study or in the Mount Rogers area of the French Broad massif (Tollo and others, 2017).

2. The *ca.* 1100 to 1200 Ma Shawinigan age mode is resolvable in most samples into Shawinigan (most probable ages of 1170–1140 Ma) and Elzevirian (most probable ages of 1230–1210 Ma) modes (table 6). The latter age range overlaps the younger end of Elzevirian magmatism in the Adirondacks and Canada (Rivers and others, 2012; McLelland and others, 2013). There are four ages of 1250 to 1200 Ma from orthogneisses in the the Mars Hill terrane (Ownby and others, 2004). Detrital magmatic zircons of this age range are common in pre- and post-Ottawan paragneisses, supporting the presence of Elzevirian magmatic rocks in the south-central Appalachian basement. Also, a Rigolet age mode (940–1010 Ma) is resolvable in some samples and consists of metamorphic and magmatic zircon grains. Thus, the five major phases of the Grenville orogeny as defined in the type region (Ontario and Quebec: Rivers and others, 2012: fig. 2) are present in the post-Grenville-age sediments that were deposited in or on the Late Neoproterozoic, rifted Laurentian continental margin, or that were deposited on the transitional continental-oceanic margin of Laurentia that formed during post-Rodinian rifting.

3. Although the oldest magmatic rocks exposed in the French Broad Massif are *ca.* 1.37 to 1.31 Ma, the oldest crustal age component is represented by detrital zircons with ages of *ca.* 2.0 to 1.6 Ga that comprise a significant fraction of the detrital zircon ages in pre-Ottawan paragneisses and that appear as rare scattered ages in post-Ottawan paragneisses (CLY15-1, H14-011, H14-007; figs. 9–11). Inherited zircon grains of *ca.* 1.8 to 1.6 Ga are present in a sample of the felsic orthogneiss and a mafic xenolith. The older (2.0–1.6 Ga) ages are also present in detrital zircons from metasedimentary rocks of the Mars Hill terrane of the French Broad massif (Aleinikoff

and others, 2013) that were metamorphosed during the late Ottawan/Rigoletan phase. The depositional age of the sediment containing the oldest zircon modes was determined here to be *ca.* 1100 to 1000 Ma. This interval coincides with the period of collisional "tectonic quiescence" between the Ottawan and Shawinigan orogenies (Rainbird and others, 2017) and with the formation of the Midcontinent Rift System (fig. 2). These sediments could therefore correspond to a late Shawinigan to early Ottawan clastic wedge that was subsequently metamorphosed during Ottawan-Rigolet orogenesis, evidence for which is also present in metasedimentary rocks from the northeasternmost French Broad massif (Aleinikoff and others, 2013; Tollo and others, 2017).

4. The pre-Ottawan paragneisses record a distinctly different balance of source terranes than the Neoproterozoic sediments of this study and of most other Phanerozoic sediments in eastern Laurentia (for example, Thomas and others, 2017). The differences include: (a) domination by pre-Elzevirian and Paleoproterozoic sources with minor Elzevirian and Shawinigan contributions; (b) presence of Ottawan-Rigolet metamorphic zircon grains; (c) lack of Geons 14 and 15 and late Archean (2800–2600 Ma) grains. The pre-Ottawan paragneisses therefore do not correlate with the *ca.* 1.3 to 1.2 Ga Grenville Supergroup sediments of the Grenville province in Ontario-Quebec, the Adirondacks, and the New Jersey Highlands that were deposited in back-arc basins from *ca.* 1.3 to 1.2 G and metamorphosed during the Shawinigan orogeny (Peck and others, 2019). The pre-Ottawan paragneisses and Elzevirian Grenville Supergroup do have in common abundant 1.9 to 1.6 Ga detrital zircons and therefore could have contributions from similar sources. Paleoproterozoic terranes are major components of Laurentia and Amazonia cratonward of Grenvillian belts so that detrital zircon ages of 2.0 to 1.6 Ga do not yield unique constraints on provenance.

Tectonic Implications

A Greater Mars Hill Terrane?.—The exotic origin and crustal affinity of south-central Appalachian basement (SCAB), including the Mars Hill terrane, with Amazonia was initially defined based on Pb isotope systematics (Sinha and others, 1996; Tosdal, 1996; Sinha and McLelland, 1999). The exotic aspect of the Mars Hill terrane was further manifested as zircon U-Pb SIMS ages for the Carvers Gap granulite gneiss of the Mars Hill terrane that were as old as *ca.* 1.8 Ga and interpreted as the age of the magmatic protolith of the Carvers Gap gneiss (Carrigan and others, 2003). However, other bedrock units from the Mars Hill terrane (Cloudland gneiss) with similarly old zircon ages were interpreted as metasedimentary units (Carrigan and others, 2003). Recent higher precision zircon U-Pb analyses and more thorough CL imaging distinguished between diverse detrital magmatic zircon grains and younger metamorphic overgrowths on magmatic grains (Aleinikoff and others, 2013). This led to the spelling of the Carvers Gap granulite gneiss as metasedimentary in origin with its oldest detrital zircon ages being 2.0 to 1.6 Ga. Furthermore, metamorphic zircon and monazite in the gneisses demonstrated that the sediments were metamorphosed during the Ottawan and Rigolet phases (Aleinikoff and others, 2013).

The present study demonstrates that rocks exhibiting evidence of the old (*ca.* 2.0–1.6 Ga) age component initially demonstrated in the Mars Hill terrane are more widespread within the French Broad massif, being observed in pre-Ottawan metasedimentary units in the Great Smoky Mountains basement complex where 1.9 to 1.6 Ga detrital zircon ages are more abundant than Grenville-age (that is, Shawinigan and Ottawan) detrital zircon ages. Although there is evidence of zircon inheritance of *ca.* 1.8 to 1.7 Ga in two igneous samples in the Great Smoky Mountains basement complex (figs. 7 and 8), the greater abundance and wider distribution of 1.9 to 1.6 Ga detrital zircons in metasedimentary rocks suggests that the old crustal component was intro-

duced as detritus from Geons 19 through 16 erosion of 2.0 to 1.6 Ga crust of Amazonian provenance.

The old crustal component is also apparent from T_{DM} ages of 2.0 to 1.5 Ga in the Great Smoky Mountains basement complex magmatic rocks and throughout the French Broad massif that indicate the presence of an evolved crustal component in the source region for the French Broad massif magmatic rocks. This range in T_{DM} ages is identical to southwestern Amazonian rocks (Tohver and others, 2004; Santos and others, 2008), which stand in marked contrast to most native Laurentian rocks that uniformly exhibit juvenile Nd isotope systematics. The present study thus supports inferences that the Mars Hill terrane may be more widespread within the south central Appalachian basement (Ownby and others, 2004) and to the proposal here of a Mars Hill terrane that effectively encompasses the entire French Broad massif.

The correlation of metasediments from the Mars Hill terrane and Great Smoky Mountains basement complex is further supported by the presence in both of a significant fraction of 1.4 to 1.3 Ga detrital zircon grains (figs. 9B-9C; fig. 3 of Aleinikoff and others, 2013). Furthermore, the inherited zircon grains in the 1.35 Ga protoliths of the Great Smoky Mountains basement complex rocks implies they were derived from or passed through *ca.* 1.8 Ga crust. This composite pre-Elzevirian metasedimentary-igneous terrane was then exposed along with Elzevirian and Shawinigan rocks during post-Shawinigan exhumation to produce sediment that was incorporated into the Ottawan to Rigolet metamorphic infrastructure of the French Broad massif during the final phase of the Grenville orogeny.

Refined Laurentian-Amazonia connections.—The latest Mesoproterozoic to early Neoproterozoic chronologies of the Great Smoky Mountains basement complex and greater French Broad massif are essentially identical to the type-Grenville province in Canada, the Adirondacks, and northern Appalachian basement massifs in terms of major zircon-forming tectonic events (fig. 2, tables 2 and 3), supporting a shared tectonic history from *ca.* 1.35 to 0.9 Ga. However, the Pb isotope systematics require that basement in the southern Appalachians is ultimately of Amazonian crustal origin. Even before publication of the Pb isotope evidence, the available geochronology led to various scenarios for potential Laurentian-Amazonian paleogeographic connections during Grenville orogenesis and Rodinian assembly. Most of the scenarios had the southeast Laurentian margin colliding with the southwestern Amazonian margin defined by Grenville-age rocks of the Sunsás belt (for example, Hoffman, 1991; Dalziel, 1992; Sadowski and Bettencourt, 1996; Bettencourt and others, 1999). Any tectonic model that attempts to juxtapose Laurentia and Amazonia must, however, incorporate the new Pb isotope and U-Pb zircon geochronological constraints, and consider the paleomagnetic evidence that supports such a configuration.

As with comparisons between the type-Grenville province and French Broad massif, the southeastern Laurentian and southwestern Amazonian Grenville margins are grossly similar but different in sufficient detail (table 7) that proposed matches remain unconvincing or even untenable based solely on geochronology (for example, Amazonia located along western Laurentia at *ca.* 1.0 Ga: Santos and others, 2008). The Pb and Nd isotope data are the most compelling evidence that the French Broad massif is exotic (Fisher and others, 2010). Paleogeographic constraints from high quality paleomagnetic data further support that transfer of the exotic crust from Amazonia occurred during sinistral oblique collision with southeastern Laurentia *ca.* 1.20 to 1.15 Ga (Tohver and others, 2002, 2004a, 2004b; D'Agrella-Filho and others, 2008). However, the specific location in Amazonia from which the exotic fragment detached, precisely when transfer occurred, and how the exotic component evolved in the context of western Amazonia warrant further consideration based on the new evidence presented here.

TABLE 7

Comparison of the GSMBC (French Broad Massif) and Paraguá Terrane

	Paraguá Terrane	**GSMBC**	**Laurentia**
Whole Rock Pb Isotopes	Amazonian	Amazonian	Laurentian
T_{DM} (pre-Elzevirian rocks)	2.2-1.6 Ga Evolved source	1.8-1.5 Ga Evolved source	1.4-1.3 Ga Juvenile source
Zircon Inheritance	1.6-1.9 Ga	1.6-1.9 Ga	None
Basement	pre-San Ignacio gneiss Complex (1.6-1.9 Ga)	None observed	None observed
Pre-Elzevirian Intrusive Suites (age)	Pensamiento Complex (1.37-1.32 Ga)	Felsic orthogneiss & xenoliths (1.36-1.31 Ga)	Dysart - Mt. Holly Suite (1.37-1.32 Ga)
Regional Metamorphism (Age)	Rondônian-San Ignacio Orogeny (1.34-1.32 Ga) Sunsás Orogeny (1.11-0.90 Ga)	Ottawan-Rigolet (1.09-0.96 Ga)	Ottawan-Rigolet (1.09-0.96 Ga)
Cover/post intrusion sediments	Sunsás -Nova Brasilândia-Aguapeí Gps.	Pre-Ottawan paragneiss	Grenville Supergroup (Elzevirian)
Maximum Depo. Age	1.15 Ga	1.1 Ga	1.25 Ga
Sediment Provenance	Geons 11-18 Paraguá - Amazonia	Geons 11-14, 16-19 FBM: Amazonia GSMBC: Amazonia-Laurentia	Geons 12-19 Laurentian terranes

The boundary between native Laurentian Grenville and exotic Amazonian Grenville is effectively a geochemical boundary defined by Pb and Nd isotope systematics. The boundary is located between Mesoproterozoic basement exposed in the Grenville-age massifs of the New Jersey Highlands and the Honey Brook Uplands (Pennsylvania). It is extrapolated southwest beneath the Appalachian foreland through eastern Tennessee (Fisher and others, 2010; Rivers and others, 2012; McLelland and others, 2013). Not including crust older than 1.4 Ga, which occurs on both cratons immediately inboard of the Grenville-age belts, the oldest rocks in common across the boundary are the 1.35 to 1.31 Ga pre-Elzevirian magmatic rocks. The Laurentian pre-Elzevirian (LpE) rocks are interpreted to be fragments of a juvenile 1.4 to 1.3 Ga pre-Elzevirian continental margin arc behind which a 1.3 to 1.2 Ga Elzevirian back-arc basin developed, and in which subsequent Grenville sedimentation, magmatic and metamorphic events occurred (McLelland and others, 2013). This history explains why the LpE occurs in such an outboard crustal position during the Grenville orogeny. The Amazonian pre-Elzevirian (ApE) rocks described here include the magmatic protoliths of the 1.35 to 1.31 Ga orthogneisses and a xenolith that exhibits *ca.* 1.7 to 1.8 Ga inheritance. As the Pb isotope array essentially defines the initial Laurentian-Amazonian collision zone, the ApE rocks would have formed in a continental arc on the Amazonian margin facing Laurentia, analogous to the LpE arc.

A close lithologic, geochronological, and geochemical match for the exotic ApE (and potentially the greater French Broad massif) are rocks that comprise the Paraguá terrane (Bettencourt and others, 2010) or Paraguá Block (Rizzotto and others, 2013) of northeastern Bolivia and southwestern Brazil, as proposed by Tohver and others (2006). The Paraguá terrane consists primarily of 1.8 to 1.5 Ga ortho- and paragneisses intruded by 1.37 to 1.32 Ga granitoids of the Pensamiento Complex. Three samples of Pensamiento Complex rocks from the Paraguá terrane have Pb isotope compositions

that help define the Amazonian Pb isotope array (fig. 13B) and possess evolved Nd isotope compositions (Tohver and others, 2004a). Collectively the gneisses and granites of the Pensamientio Complex were deformed and emplaced, respectively, during the San Ignacio orogeny at 1.34 to 1.32 Ga (Bettencourt and others, 2010). The ApE and Paraguá terrane have in common the *ca.* 1.37 to 1.32 Ga granitic rocks that exhibit 1.6 to 1.8 Ga zircon inheritance and have T_{DM} ages of 2.0 to 1.6 Ga, and paragneisses containing abundant 1.6 to 1.9 detrital zircon.

The Pensamiento granitoids intrude basement paragneiss (Litherland and others, 1989; Boger and others, 2005), whereas the relationship between 1.37 to 1.32 Ga felsic orthogneiss protoliths and paragneiss in the ApE rocks of the Great Smoky Mountains basement complex is obscured by Paleozoic orogenesis and/or is not exposed. However, the presence of 1.37 to 1.30 Ma (pre-Elzevirian) magmatic detrital zircon grains indicates that the sedimentary protoliths of the pre-Ottawan paragneisses in the Great Smoky Mountains basement complex are younger than the ApE, suggesting a basement-cover relationship. In spite of this difference there is a striking chronologic, isotopic, and lithologic correlation between the ApE rocks of the French Broad massif and Paraguá terrane (table 7), answering two of the questions posed above – the region of origin and context for western Amazonian evolution of the exotic Mars Hill terrane, Franch Broad massif, and greater SCAB may be found in southwestern Amazonia specifically within the Paraguá terrane.

In addition to geochronology consistent with a paleogeographic link, whole rock Pb isotope compositions for the *ca.* 1.33 Ga felsic orthogneiss and three pre-Ottawan paragneisses of the Great Smoky Mountains basement complex fall squarely among Amazonian values, affirming the link. In contrast feldspar Pb isotope compositions are not as "Amazonian" in their Pb isotope characteristics, spreading to lower $^{207}Pb/^{204}Pb$ for a given $^{206}Pb/^{204}Pb$ (fig. 13A), and consistent with either mixing of Amazonian and Laurentian crustal reservoirs or a direct Laurentian link. Mafic xenoliths have the lowest feldspar $^{207}Pb/^{204}Pb$ values, which fall within the Laurentian field. However, the mafic xenoliths are now hornblende-plagioclase amphibolites that were reconstituted during Taconian regional metamorphism (Anderson and Moecher, 2009). Their feldspar Pb isotope compositions are therefore unlikely to record the original Pb isotope composition of their mafic protoliths (basalt, gabbro) at *ca.* 1.35 Ga. The highest $^{207}Pb/^{204}Pb$ values overlap the lowest Amazonian whole-rock values and correspond to *ca.* 1150 and 1050 augen orthogneisses that are most likely to preserve their original feldspars. Because of the paucity of feldspar Pb isotopic data, combined with the possibility of isotopic disturbance in our studied feldspars, we take the whole rock Pb isotope compositions to be more relevant for comparison with the extensive whole rock Pb database for the southern Appalachian basement.

The more challenging question is how a fragment of the Paraguá terrane-equivalent crust was transferred to Laurentia by 1.30 Ga, and how transfer fits in with the complete Grenville orogenic cycle (Elzevirian through Rigoletan). Paleomagnetic, structural, metamorphic, and geochronologic evidence indicate sinistral oblique collision between Laurentia and Amazonia was occurring at 1.20 to 1.15 and potentially continued to *ca.* 1.0 Ga (Tohver and others, 2002, 2004a, 2004b, 2005; D'Agrella-Filho and others, 2008). This time for the earliest occurrence of oblique collision is long after formation of the 1.37 to 1.32 Ga LpE and ApE magmatic rocks on the Laurentian and Amazonian continental margins, respectively. There also occurred an additional *ca.* 100 m.y. of back-arc extension and magmatism assigned to the Elzevirian orogeny in the Laurentian Grenville. A few magmatic zircon crystallization ages in the range 1.30 to 1.20 Ga are reported from southwestern Amazonian (Santos and others, 2008), but there is certainly no crustal equivalent in southwest Amazonia to the extensive Elzevirian aged Composite Arc Belt of the Grenville orogen in Canada and

the Adirondacks. Most chronologies for southwest Amazonia indicate 1.30 to 1.20 Ga as a time of "orogenic quiescence" (Boger and others, 2005; Santos and others, 2008). The collisional records for Laurentian and Amazonian Grenville thus appear to diverge after *ca.* 1.30 Ga but converge again commencing at *ca.* 1.20 with sinistral oblique collision (Tohver and others, 2002, 2004a, 2006).

The collision of the Paraguá terrane with Amazonia during the San Ignacio orogeny (Rizzotto and others, 2013) is identical to the time for generation of the 1.37 to 1.32 Ga magmatic rocks of the LpE and ApE. It is proposed here that this event represents the collision of southeastern Laurentia with the outboard Paraguá terrane margin during the San Ignacio orogeny. This would imply an initial Laurentian-Amazonian continental collision well before sinistral transcurrent displacement began *ca.* 1.20 Ga. The actual transfer of the exotic SCAB terrane to Laurentia occurred during transcurrent displacement in the same sinistral oblique system that evolved to a transpressional system after 1.20 Ga (Tohver and others, 2004, their fig. 12), followed by the rapid onset of the Shawinigan "magmatic flareup" throughout the entire Grenville orogen beginning at *ca.* 1.19 Ga (Rivers and others, 2012). This timing further implies that the Mars Hill terrane and French Broad massif were fully integrated into the Laurentian margin by 1.19 Ga (Carrigan and others, 2003; Southworth and others, 2010; Tollo and others, 2010, 2017). The post-1.30 Ga history of the Great Smoky Mountains basement complex more closely matches that of the Laurentian Grenville than Amazonian Grenville in terms of evidence for Elzevirian, Shawinigan, and Ottawan magmatism, Ottawan and Rigolet metamorphism, and pre- and post-Ottawan sedimentation.

CONCLUSIONS

1. Field relations, petrology, whole rock major element geochemistry, zircon textures, and zircon U-Pb age systematics document the existence of a previously unrecognized "old" magmatic unit within the Great Smoky Mountains basement complex of the southwestern French Broad basement massif. Relatively undeformed felsic orthogneisses and their deformed (foliated) equivalents are 1.35 to 1.31 Ga in age. Entrained mafic xenoliths are 1.36 to 1.34 Ga in age. Both are among the oldest magmatic rocks within the Appalachian crystalline core. They correlate temporally with pre-Elzevirian (1.4–1.3 Ga) rocks elsewhere in Appalachian basement massifs, the Adirondack terrane, and the Grenville orogen in Canada. Some samples exhibit metamorphic zircon overgrowths of ~1.0 Ga age, indicating the rocks experienced Ottawan regional metamorphism during the Grenville orogenic cycle.

2. Migmatitic gneisses with inferred sedimentary prototliths within the basement complex are distinguished from orthogneisses by multiple detrital zircon age modes and zircon grains exhibiting magmatic cores with metamorphic overgrowths. Two groups of paragneisses are apparent: (1) those that lack the Ottawan-Shawinigan detrital zircon age doublet and contain late Ottawan/Rigolet (~1.05–0.95 Ga) metamorphic zircon, requireing clastic protoliths possessing depositional ages of *ca.* 1.1 Ga (pre-Ottawan); and (2) those with a depositional age of *ca.* 0.6 Ga (post-Ottawan) and exhibit the Ottawan-Shawinigan detrital zircon age doublet. The former correlate with late Grenville sediments that experienceed late Ottawan/Rigolet metamorphism elsewhere in the southern French Broad Massif. The latter correlate with latest Neoproterozoic Laurentian margin rift and passive margin clastic sequences deposited during the breakup of Rodinia that were metamorphosed during Taconian arc collision.

3. Pre-Ottawan paragneisses exhibiting detrital zircon age modes of *ca.* 2.0 to 1.8 Ga, 1.7 to 1.6 Ga, and 1.4 to 1.3 Ga are consistent with clastic input from Paleo- and Mesoproterzoic sources in either Laurentian or Amazonia. These modes are minor in

post-Ottawan paragneisses but attest to the presence of the older paragneisses among the multiple Grenvillian sources for Neoproterozoic clastic sediments.

4. Augen orthogneisses with granitic protoliths within the basement complex are 1.16 to 1.14 Ma in age, corresponding to the widespread Shawinigan magmatic event througout eastern Laurentia and consistent with previous geochronology in the study area.

5. Metamorphism at *ca.* 1040 Ma, expressed as metamorphic zircon overgrowths on 1.35 Ga magmatic zircon in orthogneisses and on 2.0 to 1.8, 1.7 to 1.6 Ga, and 1.4 to 1.3 Ga magmatic detrital zircon in paragneisses, correlates with Ottawan regional metamorphism throughout the Grenville orogen in eastern Laurentia.

6. All rocks are overprinted to varying degrees by Taconian regional metamorphism (*ca.* 460 Ma) that variably disturbs U-Pb zircon age systematics. The primary manifestation of disturbance is age discordance in detrital zircons of migmatitic paragneiss protoliths or growth of a new generation of magmatic zircon in Taconian-aged migmatites.

7. T_{DM} ages based on whole rock Sm-Nd isotope analyses of ortho- and paragneisses are 1.8 to 1.5 Ga, similar to T_{DM} ages from throughout south-central Appalachian basement, and distinctly older than Laurentian Grenville values that support juvenile crustal sources. The ages are consistent with an older, evolved crustal source, similar to Amazonian crust proposed to be the conjugate margin to eastern Laurentia during Rodinian assembly.

8. Whole rock Pb isotope compositions for the 1.35 to 1.31 orthogneisses and xenoliths, and for pre-Ottawan paragneisses, overlap the Amazonian Pb isotope array in the same manner as other southern Appalachian basement rocks, for example, the Mars Hill terrane. This overlap, along with Sm-Nd isotope and zircon age systematics indicate the exotic Mars Hill terrane potentially comprises the entire southern French Broad massif.

9. Although the ages of orthogneisses and xenoliths correlate with pre-Elzeverian rocks elsewhere in the Grenville orogen, the Pb isotope values preclude a paleogeographic link with Laurentian Grenville before *ca.* 1.2 Ga. The 1.8 to 1.3 Ga Paragua terrane of southwestern Amazonia provides a closer Pb isotope and geochronologic correlation for the conjugate margin to southeastern Laurentian in the Mesoproterozoic.

ACKNOWLEDGMENTS

Research was supported by NSF grants EAR 0635688 and 1447605, and instrumentation grants EAR 0824713 and 1551341; U.S.G.S. EDMAP grants G14AC000113 and G12AC20190; the Ferm fund of the Department of Earth and Environmental Sciences; and the Geological Society of America Student Research grant program. Jason Backus of the Kentucky Geological Survey assisted with whole rock XRF analysis and the KGS made the facility available for our use. We appreciate the encouragement and support of Bob Hatcher, Scott Southworth, Carl Merschat, and Bart Cattanach throughout the course of this research. The staff of the University of Arizona Laserchron lab patiently assisted our work at their facility. John Aleinikoff and Calvin Miller provided thorough reviews that greatly improved the manuscript.

APPENDIX

METHODS

XRF Whole Rock Geochemistry

Whole-rock analysis of major, minor and, trace elements was conducted on a 4-kW Bruker S4 Pioneer wavelength dispersive X-ray fluorescence spectrometer at the Kentucky Geologic Survey. Each unknown was weighed out to 4.0 g ± 0.0005 g and mixed with 8.0 ± 0.0005 g of Fluxite® (90 $Li_2Br_4O_7$:10 LiF) with two

added drops of 5.8 M LiBr. The powdered mixture was melted at 1080 °C in a platinum crucible and poured into fused disks using a Katanax K1 primer electric fluxer. Standards used are from the USGS – (DNC-1, BIR-1, W2a, BCR-2, BHVO-1, BHVO-2, AVG-2, G-2, STM-1, GSP-1), Irish Geologic Association – (OU-3, OU-4, AMH-1, YG-1, KPT-1), Canadian Certified References Materials Project – (MRG-1, SY-2, S-3), South African Reference Materials – (SARM 4, SARM 50), Centre de Recherches Pétrographiques et Géochimiques – (BE-N), and Chinese 13 National Standard – (GBW 07105).

U-Pb Geochronology

Approximately two kilograms of rock sample was crushed then milled in a Biko disk mill with ceramic plates. Zircon grains were concentrated by wet sieving using disposable nylon mesh, heavy liquids, and magnetic separation to obtain a 50 to 125 and 125 to 250 micron size fraction for each sample. Both size fractions were analyzed for several of the orthogneisses and some of the paragneisses. Zircon grains from igneous rock samples were hand picked; these include euhedral, acicular, and colorless grains in the concentrate. Detrital zircon grains from metasedimentary rocks were poured into a square mold to limit discrimination based on size or shape. Zircon grains were mounted in epoxy, ground and polished using 1500 and 2000 grit and 0.3 micron alumina powder. Zircon grains in polished mounts were imaged via BSE and CL on the JEOL IT-100 SEM at the University of Kentucky before analysis to guide location of the primary laser beam. Many targeted grains were imaged after analysis to assess the possibility of overlap of growth/age zones, and to aid in interpretation of dates based on zoning patterns. An attempt was made to target the widest oscillatory-zoned areas of grains from igneous samples. Detrital grains were randomly selected without preference for shape, size or zoning characteristics; the approximate center of a grain or the largest area of that grain that was free of imperfections was targeted for analysis. One spot per grain was analyzed, with the spot landing on an igneous core, metamorphic overgrowth, or the contact between the two zones. The large number of detrital grains targeted and time constraints per analytical session precluded greater discrimination of zoning patterns from CL images during targeting. Data from spots that overlapped two age zones was excluded for further use. The large number of detrital grains analyzed (usually ~300) yielded 150 to 290 ages that were less than ±5 percent discordant.

IsoPlot v. 4 (Ludwig, 2009) was used to display isotopic data. Error ellipses on Concordia diagrams and error bars on weighted mean plots are shown at the 2σ level. Calculated dates always are listed with 2-sigma uncertainties. Results of U-Pb geochronology are listed in Appendices 1-4 in Supplemental Material, http://earth.geology.yale.edu/%7eajs/SupplementaryData/2020/Moecher.

LA-ICP-MS U-Pb zircon geochronology.—Zircon U-Pb laser ablation-inductively coupled plasma-mass spectrometry was conducted on the Nu multi-collector or Element2 single collector mass spectrometers at the Arizona Laserchron facility following the general methods of Gehrels and others (2008). The circular laser spot size was 20 μm in diameter and ~ 5 μm deep (for example, figs. 7-11). Zircon age standards used were SL and R33 on the Nu instrument, and FC-1, SL mix, and R33 on the Element2. A total of ~100 and ~300 zircon grains were analyzed on the Nu and Element2, respectively. Repeated analysis of FC-1 yielded a concordant weighted mean age of 1098 ± 1 Ma (n = 825, MSWD = 1.00; accepted age = 1099 ± 1 Ma: Paces and Miller, 1993; Schmitz and others, 2003).

SIMS U-Pb geochronology.—Zircon U-Pb secondary ion mass spectrometry (SIMS) analysis of granitic orthogneisses was completed on the CAMECA ims1270 ion microprobe at the UCLA Keck facility over the course of several years (Loughry, ms, 2010; Anderson, ms, 2011; Larkin, ms, 2016). The older studies yielded preliminary age information that helped guide re-sampling for subsequent SHRIMP and LA-ICP-MS analysis. However, analytical conditions, zircon standard, and data reduction methods were the same for all SIMS sessions. Ion beam spot size was ~15 × 20 μm and ~2 μm deep. The zircon age standard was AS3 (accepted age of 1099 ± 1 Ma: Schmitz and others, 2003). Four to five standard grains were analyzed at the beginning of each session and then every sixth grain and four to five grains at the end of the session. Analysis of standard AS3 for each session yielded concordant U-Pb ages within 2σ error of the accepted age. Zircon SIMS analysis and common Pb correction followed Schmitt and others (2003).

SHRIMP U-Pb zircon geochronology.—Sensitive high resolution ion microprobe (SHRIMP) U-Pb geochronology was conducted on zircon separated from the felsic orthogneiss (DEL10-7b) and one augen orthogneiss (DEL10-30) using the SHRIMP IIB at Curtin University. Analytical methods and data reduction followed Tohver and others (2012, and references therein). The ion beam spot size was ~15 × 20 μm and ~2 μm deep. The $^{206}Pb/^{238}U$age standard was zircon BR266 (accepted age = 562.2 ± 0.5 Ma (2σ): Stern, 2001).

Nd and Pb Isotope Geochemistry – Thermal Ionization Mass Spectrometry

Whole-rock analysis of Sm and Nd, and feldspar analysis of common Pb were completed at the Syracuse University Radiogenic Isotope Laboratory. For whole-rock Sm, Nd, and Pb analyses approximately 90 ml of each sample were powdered using a single puck alumino-silicate shatterbox. Care was taken to homogenize the sample and to ensure a representative aliquot was obtained. The puck and chamber of the shatterbox

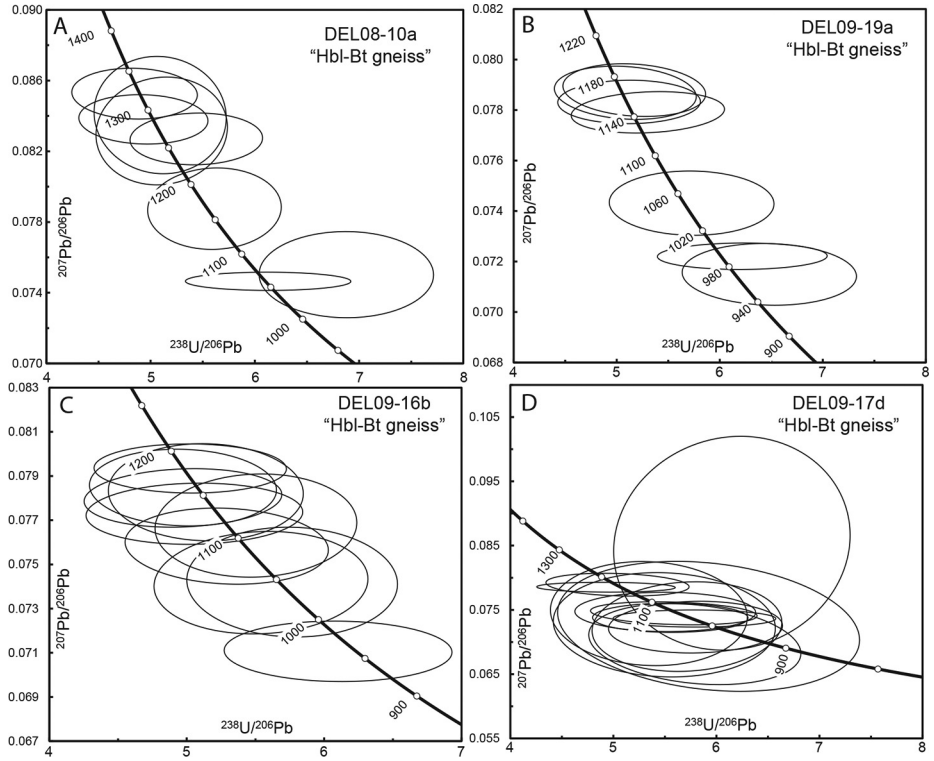

Fig. A8. Preliminary SIMS U-Pb zircon Tera-Wasserburg concordia plots for basement gneisses that were originally mapped as hornblende-biotite gneiss (Hadley and Goldsmith, 1963). All samples except A are now interpreted to be Grenville Shawinigan orthogneisses based on these analyses (Loughry, ms, 2010). A is interpreted to be related to the *ca.* 1330 Ma felsic orthogneisses (fig. 7).

were vacuumed, blasted with compressed air, and washed with soap and water between samples. For each sample, the shatterbox chamber was pre- contaminated by running a portion of the sample, discarding the powder, and cleaning the shatterbox again before loading the sample. Seven basement samples collected by Chakraborty (ms, 2010), Loughry (ms, 2010), and Anderson (ms, 2011) were also analyzed.

Whole-rock powders analyzed for Sm and Nd were dissolved in Teflon bombs. Bombs were cleaned by a series of overnight acid rinses in an oven at 160 °C. Three individual rinses were with a 4.8 ml 29 M HF and 0.2 ml HNO_3 mixture, 6 M HCl, and another HF and HNO_3 mixture of the same proportions. Savillex® vials (50 ml) were cleaned by filling the vials with the same 2.4 HF : 1 HNO_3 mixture, capping, and leaving on a hot plate for three nights. To prepare the samples for bomb dissolution, approximately 0.300 g were weighed into the 50 ml vials. The walls of the vials were rinsed and swirled with HNO_3 to collect all powder. 10 ml of 29 M HF was added to the vial, which was then capped and heated for 24 hrs. Vials were then uncapped and evaporated to dryness. 2.8 ml of 29 M HF and 0.2 ml of HNO_3 were added to the vials to re-dissolve the powder. This solution was poured into the bombs with approximately 0.1500 g of an enriched $^{149}Sm/^{150}Nd$ spike and another 2.0 ml of 29 M HF. The bombs were heated in the oven at 160 °C for 6 or 7 days. After the bombs were removed, samples were poured back into their respective Savillex® vials. The bombs were rinsed with 29 M HF to ensure the entire aliquot was collected. Samples were dried and dissolved in 6 M HCl over a 12 hr period and then dried again. Samples were heated for 30 min in 5 ml of 6 M HCl and then contents were added to their respective bombs. The bombs were then placed in an oven overnight at 160 °C. Contents were then transferred back into their respective vials and dried. Approximately 10 ml of 6 M HCl was added to the vials, which were then capped and heated for 30 min. After the entire sample was dissolved the contents were transferred into 2 equal volumes in centrifuge tubes and ran in a centrifuge for 6 min at 11 rpm. Samples were then added to cation exchange resin columns. To extract Pb, 6 ml of 2.5 M HCl was passed through the column and collected in a beaker. Columns were rinsed with 94 ml of 2.5 M HCl. 6 M

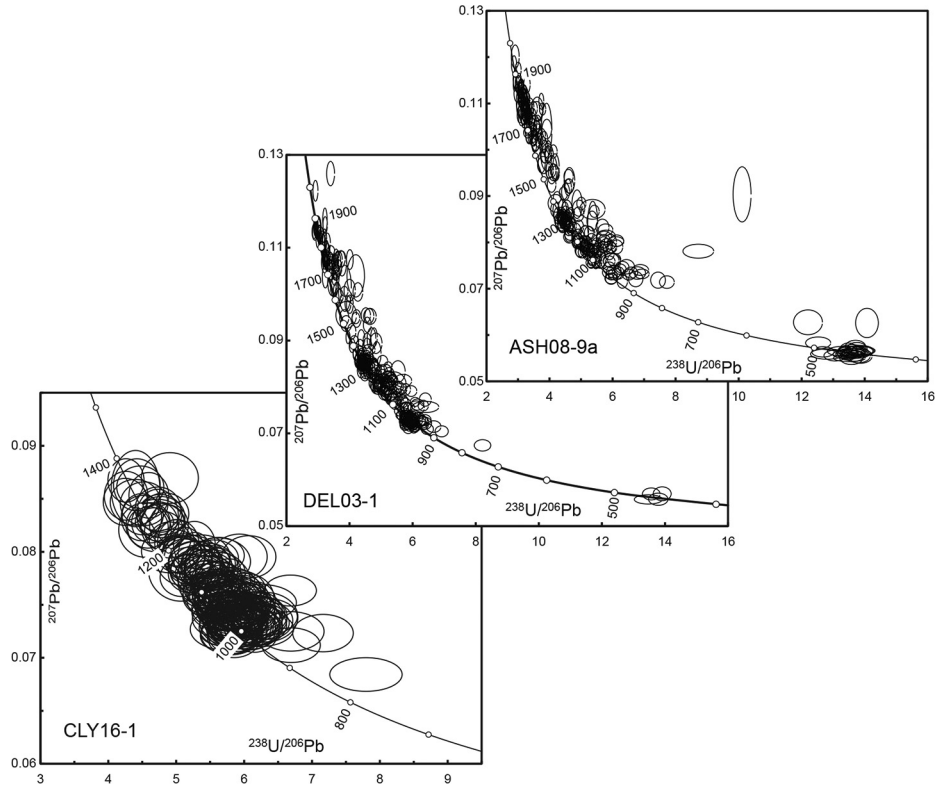

Fig. A9. Tera-Wasserburg concordia plots for pre-Ottawan paragneiss from Dellwood and Clyde illustrating degree and pattern of discordancy among detrital zircon grains.

HCl was passed through the columns to collect the heavy rare earth elements. 22 ml of each sample was collected and dried. These aliquots were dissolved in 0.18 M HCl and loaded into the second stage rare earth element cation exchange resin columns. 5 ml were collected for Nd and then the columns were re-equilibrated with 0.5 M HCl and 10-15 ml were collected for Sm. These aliquots were dried to a solid.

Samples were then analyzed on the IsotopX Phoenix thermal ionization mass spectrometer (TIMS) for whole-rock Sm and Nd concentrations. These Sm-Nd data were used to calculate epsilon Nd values at the present time, at the time of crystallization, and at the time of mantle extraction. Present day isotopic ratios used for CHUR were $^{147}Sm/^{144}Nd = 0.1967$ and $^{143}Nd/^{144}Nd = 0.512638$ (DePaolo, 1981). Depleted mantle ages were calculated using the depleted mantle curve of DePaolo (1981).

For Pb analysis samples were processed through an iron mill after the jaw crusher to produce sand composed of individual mineral grains. The resulting sand was dry sieved through 250 μm mesh. Between each sample the jaw crusher and mill were thoroughly vacuumed, air blasted, and cleaned with isopropanol. Mill discs and jaw crusher plates were removed and cleaned with a vacuum, straight wire brush grinder, and isopropanol. The sieve jar was vacuumed and washed with soap and water. Sieve mesh was discarded after each sample. All worktable surfaces were vacuumed, air blasted, and wiped down with isopropanol and new paper towels were laid down so that the sample never touched any workspace surfaces. The floor was sprayed with water and swept between each sample.

The >250 μm fraction of the samples was run through the Frantz magnetic separator model LB-1 at 0.25 and 1.5 amps. The 1.5 A non-magnetic portions were collected and stored. To avoid contamination, all removable parts of the Frantz were washed in soapy water and the rest was vacuumed and wiped with isopropanol between samples. The feldspars were picked using a Leica S8 120X binocular microscope equipped with a polarizer and analyzer. 20 test grains of each sample were hand-picked and mounted on a glass slide with carbon tape and examined on the JEOL JXA8600V200 scanning electron microscope at

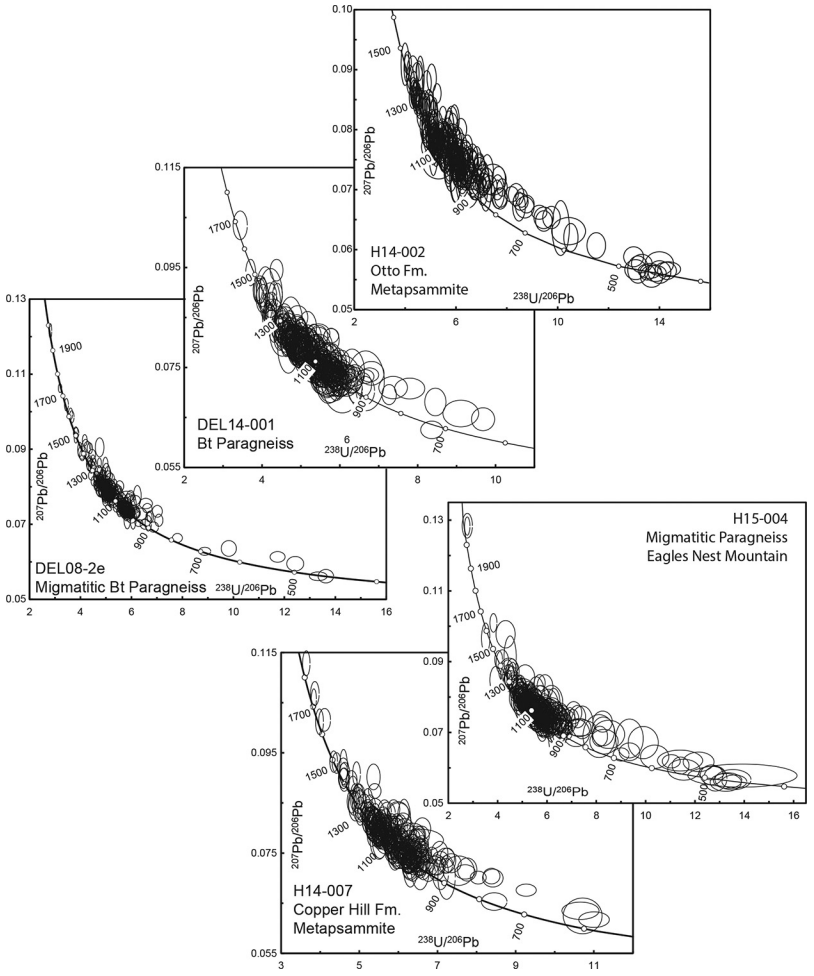

Fig. A10. Tera-Wasserburg concordia plots for post-Ottawan paragneisses from Dellwood and Hazelwood quadrangles shown in figure 10.

Syracuse University using energy dispersive spectrometry to ensure K-feldspar grains could be distinguished confidently from plagioclase, quartz, and other minerals. Some samples did not contain K-feldspar, in which case sodic plagioclase was picked.

Two-hundred feldspar grains from each sample were hand-picked. Care was taken to select the purest and least fractured grains. Picked grains were crushed using a mortar and pestle while submerged in isopropanol. Using a pipette, the powder was transferred into 15 ml Savillex® vials. Isopropanol was then pipetted out of the vial; any remaining isopropanol was evaporated. After the powder was dried each sample went through a series of rinses in acid and water. Each sample was bathed in 10 ml of HNO_3 in a capped vial on a hot plate for approximately 24 hrs. HNO_3 was pipetted out and then the sample was rinsed with 18 MΩ deionized H_2O. 10 ml of 6 M HCl was added to the vial and was set capped on a hot plate for another 24 hrs. HCl was then pipetted out and the sample was rinsed with distilled H_2O. This was followed by two half-hour rinses in room-temperature 5 percent 29 M HF. After each rinse the leach was discarded and the sample rinsed in distilled H_2O. Two 5-minute hot leaches in 5 percent 29 M HF were done for each sample, which were discarded. Three more ten-minute hot leaches in 5 percent 29 M HF were done. For each leach the leachate was collected in a separate beaker and dried down on a hot plate. After all HF volatilized 15 drops of 0.55 M HBr was added to the aliquot.

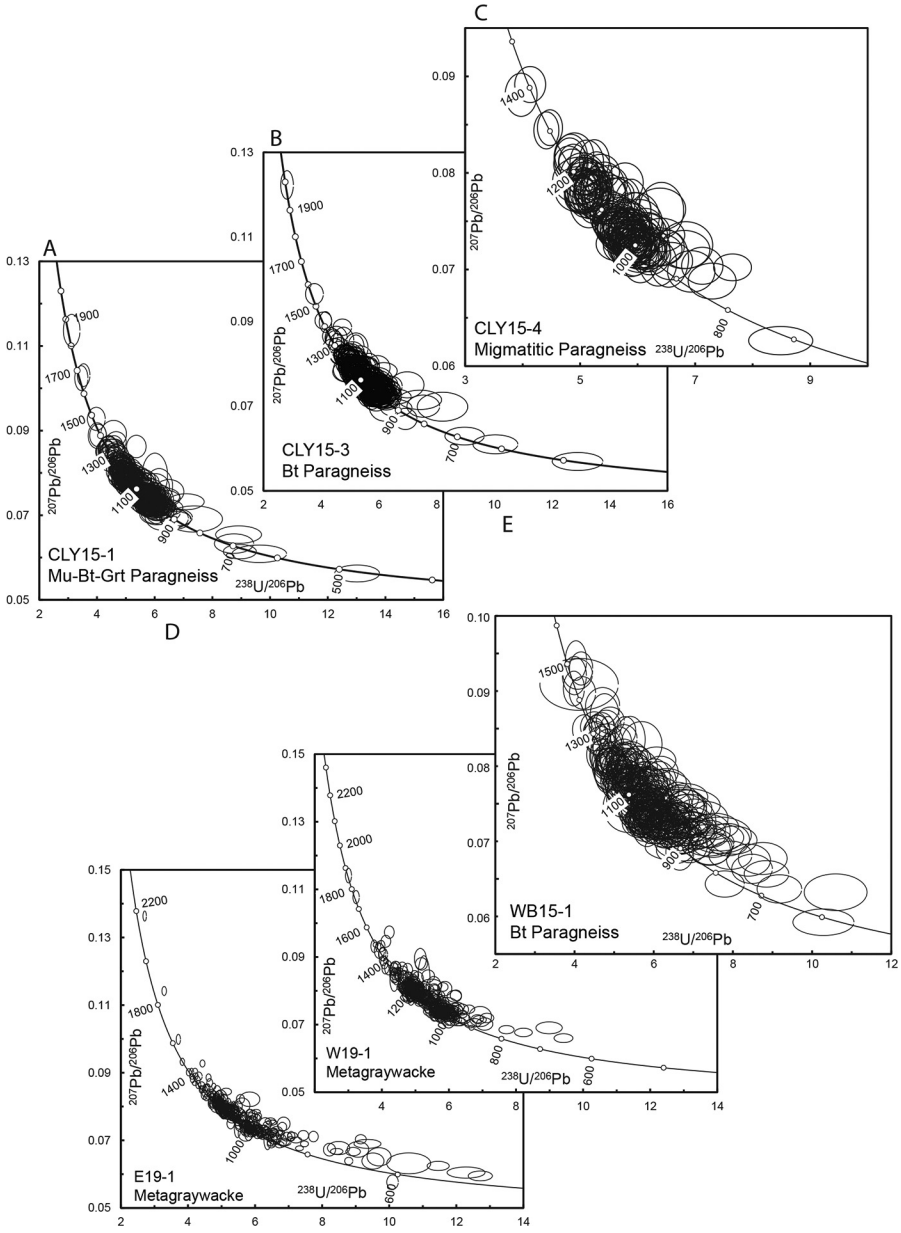

Fig. A11. Tera-Wasserburg concordia plots for post-Ottawan paragneisses from Clyde, Enka, Wayah Bald, and Weaverville quadrangles shown in figure11.

Aliquots were run through cation exchange resin columns to extract Pb. Columns were rinsed three times with 6 M HCl. After all HCl was through the column a squirt of distilled H_2O was added to each column. Columns were then equilibrated with 25 drops of 0.55 M HBr. Samples were loaded and processed through the columns. Two sets of 15 drops of 0.55 M HBr, two sets of 25 drops of 0.55M HBr, and two sets of 50 drops of 0.55M HBr were added and drained successively. The collected acid was removed and collection beakers were switched to collect Pb in the original sample in vials. To collect Pb, 20 drops of 6 M HCl were

added and then 100 drops of 6 M HCl were added and collected. Feldspar Pb samples were loaded onto rhenium filaments with silica gel and analyzed on a VG Sector 54 by thermal ionization mass spectrometer.

Pb Isotope Geochemistry - Inductively Coupled Plasma-Mass Spectrometry

Whole-rock Pb isotope geochemistry was conducted at the University of Texas - Austin. Whole rock powders were produced from a split of rough crush of 2 to 3 kilogram of bulk rock. Powders were dissolved in $HF+HNO_3$ in an oven for ~3 days. Once dry, samples were returned to the oven for 24 hours with 6M HCl to convert to chloride form. Samples were then passed through anion-exchange resin using a mixture of HCl + HBr and Pb was eluted using 6M HCl.

Lead isotope analysis was performed on a Nu Instruments Nu Plasma 3D MC-ICP-MS equipped with a DSN100 desolvating nebulizer. Solutions were aspirated at 100 μl/min. Samples were diluted to match the total ion intensity of the standards. Instrumental mass bias was corrected using thallium ($^{205}Tl/^{203}Tl$ = 2.389650) added to samples with a Pb/Tl ratio between 5 and 10 and then normalized to NBS-981. Based on the precision of standard analyses of NBS-981 the uncertainty in $^{206}Pb/^{204}Pb$, $^{207}Pb/^{204}Pb$, and $^{208}Pb/^{204}Pb$ is estimated to be 0.020% per amu (2SD, n = 22). For rock standard JR-1 we measured $^{206}Pb/^{204}Pb$ = 18.364, $^{207}Pb/^{204}Pb$ = 15.568 and $^{208}Pb/^{204}Pb$ = 38.434 which are consistent with the data reported by Koide and Nakamura (1990).

REFERENCES

Aleinikoff, J. N., Zartman, R. E., Walter, M., Rankin, D. W., Lyttle, P. T., and Burton, W. C., 1995, U-Pb ages of metarhyolites of the Catoctin and Mount Rogers Formations, central and southern Appalachians: Evidence for two pulses of Iapetan rifting: American Journal of Science, v. 295, n. 4, p. 428–454, https://doi.org/10.2475/ajs.295.4.428

Aleinikoff, J. N., Southworth, S., and Kunk, M. J., 2007, SHRIMP U-Pb geochronology of zircon and titanite and $^{40}Ar/^{39}Ar$ of hornblende and muscovite from Mesoproterozoic rocks of the western Blue Ridge, Great Smoky Mountains National Park area, TN and NC: Geological Society of America Abstracts with Programs, v. 39, n. 2, p. 78.

Aleinikoff, J. N., Southworth, S., Fanning, C. M., and Mazdab, F. K., 2010, Evidence for late Neoproterozoic age of Ocoee Supergroup: SHRIMP U-Pb and trace elements analysis of diagenetic xenotime and monazite; Geological Society of America Abstracts with Programs, v. 41, n. 2, p. 59.

Aleinikoff, J. N., Ratcliffe, N. M., and Walsh, G. J., 2011. Provisional zircon and monazite uranium-lead geochronology for selected rocks from Vermont: U.S. Geological Survey Open-File Report 2011-1309, 46 p, https://doi.org/10.3133/ofr20111309

Aleinikoff, J. N., Grauch, R. I., Mazdab, F. K., Kwak, L., Fanning, C. M., and Kamo, S. L., 2012, Origin of an unusual monazite-xenotime gneiss, Hudson Highland, New York: SHRIMP U-Pb geochronology and trace element geochemistry: American Journal of Science, v. 312, n. 7, p. 723–765, https://doi.org/10.2475/07.2012.02

Aleinikoff, J.N., Southworth, S., and Merschat, A.J., 2013, Implications for late Grenvillian (Rigolet phase) construction of Rodinia using new U-Pb data from the Mars Hill terrane, Tennessee and North Carolina, United States: Geology, v. 41, n. 10, p. 1087–1090, https://doi.org/10.1130/G34779.1

Anderson, E. D., ms, 2011, Petrologic, geochemical, and geochronologic constraints on the tectonic evolution of the southern Appalachian orogen, Blue Ridge Province of western North Carolina: Lexington, Kentucky, University of Kentucky, Ph. D. thesis, 279 p., https://uknowledge.uky.edu/gradschool_diss/820/

Anderson, E. D., and Moecher, D. P., 2009, Formation of high-pressure metabasites in the southern Appalachian Blue Ridge via Taconic continental subduction beneath the Laurentian margin: Tectonics, v. 28, n. 5, https://doi.org/10.1029/2008TC002319

Becker, T. P., Thomas, W. A., Samson, S. D., and Gehrels, G. E., 2005, Detrital zircon evidence of Laurentian crustal dominance in the lower Pennsylvanian deposits of the Alleghanian clastic wedge in eastern North America: Sedimentary Geology, v. 182, n. 1–4, p. 59–86, https://doi.org/10.1016/j.sedgeo.2005.07.014

Berquist, P. J., ms, 2005, U-Pb zircon geochronology and geochemistry of southern Appalachian basement: Tectonic implications and constraints on age, extent, and origin: Nashville, Tennessee, Vanderbilt University, M. S. thesis, 69 p.

Bettencourt, J. S., Tosdal, R. M., Leite, Jr., W. B., and Payolla, B. L., 1999, Mesoproterozoic rapakivi granites of the Rondônia Tin Province, southwestern border of the Amazonian craton, Brazil – I. Reconnaissance U-Pb geochronology and regional implications: Precambrian Research, v. 95, n. 1–2, p. 41–67, https://doi.org/10.1016/S0301-9268(98)00126-0

Bettencourt, J. S., Leite, Jr., W. B., Ruiz, A. S., Matos, R., Payolla, B. L., and Tosdal, R. M., 2010, The Rondonian-San Ignacio province in the SW Amazonian craton: An overview: Journal of South American Earth Sciences, v. 29, n. 1, p. 28–46, https://doi.org/10.1016/j.jsames.2009.08.006

Bickford, M. E., Van Schmus, W. R., Karlstrom, K. E., Mueller, P. A., and Kamenov, G. D., 2015, Mesoproterozoic-trans-Laurentian magmatism: A synthesis of continent-wide age distributions, new SIMS U-Pb ages, zircon saturation temperatures, and Hf and Nd isotope compositions: Precambrian Research, v. 265, p. 286–312, https://doi.org/10.1016/j.precamres.2014.11.024

Boger, S. D., Raetz, M., Giles, D., Etchart, E., and Fanning, C. M., 2005, U-Pb age date from the Sunsás region

of eastern Bolivia, evidence for the allochthonous origin of the Paragua Block: Precambrian Research, v. 139, n. 3–4, p. 121–146, https://doi.org/10.1016/j.precamres.2005.05.010
Bream, B. R., Hatcher, Jr., R. D., Miller, C. F., and Fullagar, P. D., 2004, Detrital zircon ages and Nd isotopic data from the southern Appalachian crystalline core, Georgia, South Carolina, North Carolina, and Tennessee: New provenance constraints for part of the Laurentian margin, *in* Tollo, R. P., Corriveau, L., McLelland, J., and Bartholomew, M. J., editors, Proterozoic Tectonic Evolution of the Grenville Orogen in North America: GSA Memoirs, v. 197, p. 459–475, https://doi.org/10.1130/0-8137-1197-5.459
Carrigan, C. W., Miller, C. F., Fullager, P. D., Bream, B. R., Hatcher, Jr., R. D., and Coath, C. D., 2003, Ion microprobe age and geochemistry of southern Appalachian basement, with implications for Proterozoic and Paleozoic reconstructions: Precambrian Research, v. 120, n. 1–2, p. 1–36, https://doi.org/10.1016/S0301-9268(02)00113-4
Carter, B. T., Hibbard, J. P., Tubrett, M., and Sylvester, P., 2006, Detrital zircon geochronology of the Smith River Allochthon and Lynchburg Group, southern Appalachians: Implications for Neopoterozoic-Early Cambrian paleogeography: Precambrian Research, v. 147, n. 3–4, p. 279–304, https://doi.org/10.1016/j.precamres.2006.01.024
Cawood, P. A., McCausland, P. J. A., and Dunning, G. R., 2001, Opening Iapetus: Constraints from the Laurentian margin in Newfoundland: GSA Bulletin, v. 113, n. 4, p. 443–453, https://doi.org/10.1130/0016-7606(2001)113<0443:OICFTL>2.0.CO;2
Cawood, P. A., Hawkesworth, C. J., and Dhuime, B., 2013, The continental record and the generation of continental crust: GSA Bulletin, v. 125, n. 1–2, p. 14–32, https://doi.org/10.1130/B30722.1
Chakraborty, S., ms, 2010, Provenance of the Neoproterozoic Ocoee Supergroup, eastern Great Smoky Mountains: Lexington, Kentucky, University of Kentucky, Ph. D. thesis, 307 p.
Chakraborty, S., Moecher, D. P., and Samson, S. D. 2012, Provenance of the lower Ocoee Supergroup, eastern Great Smoky Mountains: GSA Bulletin, v. 124, n. 7–8, p. 1278–1292, https://doi.org/10.1130/B30578.1
Clemons, K. M., and Moecher, D. P., 2009, Reinterpretation of the Greenbrier fault, Great Smoky Mountains: New petrofabric constraints and implications for southern Appalachian tectonics: GSA Bulletin, v. 121, n. 7–8, p. 1108–1122, https://doi.org/10.1130/B26480.1
Condie, K. C., 1990, Growth and accretion of continental crust: Inferences based on Laurentia: Chemical Geology, v. 83, n. 3–4, p. 183–194, https://doi.org/10.1016/0009-2541(90)90279-G
Condie, K. C., and Aster, R. C., 2010, Episodic zircon age spectra of orogenic granitoids: The supercontinent connection and continental growth: Precambrian Research, v. 180, n. 3–4, p. 227–236, https://doi.org/10.1016/j.precamres.2010.03.008
Corrie, S. L., and Kohn, M. J., 2007, Resolving the timing of orogenesis in the Western Blue Ridge, southern Appalachians, via *in situ* ID-TIMS monazite geochronology: Geology, v. 35, n. 7, p. 627–630, https://doi.org/10.1130/G23601A.1
D'Agrella-Filho, M. S., Tohver, E., Santos, J. O. S., Elming, S.-A., Trindade, R. I. F., Pacca, I. I. G., and Geraldes, M. C., 2008, Direct dating of paleomagnetic results from Precambrian sediments in the Amazon craton: Evidence for Grenvillian emplacement of exotic crust in SE Appalachians of North America: Earth and Planetary Science Letters, v. 267, n. 1–2, p. 188–199, https://doi.org/10.1016/j.epsl.2007.11.030
Daly, J. S., and McLelland, J. M., 1991, Juvenile Middle Proterozoic crust in the Adirondack highlands, Grenville province, northeastern North America: Geology, v. 19, n. 2, p. 119–122, https://doi.org/10.1130/0091-7613(1991)019<0119:JMPCIT>2.3.CO;2
Dalziel, I. W. D., 1992, On the organization of American plates in the Neoproterozoic and the breakout of Laurentia: GSA Today, v. 2, p. 1–2.
DePaolo, D. J., 1981, Neodymium isotopes in the Colorado Front Range and crust-mantle evolution in the Proterozoic: Nature, v. 291, p. 193–196, https://doi.org/10.1038/291193a0
DeWolf, C. P., and Mezger, K., 1994, Lead isotope analysis of leached feldspars: Constraints on the early crustal history of the Grenville Orogen: Geochimica et Cosmochimica Acta, v. 58, n. 24, p. 5537–5550, https://doi.org/10.1016/0016-7037(94)90248-8
Eckert, Jr. , J. O., Hatcher, Jr., R. D., and Mohr, D. W., 1989, The Wayah granulite-facies metamorphic core, southwestern North Carolina: High-grade culmination of Taconic metamorphism in the southern Blue Ridge: GSA Bulletin, v. 101, n. 11, p. 1434–1447, https://doi.org/10.1130/0016-7606(1989)101<1434:TWGFMC>2.3.CO;2
Eriksson, K. A., Campbell, I. H., Palin, J. M., and Allen, C. M., 2003, Predominance of Grenvillian magmatism recorded in detrital zircons from modern Appalachian rivers: The Journal of Geology, v. 111, n. 6, p. 707–717, https://doi.org/10.1086/378338
Fisher, C. M., Loewy, S. L., Miller, C. F., Berquist, P., Van Schmus, W. R., Hatcher, Jr., R. D., Wooden, J. L., and Fullagar, P. D., 2010, Whole-rock Pb and Sm-Nd isotopic constraints on the growth of southeastern Laurentia during Grenvillian orogenesis: GSA Bulletin, v. 122, n. 9–10, p. 1646–1659, https://doi.org/10.1130/B30116.1
Fosdick, J. C., Grove, M., Graham, S. A., Hourigan, J. K., Lovera, O., and Romans, B. W., 2014, Detrital thermochronologic record of burial heating and sediment recycling in the Magallanes foreland basin, Patagonian Andes: Basin Research, v. 27, n. 4, p. 546–572, https://doi.org/10.1111/bre.12088
Gehrels, G. E., Valencia, V. A., and Ruiz, J., 2008, Enhanced precision, accuracy, efficiency, and spatial resolution of U-Pb ages by laser ablation-multicollector-inductively coupled plasma-mass spectrometery: Geochemistry, Geophysics, Geosystems, v. 9, n. 3, https://doi.org/10.1029/2007GC001805
Hadley, J. B., and Goldsmith, R., 1963, Geology of the eastern Great Smoky Mountains, North Carolina and Tennessee: U.S. Geological Survey Professional Paper 349-B, 118 p., https://doi.org/10.3133/pp349B
Halpin, J. A., Daczko, N. R., Milan, L. A., and Clarke, G. L., 2012, Decoding near-concordant U-Pb zircon

ages spanning several hundred million years: Recrystallization, metamictisation, or diffusion?: Contributions to Mineralogy and Petrology, v. 163, p. 67–85, https://doi.org/10.1007/s00410-011-0659-7
Hanmer, S., Corrigan, D., Pehrsson, S., and Nadeau, L., 2000, SW Grenville Province, Canada: The case against post–1.4 Ga accretionary tectonics: Tectonophysics, v. 319, n. 1, p. 33–51, https://doi.org/10.1016/S0040-1951(99)00317-0
Hatcher, Jr., R. D., 1987, Tectonics of the southern and central Appalachian internides: Annual Review of Earth and Planetary Sciences, v. 15, p. 337–362, https://doi.org/10.1146/annurev.ea.15.050187.002005
Hatcher, Jr., R. D., Bream, B. R., Miller, C. F., Eckert, J. O., Fullagar, P. D., and Carrigan W. W., 2004, Paleozoic structure of internal basement massifs, southern Appalachian Blue Ridge, incorporating new geochronologic, Nd and Sr isotopic, and geochemical data, *in* Tollo, R. P., Corriveau, L., McLelland, J., and Bartholomew, M. J., editors, Proterozoic tectonic evolution of the Grenville orogen in North America: GSA Memoirs, v. 197, p. 459–475, https://doi.org/10.1130/0-8137-1197-5.525
Hoffman, P. F., 1988, United plates of America, the birth of a craton: Early Proterozoic assembly and growth of Laurentia: Annual Review of Earth and Planetary Sciences, v. 16, p. 543–603, https://doi.org/10.1146/annurev.ea.16.050188.002551
_____ 1991, Did the breakout of Laurentia turn Gondwanaland inside-out?: Science, v. 252, n. 5011, p. 1409–1412, https://doi.org/10.1126/science.252.5011.1409
Hynes, A., and Rivers, T., 2010, Protracted continental collision – evidence from the Grenville Orogen: Canadian Journal of Earth Science, v. 47, n. 5, p. 591–620, https://doi.org/10.1139/E10-003
Kelly, E. M., and Moecher, D. P., 2014, Age of the Walden Creek Group revisited, rehashed, and finally resolved? Evidence from ages of detrital zircon, detrital monazite, and metamorphic/diagenetic monazite from the Whilhite, Sandsuck, and Shields Formations, western Greak Smoky Mountains: GSA Abstracts with Programs, v. 46, no. 3, p. 84.
Kunz, B. E., Regis, D., and Engi, M., 2018, Zircon ages in granulite facies rocks: Decoupling from geochemistry above 850 °C?: Contributions to Mineralogy and Petrology, v. 173, article n. 26, https://doi.org/10.1007/s00410-018-1454-5
Larkin, E. A., ms, 2016, Field, geochronologic, and geochemical constraints on late Precambrian to early Paleozoic terrane accretion in the southern Appalachian Blue Ridge Province: Lexington, Kentucky, University of Kentucky, M.S. thesis, 127 p., https://uknowledge.uky.edu/ees_etds/39/
Litherland, M., Annells, R. N., Darbyshire, D. P. F., Fletcher, C. J. N., Hawkins, M. P., Klinck, B. A., Mitchell, W. I., O'Connor, E. A., Pitfield, P. E. J., Power, G., and Webb, B. C., 1989, The Proterozoic of eastern Bolivia and its relationship to the Andean mobile belt: Precambrian Research, v. 43, n. 3, p. 157–174, https://doi.org/10.1016/0301-9268(89)90054-5
Loewy, S. L., Connelly, J. N., Dalziel, I. W. D., and Gower, C. F., 2003, Eastern Laurentia in Rodinia: Constraints from whole-rock Pb and U/Pb geochronology: Tectonophysics, v. 375, n. 1–4, p. 169–197, https://doi.org/10.1016/S0040-1951(03)00338-X
Loughry, D. F., ms, 2010, Origin of Blue Ridge basement rocks, Dellwood Quad, western NC: New evidence from U-Pb zircon geochronology and whole rock geochemistry: Lexington, Kentucky, University of Kentucky, M. S. thesis, 136 p., https://uknowledge.uky.edu/gradschool_theses/11/
Ludwig, K. R., 2009, IsoPlot 4.1. A geochronological toolkit for Microsoft Excel: Berkeley Geochronology Center Special Publication 4, 76 p.
Massey, M. A., and Moecher, D. P., 2005, Deformation and metamorphic history of the Western Blue Ridge-Eastern Blue Ridge terrane boundary, southern Appalachian orogen: Tectonics, v. 24, n. 5, https://doi.org/10.1029/2004TC001643
McLelland, J. M., Daly, J. S., and Chiarenzelli, J., 1993, Sm-Nd and U-Pb isotopic evidence of juvenile crust in the Adirondack Lowlands and implications for the evolution of the Adirondack Mts.: The Journal of Geology, v. 101, n. 1, p. 97–105, https://doi.org/10.1086/648198
McLelland, J. M., Daly, J. S., and McLelland, J. M., 1996, The Grenville orogenic cycle (*ca.* 1350–1000 Ma): An Adirondack perspective: Tectonophysics, v. 265, n. 1–2, p. 1–28, https://doi.org/10.1016/S0040-1951(96)00144-8
McLelland, J. M., Selleck, B. W., and Bickford, M. E., 2010, Review of the Proterozoic evolution of the Grenville Province, its Adirondack outlier, and the Mesoproterozoic inliers of the Appalachians, *in* Tollo, R. P., Bartholomew, M. J., Hibbard, J. P., and Karabinos, P. M., editors, From Rodinia to Pangea: The Lithotectonic Record of the Appalachian Region: GSA Memoirs, v. 206, p. 795–836, https://doi.org/10.1130/2010.1206(02)
McLelland, J. M., Selleck, B. W., and Bickford, M. E., 2013, Tectonic evolution of the Adirondack Mountains and Grenville Orogen inliers with in the USA: Geoscience Canada, v. 40, n. 4, https://doi.org/10.12789/geocanj.2013.40.022
Merschat, A. J., ms, 2009, Assembling the Blue Ridge and Inner Piedmont: Insights into the nature and timing of terrane accretion in the southern Appalachian orogen from geologic mapping, stratigraphy, kinematic analysis, petrology, geochemistry, and modern geochronology: Knoxville, Tennessee, University of Tennessee, Ph. D. thesis, 455 p.
Merschat, C. E., and Cattanach, B. L., 2008, Bedrock geologic map of the western half of the Asheville 1:100,000-scale quadrangle, North Carolina and Tennessee: North Carolina Geological Survey Geologic Map Series 13, scale 1:100,000.
Mezger, K., and Krogstad, E. J., 1997, Interpretation of discordant U-Pb zircon ages: An evaluation: Journal of Metamorphic Geology, v. 15, n. 1, p. 127–140, https://doi.org/10.1111/j.1525-1314.1997.00008.x
Miller, C. F., Hatcher, Jr., R. D., Harrison, T. M., Coath, C. D., and Gorisch, E. B., 1998, Cryptic crustal events elucidated through zone imaging and ion microprobe studies of zircon, southern Appalachian Blue Ridge, North Carolina-Georgia: Geology, v. 26, n. 5, p. 419–422, https://doi.org/10.1130/0091-7613(1998)026<0419:CCEETZ>2.3.CO;2
Miller, C. F., Hatcher, Jr., R. D., Ayers, J. C., Coath, C. D., and Harrison, T. M., 2000, Age and zircon

inheritance of Eastern Blue Ridge plutons, southwestern North Carolina and northeastern Georgia, with implications for magma history and evolution of the southern Appalachian orogen: American Journal of Science, v. 300, n. 2, p. 142–172, https://doi.org/10.2475/ajs.300.2.142

Moecher, D. P., Samson, S. D., Miller, C. F., 2004, Precise time and conditions of peak Taconian granulite facies metamorphism in the southern Appalachian orogen, U.S.A., with implications for zircon behavior during crustal melting events: The Journal of Geology, v. 112, n. 3, p. 289–304, https://doi.org/10.1086/382760

Moecher, D. P., Hietpas, J., Samson, S. D., and Chakraborty, S., 2011, Insights into southern Appalachian tectonic history from ages of detrital monazite and zircon in modern alluvium: Geosphere, v. 7, n. 2, p. 494–512, https://doi.org/10.1130/GES00615.1

Moecher, D. P., Anderson, E. D., Loughry, Jr., D. F., Quinn, R. J., Larkin, E. A., Walsh, K. B., Samson, S. D., Satkoski, A. M., and Tohver, E., 2018, Evolution of the Blue Ridge basement complex in the eastern Great Smoky Mountains: Evidence from zircon U-Pb geochronology and Nd-Pb isotope geochemistry of basement gneisses, *in* Engel, A. S., and Hatcher, Jr., R. D., editors, Geology at Every Scale: Field Excursions for the 2018 GSA Southeastern Section Meeeting in Knoxville, Tennessee: Geological Society of America Field Guide 50, p. 121–139, https://doi.org/10.1130/2018.0050(08)

Moecher, D. P., Kelly, E. A., Hietpas, J., and Samson, S. D., 2019, Proof of recycling in clastic sedimentary systems from detrital monazite textures and geochronology: GSA Bulletin, v. 131, n. 7–8, p. 1116–1132, https://doi.org/10.1130/B31947.1

Montes, C., ms, 1997, The Greenbrier and Hayesville faults in central-western North Carolina: Knoxville, Tennessee, University of Tennessee, M. S. thesis, 145 p.

Nemchin, A. A., and Cawood, P. A., 2005, Discordance of the U-Pb system in detrital zircons: Implications for provenance studies of sedimentary rocks: Sedimentary Geology, v. 182, n. 1–4, p. 143–162, https://doi.org/10.1016/j.sedgeo.2005.07.011

Ownby, S. E., Miller, C. F., Berquist, P. J., Carrigan, C. W., Wooden, J. L., and Fullager, P. D., 2004, U-Pb geochronology and geochemistry of a portion of the Mars Hill terrane, North-Carolina-Tennessee: Constraints on origin, history, and tectonic assembly, *in* Tollo, R. P., Corriveau, L., McLelland, J., and Bartholomew, M. J., editors, Proterozoic tectonic evolution of the Grenville orogen in North America: GSA Memoirs, v. 197, p. 609–632, https://doi.org/10.1130/0-8137-1197-5.609

Paces, J. B., and Miller, Jr., J. D., 1993, Precise U-Pb ages of Duluth Complex and related mafic intrusions, northeastern Minnesota: Geochronological insights to physical, petrogenetic, paleomagnetic, and tectonometamorphic processes associated with the 1.1 Ga Midcontinent Rift System: Journal of Geophysical Research-Solid Earth, v. 98, n. B8, p. 13997–14,013, https://doi.org/10.1029/93JB01159

Peck, W. H., Quinan, M. P., and Selleck, B. W., 2019, Detrital zircon constraints on Grenville sedimentation at the margin of Laurentia: Precambrian Research, v. 331, https://doi.org/10.1016/j.precamres.2019.105342

Pullen, A., Ibañez-Mejia, M., Gehrels, G. E., Ibañez-Mejia, J. C., and Pecha, M., 2014, What happens when n=1000? Creating large-*n* geochronologic datasets with LA-ICP-MS for geologic investigations: Journal of Analytical Atomic Spectrometry, v. 29, n. 6, p. 971–980, https://doi.org/10.1039/C4JA00024B

Quinn, M. J., ms, 1991, Two lithotectonic boundaries in western North Carolina: Geologic interpretation of a region surrounding Sylva, Jackson County: Knoxville, Tennessee, University of Tennessee, M. S. thesis, 223 p.

Quinn, R. J., ms, 2012, The evolution of Grenville basement in the eastern Great Smoky Mountains; Constraints from U-Pb zircon, whole rock Sm-Nd, and feldspar Pb geochemistry: Lexington, Kentucky University of Kentucky, M.S. thesis, 115 p., https://uknowledge.uky.edu/ees_etds/7/

Rainbird, R. H., Rayner, N. M., Hadlari, T., Heaman, L. M., Ielpi, A., Turner, E. C., and MacNaughton, R. B., 2017, Zircon provenance data record the lateral extent of pancontinental, early Neoproterozoic rivers and erosional unroofing history of the Grenville orogen: GSA Bulletin, v. 129, n. 11–12, p. 1408–1423, https://doi.org/10.1130/B31695.1

Rankin, D. W., 1975, The continental margin of eastern North America in the southern Appalachians: The opening and closing of the proto-Atlantic ocean: American Journal of Science, v. 279A, p. 298–336.

Rankin, D. W., Drake, Jr., A.A., Glover, III, L., Goldsmith, R., Hall, L. M., Murray, D. P., Ratcliffe, N. M., Read, J. F., Secor, Jr., D. T., and Stanley, R. S., 1989, Pre-orogneic terranes, *in* Hatcher, Jr., R. D., Thomas, W. A., and Viele, G. W., editors, The Appalachian-Orogen in the United States: Geological Society of America, The Geology of North America, v. F-2, p. 7–100, https://doi.org/10.1130/DNAG-GNA-F2.7

Rankin, D. W., Drake, Jr., A. A., and Ratcliffe, N. M., 1990, Plate 2, Geologic map of the U.S. Appalachians showing the Laurentian margin and the Taconic Orogen, *in* Hatcher, Jr., R. D., Thomas, W. A., and Viele, G. W., editors, The Appalachian-Orogen in the United States: Geological Society of America, The Geology of North America, v. F-2, Plate 2, map scale 1:1,538,000.

Ratcliffe, N. M., and Aleinikoff, J. N., 2008, Pre-Ottawan (1.09 Ga) infrastructure and tectonics of the Hudson Highlands and Manhattan prong of New York, *in* Van Baalen, M.R., editor, Guidebook for field trips in Massachusetts and adjacent regions of Connecticut and New York: Westfield, Massachusetts, New England Intercollegiate Geological Conference, 100th, p. 307–340.

Ratcliffe, N. M., Aleinikoff, J. N., Burton, W. C., and Karabinos, P., 1991, Trondhjemitic, 1.35–1.31 Ga gneisses of the Mount Holly Complex of Vermont: Evidence for an Elzevirian event in the Grenville basement of the United States Appalachians: Canadian Journal of Earth Science, v. 28, n. 1, p. 77–93, https://doi.org/10.1139/e91-007

Raymond, L. A., Yurkovich, S. P., and McKinney, M., 1989, Block-in-matrix structures in the North Carolina Blue Ridge Belt and their significance for the tectonic history of the Southern Appalachian orogen, *in* Horton, Jr., J. W., and Rast, N., editors, Melanges and olistostromes of the U.S. Appalachians: Geological Society of America Special Paper 228, p. 195–215, https://doi.org/10.1130/SPE228-p195

Rivers, T., 1997, Lithotectonic elements of Grenville province: Review and tectonic implications: Precambrian Research, v. 86, n. 3–4, p. 117–154, https://doi.org/10.1016/S0301-9268(97)00038-7

_____ 2008, Assembly and preservation of lower, mid, and upper orogenic crust in the Grenville Province – Implications for the evolution of large hot long-duration orogens: Precambrian Research, v. 167, n. 3–4, p. 237–259, https://doi.org/10.1016/j.precamres.2008.08.005

Rivers, T., Culshaw, N., Hynes, A., Indares, A., Jamieson, R., and Martignole, J., 2012, Chapter 3: The Grenville Orogen – a post-LITHOPROBE perspective, *in* Percival, J. A., Cook, F. A., and Clowes, R. M., editors, Tectonic Styles in Canada: The LITHOPROBE Perspective, Geological Association of Canada, Special Paper 49, p. 97–236.

Rizzotto, G. J., Santos, J. O. S., Hartmann, L. A., Tohver, E., Pimental, M. M., and McNaughton, N. J., 2013, The Mesoproterozoic Guaporé suture in the SW Amazonian Craton: Geotectonic implications based on field geology, zircon geochronology and Nd-Sr isotope geochemistry: Journal of South American Earth Sciences, v. 48, p. 271–295, https://doi.org/10.1016/j.jsames.2013.10.001

Roberts, N. M. W., and Spencer, C. J., 2015, The zircon archive of continent formation through time: Geological Society, London, Special Publications, v. 389, p. 197–225, https://doi.org/10.1144/SP389.14

Robinson, P., Tucker, R. D., Bradley, D. C., Berry, IV, H. N., and Osberg, P. H., 1998, Paleozoic orogens in New England, U.S.A.: Geologiska Foreningen i Stockholm Forhandlingar (GFF), v. 120, n. 2, p. 119–148, https://doi.org/10.1080/11035899801202119

Sadowski, G. R., and Bettencourt, J. S., 1996, Mesoproterozoic tectonic correlations between eastern Laurentia and the western border of the Amazon Craton: Precambrian Research, v. 76, n. 3–4, p. 213–227, https://doi.org/10.1016/0301-9268(95)00026-7

Santos, J. O. S., Rizzotto, G. J., Potter, P. E., McNaughton, N. J., Matos, R. S., Hartmann, L. A., Chemale, F., and Quadros, M. E. S., 2008, Age and authochthonous evolution of the Sunsás Orogen in West Amazonia Craton based on mapping and U-Pb Geochronology: Precambrian Research, v. 165, p. 120–152, https://doi.org/10.1016/j.precamres.2008.06.009

Schmitt, A. K., Grove, M., Harrison, T. M., Lovera, O., Hulen, J., and Walters, M., 2003, The Geysers-Cobb Mountain magma system, California (Part 1): U-Pb zircon ages of volcanic rocks, conditions of zircon crystallization and magma residence times: Geochimica et Cosmochimica, v. 67, n. 18, p. 3423–3442, https://doi.org/10.1016/S0016-7037(03)00140-6

Schmitz, M. D., Bowring, S. A., and Ireland, T. R., 2003, Evaluation of the Duluth Complex anorthositic series (AS3) zircon as a U-Pb geochronological standard: New high-precision isotope dilution thermal ionization mass spectrometry results: Geochimica et Cosmochimica Acta, v. 67, n. 19, p. 3665–3672, https://doi.org/10.1016/S0016-7037(03)00200-X

Sinha, A. K., and McLelland, J. M., 1999, Lead isotope mapping of crustal reservoirs within the Grenville superterrane: II. Adirondack massif, New York: Basement Tectonics, v. 13, p. 293–305, https://doi.org/10.1007/978-94-011-4800-9_17

Sinha, A. K., Hogan, J. P., and Parks, J., 1996, Lead isotope mapping of crustal reservoirs within the Grenville Superterrane: I: Central and Southern Appalachians, *in* Basu, A., and Hart, S., editors, Earth Processes: Reading the Isotopic Code: Geophyscial Monograph Series, v. 95, p. 293–305, https://doi.org/10.1029/GM095p0293

Southworth, S., Aleinikoff, J. N., Tollo, R. P., Bailey, C. M., Burton, W. C., Hackley, P. C., and Fanning, M. C., 2010, Mesoproterozoic magmatism and deformation in the northern Blue Ridge, Virginia and Maryland: Application of SHRIMP U-Pb geochronology and integrated field studies in the definition of Grenvillian tectonic history, *in* Tollo, R. P., Bartholomew, M. J., Hibbard, J. P., and Karabinos, P. M., editors, From Rodinia to Pangea: The Lithotectonic Record of the Appalachian Region: GSA Memoirs, v. 206, p. 795–836, https://doi.org/10.1130/2010.1206(31)

Southworth, S., Schultz, A., Aleinikoff, J. N., and Merschat, A. J., 2012, Geologic map of the Great Smoky Mountains National Park Region, Tennessee and North Carolina: U.S. Geological Survey Scientific Investigations Map 2997, https://doi.org/10.3133/sim2997

Spaulding, D., 2014, Geology of the west half of the Cove Creek Gap 7.5 minute quadrangle and adjacent areas, western North Carolina: Insights into eastern Great Smoky Mountains tectonometamorphism: Lexington, Kentucky, University of Kentucky, 121 p., https://uknowledge.uky.edu/ees_etds/23/

Spencer, C. J., 2020, Continuous continental growth as constrained by the sedimentary record: American Journal of Science, v. 320, n. 4, p. 373–401, https://doi.org/10.2475/04.2020.02

Spencer, C. J., Cawood, P. A., Hawkesworth, C. J., Prave, A. R., Roberts, N. M. W., Horstwood, M. S. A., Whitehouse, M. J., and EIMF, 2015, Generation and preservation of continental crust in the Grenville Orogeny: Geoscience Frontiers, v. 6, n. 3, p. 357–372, https://doi.org/10.1016/j.gsf.2014.12.001

Spencer, C. J., Kirkland, C. L., and Taylor, R. J. M., 2016, Strategies towards statistically robust interpretation of *in situ* U-Pb zircon geochronology: Geoscience Frontiers, v. 7, n. 4, p. 581–589, https://doi.org/10.1016/j.gsf.2015.11.006

Stacey, J. S., and Kramers, J. D., 1975, Approximation of terrestrial lead isotope evolution by a two-stage model: Earth and Planetary Science Letters, v. 26, n. 2, p. 207–221, https://doi.org/10.1016/0012-821X(75)90088-6

Stern, R. A., 2001, A new isotopic and trace-element standard for ion microprobe: Preliminary thermal ionization mass spectrometry (TIMS) U-Pb and electron-microprobe data: Geological Survey of Canada Current Research, 2001-F1, 11 p., https://doi.org/10.4095/212668

Streckeisen, A. J., and Le Maitre, R. W., 1979, A chemical approximation to the modal QAPF classification of the igneous rocks: Neues Jahrbuch fuer Mineralogie, Abhandlungen, v. 136, p. 169–206.

Thomas, W. A., Becker, T. P., Samson, S. D., and Hamilton, M. A., 2004, Detrital zircon evidence of a recycled orogenic foreland provenance for Alleghanian clastic-wedge sandstones: The Journal of Geology, v. 112, n. 1, p. 23–37, https://doi.org/10.1086/379690

Thomas, W. A., Gehrels, G. E., Greb, S. F., Nadon, G. C., Satkoski, A. M., and Romero, M. C., 2017, Detrital zircons and sediment dispersal in the Appalachian foreland: Geosphere, v. 13, n. 6, p. 2206–2230, https://doi.org/10.1130/GES01525.1

Tohver, E., van der Pluijm, B. A., Van der Voo, R., Rizzotto, G., and Scandolara, J. E., 2002, Paleogeography of the Amazon craton at 1.2 Ga: Early Grenvillian collision with the Llano segment of Laurentia: Earth and Planetary Science Letters, v. 199, n. 1–2, p. 185–200, https://doi.org/10.1016/S0012-821X(02)00561-7

Tohver, E., Bettencourt, J. S., Tosdal, R., Mezger, K., Leite, W. B., and Payolla, B. L., 2004a, Terrane transfer during the Grenville orogeny: Tracing the Amazonian ancestry of southern Appalachian basement through Pb and Nd isotopes: Earth and Planetary Science Letters, v. 228, n. 1–2, p. 161–176, https://doi.org/10.1016/j.epsl.2004.09.029

Tohver, E., van der Pluijm, B., Mezger, L., Essene, E., Scandolara, J., and Rizotto, G., 2004b, Significance of the Nova Brasilândia metasedimentary belt in western Brazil: Redefining the Mesoproterozoic boundary of the Amazon craton: Tectonics, v. 23, n. 6, TC6004, https://doi.org/10.1029/2003TC001563

Tohver, E., van der Pluijm, B. A., Scandolâria, J. E., and Essene, E. J., 2005, Late Mesoproterozoic deformation of SW Amazonia (Rondônia, Brazil): Geochronological and structural evidence for collision with southern Laurentia: The Journal of Geology, v. 113, n. 3, p. 309–323, https://doi.org/10.1086/428807

Tohver, E., Teixeira, W., van der Pluijm, B., Geraldes, M. C., Bettencourt, J. S., and Rizzotto, G., 2006, Restored transect across exhumed Grenville orogen of Laurentia and Amazonia, with implications for crustal architecture: Geology, v. 34, n. 8, p. 669–672, https://doi.org/10.1130/G22534.1

Tohver, E., Lana, C., Cawood, P. A., Fletcher, I. R., Jourdan, F., Sherlock, S., Rasmussen, B., Trindade, R. I. F., Yokoyama, E., Souza Filho, C. R., and Marangoni, Y., 2012, Geochronological constraints on the age of the Permo-Triassic impact event: U-Pb and $^{40}Ar/^{39}Ar$ results for the 40 km Araguainha structure of central Brazil: Geochimica et Cosmochimica Acta, v. 86, p. 214–227, https://doi.org/10.1016/j.gca.2012.03.005

Tollo, R. P., Aleinikoff, J. N., Wooden, J. L., Mazdab, F. K., Southworth, S., and Fanning, M. C., 2010, Thermomagmatic evolution of Mesoproterozoic crust in the Blue Ridge of SW Virginia and NW North Carolina: Evidence from U-Pb geochronology and zircon geothermometry, *in* Tollo, R. P., Bartholomew, M. J., Hibbard, J. P., and Karabinos, P. M., editors, From Rodinia to Pangea: The Lithotectonic Record of the Appalachian Region: GSA Memoirs, v. 206, p. 859–896, https://doi.org/10.1130/2010.1206(33)

Tollo, R. P., Aleinikoff, J. N., Dickin, A. P., Radwany, M. S., Southworth, C. S., and Fanning, C. M., 2017, Petrology and geochronology of Mesoproterozoic basement of the Mount Rogers area of southwestern Virginia and northwestern North Carolina: Implications for the Precambrian tectonic evolution of the southern Blue Ridge Province: American Journal of Science, v. 317, n. 3, p. 251–337, https://doi.org/10.2475/03.2017.01

Tosdal, R. M., 1996, The Amazon-Laurentia connection as viewed from the Middle Proterozoic rocks in the central Andes, western Bolivia and northern Chile: Tectonics, v. 15, n. 4, p. 827–842, https://doi.org/10.1029/95TC03248

Trupe C. H., Stewart, K. G., Adams, M. G., and Foudy, J. P., 2004, Deciphering the Grenville of the southern Appalachians through evaluation of the post-Grenville tectonic history in northwestern North Carolina, *in* Tollo, R. P., Corriveau, L., McLelland, J., and Bartholomew, M. J., editors, Proterozoic Tectonic Evolution of the Grenville Orogen in North America: GSA Memoirs, v. 197, p. 679–695, https://doi.org/10.1130/0-8137-1197-5.679

Vavra, G., Gebauer, D., Schmid, R., and Compston, W., 1996, Multiple zircon growth and recrystallization during polyphase Late Carboniferous to Triassic metamorphism in granulites of the Ivrea Zone (Southern Alps): An ion microprobe (SHRIMP) study: Contributions to Mineralogy and Petrology, v. 122, p. 337–358, https://doi.org/10.1007/s004100050132

Vavra, G., Schmid, R., and Gebauer, D., 1999, Internal morphology, habit and U-Th-Pb microanalysis of amphibolite-to-granulite facies zircons: Geochronology of the Ivrea Zone (Southern Alps): Contributions to Mineralogy and Petrology, v. 134, p. 380–404, https://doi.org/10.1007/s004100050492

Volkert, R. A., Aleinikoff, J. N., and Fanning, C. M., 2010, Tectonic, magmatic, and metamorphic history of the New Jersey Highlands: New insights from SHRIMP U-Pb geochronology, *in* Tollo, R. P., Bartholomew, R. P., Hibbard, M. J., and Karabinos, P. M., editors, From Rodinia to Pangea: The Lithotectonic Record of Appalachian Region: GSA Memoirs, v. 206, p. 307–346, https://doi.org/10.1130/2010.1206(14)

Walsh, K. B., ms, 2018, Geochronological and geochemical constraints on the origin of the Cartoogechaye Terrane, western North Carolina: Implications for the late Precambrian to early Paleozoic evolution of the eastern Laurentian margin: Lexington, Kentucky, University of Kentucky, M. S. thesis, 108 p., https://uknowledge.uky.edu/ees_etds/57/

Whitmeyer, S. J., and Karlstrom, K. E., 2007, Tectonic model for the Proterozoic growth of North America: Geosphere, v. 3, n. 4, p. 220–259, https://doi.org/10.1130/GES00055.1

Whitney, D. L., and Evans, B. W., 2010, Abbreviations for names of rock-forming minerals: American Mineralogist, v. 95, n. 1, p. 181–187, https://doi.org/10.2138/am.2010.3371